AD_____

AWARD NUMBER: DAMD17-02-1-0684

TITLE: Bone Sialoproteins and Breast Cancer Detection

PRINCIPAL INVESTIGATOR: Neal S. Fedarko, Ph.D.

CONTRACTING ORGANIZATION: The Johns Hopkins University School of Medicine
Baltimore, Maryland 21205

REPORT DATE: July 2006

TYPE OF REPORT: Final

PREPARED FOR: U.S. Army Medical Research and Materiel Command
Fort Detrick, Maryland 21702-5012

DISTRIBUTION STATEMENT: Approved for Public Release;
Distribution Unlimited

REPORT DOCUMENTATION PAGE

Form Approved
OMB No. 0704-0188

1. REPORT DATE *(DD-MM-YYYY)*	**2. REPORT TYPE**	**3. DATES COVERED** *(From - To)*
01-07-2006	Final	1 Jul 2002 – 30 Jun 2006

4. TITLE AND SUBTITLE

Bone Sialoproteins and Breast Cancer Detection

5a. CONTRACT NUMBER

5b. GRANT NUMBER
DAMD17-02-1-0684

5c. PROGRAM ELEMENT NUMBER

6. AUTHOR(S)

Neal S. Fedarko, Ph.D.

E-Mail: ndarko@jhmi.edu

5d. PROJECT NUMBER

5e. TASK NUMBER

5f. WORK UNIT NUMBER

7. PERFORMING ORGANIZATION NAME(S) AND ADDRESS(ES)

The Johns Hopkins University School of Medicine
Baltimore, Maryland 21205

8. PERFORMING ORGANIZATION REPORT NUMBER

9. SPONSORING / MONITORING AGENCY NAME(S) AND ADDRESS(ES)
U.S. Army Medical Research and Materiel Command
Fort Detrick, Maryland 21702-5012

10. SPONSOR/MONITOR'S ACRONYM(S)

11. SPONSOR/MONITOR'S REPORT NUMBER(S)

12. DISTRIBUTION / AVAILABILITY STATEMENT
Approved for Public Release; Distribution Unlimited

13. SUPPLEMENTARY NOTES

14. ABSTRACT

We have been studying a family of proteins that we have termed SIBLINGs for Small Integrin Binding LIgand N-linked Glycoproteins, that share similar structural domains, human chromosomal location, normal synthesis by skeletal tissue, and abnormal expression by neoplasms . The goal of our research is to test whether SIBLINGs might be informative markers for breast cancer detection. To accomplish this goal we have developed competitive enzyme-linked immunosorbent assays (ELISAs) for the SIBLINGs bone sialoprotein (BSP), osteopontin (OPN), dentin matrix protein-1 (DMP1), dentin sialophosphoprotein (DSPP) and matrix extracellular phosphoglycoprotein (MEPE). Sandwich-based ELISA assays have also been developed. When the competitive ELISAs were used to screen SIBLING protein levels, BSP and OPN exhibited the highest degree of sensitivity and specificity for the detection of breast cancer. Microarray analysis of normal and breast cancer-derived mRNA samples found a similar elevated levels of elevated SIBLING expression. The levels of certain SIBLINGs in serum were found to be correlated with cancer stage. These results suggest that SIBLINGs may have utility as serum-based markers for breast cancer detection.

15. SUBJECT TERMS
Biomarkers, immunoassay, detection, receiver operating, characteristics (ROC), sensitivity, specificity, detection

16. SECURITY CLASSIFICATION OF:			**17. LIMITATION OF ABSTRACT**	**18. NUMBER OF PAGES**	**19a. NAME OF RESPONSIBLE PERSON**
a. REPORT	**b. ABSTRACT**	**c. THIS PAGE**			USAMRMC
U	U	U	UU	75	**19b. TELEPHONE NUMBER** *(include area code)*

Table of Contents

Introduction

Tumor progression involves modulation of cell adhesion, differentiation, division, apoptosis, angiogenesis as well as migration and metastasis. We have been studying a gene family we term SIBLINGs (for Small Integrin-Binding Ligand N-linked Glycoproteins) that are induced by certain neoplasms. Members of the SIBLING family include bone sialoprotein (BSP), osteopontin (OPN), dentin matrix protein (DMP1), dentin sialophosphoprotein (DSPP), and matrix extracellular phosphoglycoprotein (MEPE). Our published work has shown that BSP and OPN are extended and flexible in solution (such lack of ordered structure is shared by a number proteins that have multiple binding partners) [1]. SIBLINGs can bind integrins including $\alpha_V\beta_3$ via their RGD sequence [2-4]. OPN and DMP1 can also bind CD44 (via an amino terminal domain) [5-7]. SIBLINGs can bind to complement Factor H and sequester it to the cell surface thereby regulating complement-mediated cell lysis [7, 8]. More recently we have shown that SIBLINGs can bind to and modulate the activity of specific MMPs [9]. It is our hypothesis that SIBLINGs promote breast cancer progression through neoplastic expression of SIBLINGs that bind to and modulate the activity of specific MMPs. MMPs play multiple roles in tumor progression including: angiogenesis; processing and presentation of certain growth factors; and metastasis. We further hypothesize that SIBLINGs are biologically plausible surrogate endpoint markers for cancer detection.

The goal of the current research is to develop SIBLINGs as serum measures for use in breast cancer detection, by determining the distribution of their serum levels in a breast cancer patient population before and after treatment, a large normal (cancer-free) population, and a patient population at risk for developing breast cancer. Serum levels of gene family members in normal and breast cancer patients will be used to establish the sensitivity, specificity and predictive value of these markers in breast cancer. In patients with defined breast cancer, serum levels will be correlated with stage, prognosis and response to treatment. This research will determine whether serum SIBLING levels have high sensitivity (low false negative rate) and high specificity (low false positive rate), can be analyzed in a general laboratory setting (does not require highly specialized procedures/equipment), and enable early detection.

Body

Overview:

The goal of the proposed research was to develop reagents and methodology to implement ELISA-based quantification of serum levels of SIBLING proteins and to apply these tests to breast cancer sera. Competitive and sandwich-based ELISAs were developed (years 1 and 2) and applied to defining the distribution of SIBLINGs in a normal group and in a group of subjects with breast cancer (years 2 and 3).

Statement of Work:

Task 1. To complete development of competitive ELISA for the SIBLINGs DMP1 and MEPE (Months 1 – 6):

a. Develop adenovirus expression vector for expressing recombinant human MEPE.
b. Perform checkerboard assays to determine optimum antigen coating and antibody concentrations for MEPE and DMP1.
c. Determine precision and yield of these new assays.

Task 2. To determine the distribution of serum SIBLING (BSP, OPN, DMP1 and MEPE) levels in serum obtained from normal donors and breast cancer patients (Months 7 - 24).

a. Measure BSP, OPN, DMP1 and MEPE in a normal population, breast cancer patients and a population at risk for breast cancer.
b. Determine sensitivity and specificity and perform ROC analysis.
c. Test for clinical correlation between serum SIBLING levels and cancer stage, prognosis, tumor burden and response to treatment.

Task 3. To refine the existing competitive ELISA assay systems to more rapid sandwich-based assay systems and verify previous results (Months 24 – 36).

a. Screen monoclonal antibodies for utility in BSP, OPN, DMP1 and MEPE assays.
b. Employ checkerboard assays to define optimum capture antibody coating, second antibody concentration and incubation time.
c. Re-analyze normal and breast cancer patient sera using the new sandwich based assays.

Progress:

This is the final year (a no cost extension) of a three year study. The no cost extension had been requested because of a delay in completing all tasks. As of the end of the final year of this grant, all Tasks have been completed, with the exception of the development of a sandwich-based ELISA for DMP1. In the original design of the study, cut-off values for serum SIBLING levels determined using the competitive ELISA results would be used in evaluating the sensitivity and specificity of the sandwich-based ELISAs. This "lock-down" of cut-off values prior to final analysis would decrease bias. The inability to devise a stable DMP1 sandwich ELISA caused a change in the experimental plan as we have no corresponding sandwich ELISA to use for the analysis. The decision has been made to leave DMP1 out of the SIBLING analysis plan and use BSP, DSPP and OPN for cross comparison of competitive and sandwich based ELISAs. As a result, we have only recently been unblinded as to staging (TNM scores) and outcome data for the subjects from whom the serum samples were derived. Even though the funding period has ended, we will continue the statistical analysis of the unblinded data and pursue writing the final manuscripts.

During the current reporting period and on the strength of data generated from our studies of SIBLING biology, the P.I. successfully applied for NIH-sponsored funding for a study examining the biochemical and physiological role of SIBLINGs in tumor progression.

Summary of Research

During the course of research on BSP and OPN, it was discovered that they are members of a gene family. This family, termed SIBLINGs (for Small Integrin Binding LIgand N-linked Glycoproteins) was found to be expressed normally in skeletal tissue [14] and in certain cancers [11]. As described in the annual report for year one, during the course of purifying recombinant SIBLINGs for use in immunoassays, proteins that co-purified with specific SIBLINGs under nondenaturing conditions were observed. These proteins have subsequently been identified as matrix metalloproteinases (MMPs).

While developing and testing the immunoassay for the SIBLING MEPE, novel observation were made on its levels, distribution as well as physiological correlations. In the paper by Jain et al. (Appendix I, [10]), we have shown that a) significant levels of MEPE in the serum of normal humans can be measured, (b) a clear age-related decrease in serum MEPE

levels, (c) a positive correlation between MEPE and phosphorus, a inverse correlation with parathyroid hormone, and (d) a significant positive correlation with total hip and neck bone mineral density. While this study demonstrates the association of serum MEPE levels with serum phosphate, PTH and bone mineral density, it does not address causality. In the very least, the results suggest that MEPE may be an interesting marker of normal human bone and mineral metabolism.

Given what we now know about SIBLING and MMP biology, experiments were designed to address whether biologically and physiologically relevant complexes of SIBLING + MMP + cell surface receptor could be measured (Appendix II, [12], [13]). Studies were performed to demonstrate that BSP interacted with MMP-2 and cell-surface integrin $\alpha_v\beta_3$ to form a trimolecular complex as shown by immunoprecipitation, flow cytometry, and *in situ* hybridization. Enhanced invasiveness of breast cancer cells by BSP addition was shown to require a_Vb_3 and MMP-2 and the formation of the trimolecular complex at the membrane surface [12]. Similarly, studying colon cancer cells, a complex of DMP1 and MMP-9 could be demonstrated and DMP1 enhanced the invasiveness of the colon cancer cells [13].

As reported in the 2005 annual report, the expression of five SIBLING gene family members – BSP, OPN, DMP1, MEPE, and DSPP in 9 distinct cancer types was determined. The expression levels of SIBLINGs were distinct within subtypes of cancer (e.g. breast ductal tumors compared to lobular tumors). SIBLING expression increased with cancer stage for breast, colon, lung and rectal cancer [11].

Also as reported in the 2005 annual report, BSP was found to alter MMP enzyme inhibition kinetics (Jain et al. 2006, submitted, included in Appendix). BSP binding to MMP-2 caused the natural inhibitor TIMP2 to function as a weaker inhibitor. Similarly, synthetic inhibitors exhibited a poorer affinity for MMP-2 in the presence of BSP. This observation may explain why clinical trials of MMP inhibitors in cancer have not been that successful.

Key Research Accomplishments

Assay Development:

Competitive ELISAs have been developed for 5 different SIBLING family proteins.
Indirect sandwich-based ELISAs have been developed for 4 different SIBLING family proteins.

Assay Application:

The normal distribution pattern of BSP, OPN, DMP1, DSPP and MEPE has been characterized ([10], 2003 and 2004 annual report).

The distribution of serum BSP, OPN, DMP1 and DSPP in breast cancer has been described. (2004 and 2005 annual report)

In an initial analysis, the SIBLINGs expression levels increase with changing tumor (T) stage ([11], 2004 and 2005 annual report).

In contrast to other SIBLINGs, MEPE serum levels exhibited:

- no elevation in breast cancer;
- an age-dependent decrease in levels;
- an inverse correlation with parathyroid hormone levels;
- a significant positive correlation with total hip and neck BMD.

([10], 2005 annual report)

SIBLING Biology:
SIBLINGs bind to and modulate specific matrix metalloproteinases [9].
The transcription factor RunX2 is more highly expressed in ductal tumors (2005 annual report).
The expression levels of the transcription factor RunX2 were found to be correlated with BSP, MMP-2, and MT1-MMP expression (2005 annual report).
BSP and MMP-2 can be co-localized to the cell surface and promote cell invasion ([12]).
DMP2 and MMP-9 can be co-localized to the cell surface and promote cell invasion ([13]).

Reportable Outcomes

(for entire period)

- Submitted Manuscripts
  - Jain, A., Fisher, L.W. and N.S. Fedarko. (2006) Bone Sialoprotein Binding To Matrix Metalloproteinase-2 Alters Enzyme Kinetics. J. Natl. Cancer Inst.
- Meeting Abstracts
  - Jain, A., Fisher, L.W. and N.S. Fedarko Small Integrin Binding Ligand N-Linked Glycoproteins (SIBLINGs) Bind and Activate Matrix Metalloproteinases. Era of Hope 2005 Department of Defense Breast Cancer Research Program Meeting. June 9th, 2005, Philadelphia, PA
  - Jain, A., Fisher, L.W. and N.S. Fedarko. Small Integrin Binding Ligand N-Linked Glycoprotein (SIBLING) Gene Family Expression In Breast Cancer. Era of Hope 2005 Department of Defense Breast Cancer Research Program Meeting. June9th, 2005, Philadelphia, PA
  - Fedarko, N.S., Fisher, L.W. and A. Jain. Small Integrin Binding Ligand N-Linked Glycoproteins Modulate Matrix Metalloproteinases and Angiogenesis. Era of Hope 2005 Department of Defense Breast Cancer Research Program Meeting. June 9th, 2005, Philadelphia, PA
- Invited Presentations:

"SIBLING binding interactions." Third International Conference on Osteopontin. 2002, San Antonio, TX.

"Serum SIBLINGs in Cancer" 8th Annual ASBMR Workshop on Aging and the Human Skeleton. 2002. 24th Annual Meeting of the American Society for Bone and Mineral Research, Phoenix, AZ.

"Markers in Malignant Bone Disease." 24th Annual ASBMR Workshop on Biochemical Markers of Bone Turnover, 2002, 24th Annual Meeting of the American Society for Bone and Mineral Research, San Antonio, TX

"The SIBLING gene family promotes tumor progression." 2004-2005 Johns Hopkins

University Oncology Translational Research Conference, November 3rd, 2004, Baltimore, MD.

"SIBLING modulation of matrix metalloproteinases and tumor progression." 2nd National Meeting of the American Society for Matrix Biology. November 12, 2004, San Diego, CA.

"What do bone proteins have to do with tumor progression?" The Sidney Kimmel Comprehensive Cancer Center At Johns Hopkins Longrifles Seminar Series, March 2nd, 2005, Baltimore MD.

"MMP activation by SIBLINGs" Gordon Research Conference on Small Integrin-Binding Proteins, September 12th, 2005 Big Sky, MT.

"The Small Integrin Binding Ligand N-linked Glycoprotein (SIBLING) family, protease activation and tumor progression. November 18th, 2005; University of Li∂ge, Belgium.

"What do bone proteins have to do with tumor progression, inflammation and wound healing?" Johns Hopkins Bayview Medical Center Research Conference, February 16th, 2006; Baltimore MD.

"The role of bone proteins in tumor progression and metastasis." Johns Hopkins University Department of Orthopedics Grand Rounds, June 30th, 2006; Baltimore, MD.

- Publications

Fisher, L., and N.S. Fedarko. (2003) Six genes expressed in bones and teeth constitute the current members of the SIBLING family of proteins. Connective Tissue Res. 44:1-8.

Koopmann, J., Zhang, Z.,White, N., Rosenzweig, J., Fedarko, N.S., Sanjay Jagannath, S., Canto, M.I., Yeo, C.J., Chan, D.W., and Michael Goggins. (2004) Serum diagnosis of pancreatic adenocarcinoma using surface-enhanced laser desorption and ionization mass spectrometry. Clin. Cancer Res.10(3):860-8.

Koopmann, J., Fedarko, N.S., Jain, A., Maitra, A., Iacobuzio-Donahue, C., Rahman, A., Hruban, R.H., Yeo, C.J., and M. Goggins. (2004) Evaluation of osteopontin as biomarker for pancreatic adenocarcinoma. Cancer Epidemiology, Biomarkers and Prevention. 13(3):487-491.

Fedarko, N.S., Jain, A., Karadag, A., and L.W. Fisher. (2004) Three small integrin binding ligand N-linked glycoproteins (SIBLINGs) bind and activate specific matrix metalloproteinases. FASEB J. 18:734-736.

Karadag, A., Ogburke K.U.E. , Fedarko, N.S., and L.W. Fisher. (2004) Bone sialoprotein promotes invasion by osteotropic cancer cells in vitro by bridging MMP-2 to $\alpha_V\beta_3$ integrin. J. Natl. Cancer Inst. 96:956-965.

Jain, A., Fedarko, N.S., Collins, M.T., Gelman, R., Ankrom, M.A., Tayback, M., and L.W. Fisher. (2004) Serum levels of matrix extracellular phosphoglycoprotein (MEPE) in normal humans correlate with serum phosphorus, parathyroid hormone and bone mineral density. J. Clin. Endo. Metab.89(8):4158-4161.

Fisher, L.W., Jain, A., Tayback, M., and N.S. Fedarko. (2004) Small Integrin Binding Ligand N-Linked Glycoprotein (SIBLING) gene family expression in different cancers**.** Clin. Cancer Res. 10(24): 10:8501-8511.

Karadag, A., Fedarko, N.S., and L.W. Fisher. (2005) Dentin matrix protein 1 enhances invasion potential of colon cancer cells by bridging matrix metalloproteinase-9 to integrins and CD44. Cancer Res. 65(24): p. 11545-52.

- Funding Received:

  - NCI, NIH U54 CA91409, Howard/Hopkins Partnership in Cancer ,NCI Minority Institution/Cancer Center Partnership, "Molecular Analysis of Co-Expression of Matrix Metalloproteinases and SIBLINGs in African American –vs- Caucasian Women." Agnes A. Day, Ph. D. (Howard University P.I.) & Neal S. Fedarko, Ph. D. (Johns Hopkins University P.I.) 09/15/04 – 10/14/07

  - DOD/CDMRP. W81XWH-04-1-0844, "Prostate Cancer Progression and Serum SIBLING (Small Integrin Binding N-linked Glycoprotein) Levels." 09/15/04 – 10/14/07

  - NCI, NIH 1 R01 CA113865. "Small integrin-binding proteins and tumor progression." 07/01/06 – 06/30/09

- Personnel Receiving Pay:

  Neal S. Fedarko
  Alka Jain
  Matthew Tayback

Conclusions

Summary. The development of competitive ELISAs and sandwich-based ELISAs to measure serum levels of SIBLING gene family members has been a necessary requirement in order to evaluate the utility of these potential markers in breast cancer detection. Initial results in applying these assays describe a gaussian distribution of SIBLINGs (with the exception of MEPE) in the serum of normal individuals. In serum from subjects with cancer, serum SIBLING levels were increased (for BSP, OPN, DMP1 and DSPP) in the presence of disease. In breast cancer, in particular, BSP and OPN display greater sensitivity and specificity then DSPP. More normal and breast cancer sera need to be analyzed for ROC analysis of DMP1 sensitivity and specificity. All of our data so far is consistent with SIBLINGs behaving as early markers of breast cancer progression. This conclusion is reached by noting that (a) increased expression levels are not associated with metastases, (b) increased expression levels are observed with increasing tumor size (T status in TNM staging) and lymph node involvement (N status in TNM staging) (c) SIBLINGs can act biologically to modulate matrix metalloproteinase (MMP) activity. MMP activation is required for early tumor progression (remodeling the extracellular matrix scaffolding to yield space for growth and for angiogenesis). The completion of the research (final statistical analysis of unblinded data) will occur over the next few months and will enable the utility of these breast cancer biomarkers to be defined. Once completed, the groundwork will be laid for subsequent larger scale clinical trials of these biomarkers.

References

1. Fisher, L.W., D.A. Torchia, B. Fohr, M.F. Young, and N.S. Fedarko, *The solution structures of two SIBLING proteins, bone sialoprotein and osteopontin, by NMR.* Biochem. Bophys. Res. Comm., 2001. 280: p. 460-465.
2. Wu, Y., D.T. Denhardt, and S.R. Rittling, *Osteopontin is required for full expression of the transformed phenotype by the ras oncogene.* Br J Cancer, 2000. 83(2): p. 156-63.
3. Takano, S., K. Tsuboi, Y. Tomono, Y. Mitsui, and T. Nose, *Tissue factor, osteopontin, alphavbeta3 integrin expression in microvasculature of gliomas associated with vascular endothelial growth factor expression.* Br J Cancer, 2000. 82(12): p. 1967-73.
4. Tuck, A.B., B.E. Elliott, C. Hota, E. Tremblay, and A.F. Chambers, *Osteopontin-induced, integrin-dependent migration of human mammary epithelial cells involves activation of the hepatocyte growth factor receptor (Met).* J Cell Biochem, 2000. 78(3): p. 465-75.
5. Ue, T., H. Yokozaki, Y. Kitadai, S. Yamamoto, W. Yasui, T. Ishikawa, and E. Tahara, *Co-expression of osteopontin and CD44v9 in gastric cancer.* Int J Cancer, 1998. 79(2): p. 127-32.
6. Zohar, R., N. Suzuki, K. Suzuki, P. Arora, M. Glogauer, C.A. McCulloch, and J. Sodek, *Intracellular osteopontin is an integral component of the CD44-ERM complex involved in cell migration.* J Cell Physiol, 2000. 184(1): p. 118-30.
7. Jain, A., A. Karadag, B. Fohr, L.W. Fisher, and N.S. Fedarko, *Three SIBLINGs (small integrin-binding ligand, N-linked glycoproteins) enhance factor H's cofactor activity enabling MCP-like cellular evasion of complement-mediated attack.* J Biol Chem, 2002. 277(16): p. 13700-8.
8. Fedarko, N.S., B. Fohr, P. Gehron Robey, M.F. Young, and L.W. Fisher, *Factor H binding to bone sialoprotein and osteopontin enables molecular cloaking of tumor cells from complement-mediated attack.* J. Biol. Chem., 2000. 275: p. 16666-16672.
9. Fedarko, N.S., A. Jain, A. Karadag, and L.W. Fisher, *Three small integrin binding ligand N-linked glycoproteins (SIBLINGs) bind and activate specific matrix metalloproteinases.* Faseb J, 2004. 18(6): p. 734-6.
10. Jain, A., N.S. Fedarko, M.T. Collins, R. Gelman, M.A. Ankrom, M. Tayback, and L.W. Fisher, *erum levels of matrix extracellular phosphoglycoprotein (MEPE) in normal humans correlate with serum phosphorus, parathyroid hormone and bone mineral density.* J. Clin. Endo. Metab., 2004. In Press.
11. Fisher, L.W., A. Jain, M. Tayback, and N.S. Fedarko, *Small Integrin Binding LIgand N-linked Glycoprotein (SIBLING) gene family expression in different cancers.* Clin. Can. Res, 2004. 10(24): p. 8501-8511.
12. Karadag, A., K.U. Ogbureke, N.S. Fedarko, and L.W. Fisher, *Bone sialoprotein, matrix metalloproteinase 2, and alpha(v)beta3 integrin in osteotropic cancer cell invasion.* J Natl Cancer Inst, 2004. 96(12): p. 956-65.
13. Karadag, A., N.S. Fedarko, and L.W. Fisher, *Dentin matrix protein 1 enhances invasion potential of colon cancer cells by bridging matrix metalloproteinase-9 to integrins and CD44.* Cancer Res, 2005. 65(24): p. 11545-52.
14. Fisher, L.W. and N.S. Fedarko, *Six genes expressed in bones and teeth encode the current members of the SIBLING family of proteins.* Connect Tissue Res, 2003. 44 Suppl 1: p. 33-40.

Connective Tissue Research, 44(Suppl. 1):33–40, 2003

0300-8207/03 $12.00 + .00
DOI: 10.1080/03008200390152061

Taylor & Francis
healthsciences

Six Genes Expressed in Bones and Teeth Encode the Current Members of the SIBLING Family of Proteins

Larry W. Fisher[1] and Neal S. Fedarko[1,2]
[1]*Matrix Biochemistry Unit, Craniofacial & Skeletal Diseases Branch, NIDCR, NIH, Bethesda, Maryland, USA*
[2]*Division of Geriatrics, Department of Medicine, Johns Hopkins University, Baltimore, Maryland, USA*

Bone sialoprotein (BSP), dentin matrix protein 1 (DMP1), dentin sialophosphoprotein (DSPP), enamelin (ENAM), matrix extracellular phosphoglycoprotein (MEPE), and osteopontin (OPN) are glycophosphoproteins expressed in bones and/or teeth. Direct comparison of their amino acid sequences do not suggest that they belong to a single genetic family, but a detailed analysis of their chromosomal location and gene structure does. Analysis of human brain mRNA by RT-PCR has led to the discovery of two additional exons thereby making it more convincing that MEPE is a member of the SIBLING (Small Integrin-Binding LIgand, N-linked Glycoprotein) family. We propose that the members of this SIBLING family are extended, flexible proteins in solution that can facilitate the formation of a number of different complexes. For example, OPN can bridge complement Factor H to either an RGD-dependent integrin or to CD44 forming a membrane-bound complex that actively suppresses the alternate complement pathway. Two possible mechanisms for inhibiting the lytic pathway of alternate complement are presented.

Keywords Bone Sialoprotein, Complement, Integrin-Binding, Osteopontin, SIBLING.

INTRODUCTION

Studies of the extracellular matrices of bones and teeth have a long and rich history. Ages before written scientific literature it was noticed that bones treated with a weak acid such as vinegar changed into supple structures that looked and behaved much like the skin, tendons, ligaments, and other soft tissue elements. The application of first modern protein biochemistry methods and then more recently, molecular biological approaches, have led us to understand much of the biology and mechanical properties of the underlying collagen scaffolding that constitutes the vast majority of the matrix of bones and dentin. Indeed, the vast majority of the genetic diseases of bones and teeth whose mutations are known are mutations in the various members of the collagen family [1].

Still, the age-old question of why bones and teeth mineralize whereas the nearly identical skin, tendon, and ligaments do not remained unanswered and the quest to understand this intriguing process was undertaken by a number of laboratories around the world. Many of the most successful of these laboratories started about 30 years ago, during the ascendancy of the idea that one gene leads to one protein and that most biological functions can be satisfactorily explained by finding and describing the protein that performs such a function. In the 1960s and 1970s a number of laboratories around the world began the search for the holy grail of "the proteins" that nucleate and/or control the growth of hydroxyapatite crystals in calcified cartilage, bone, dentin, and enamel. Logically the candidate gene products would be acidic proteins, possibly phosphoproteins, with a strong affinity for hydroxyapatite. Most investigators thought that these proteins would likely (but not necessarily) be entrapped within the mineralizing matrix and therefore be released from the mature tissues by demineralization. Only a handful of proteins were found in relative abundance in the mineralized compartment of bones and teeth and these are now the proteins whose names (often based on the names used for the cDNA sequences) we read many times in the literature: osteocalcin (OCN), osteonectin (ON), osteopontin (OPN, also known as SPP1 and Eta1), bone sialoprotein (BSP), matrix gla protein (MGP), decorin (DCN), biglycan (BGN), dentin matrix protein 1 (DMP1), dentin sialophosphoprotein (DSPP), enamelin (ENAM), amelogenin (AMEL), and others.

At least in the case of bone, the mice with null mutations in the various candidate genes do not show abject failure of mineralization. Bones are larger or smaller, thinner or thicker, perfectly

Received 9 November 2002; revised 1 February 2003; accepted 7 February 2003.

Address correspondence to Dr. Larry Fisher, Room 228, Building 30, NIDCR-NIH, Bethesda, MD, 20892-4320, USA. E-mail: LFISHER@dir.nidcr.nih.gov

formed or somewhat distorted, but all single knockout mice have grossly functional, mineralized bones. While the usual descriptions of redundancy of genes have been offered to explain why the proteins of such logical promise have disappointed us within the context of mineralization, these results also set us free to discover other functions for these curious proteins. In this paper, we argue that five of these proteins, BSP [2], DMP1 [3], DSPP [4], MEPE (matrix extracellular phosphoglycoprotein [5], also known in the rat as OF45 and osteoregulin [6], and OPN [7] are likely members of a family of proteins we have called SIBLING for Small Integrin-Binding LIgand, N-linked Glycoprotein. A sixth protein, ENAM [8], may be a more distant member of the family. Earlier work had suggested that at least four and possibly five of these genes were members of this family [9]. While we argue that at least three of the SIBLINGs do function in complement, the SIBLING name includes only biochemical descriptions and not higher biological functions because the ultimate functions of all the members of the family are not known at this time.

RESULTS AND DISCUSSION

The most common method of defining the relationship among a group of proteins is to compare their linear amino acid sequences. For the six proteins currently proposed to be in the SIBLING family, this approach does not yield satisfying results. Figure 1 illustrates this point by showing the comparison of three random pairing of members of the family using the "Compare" program of the GCG group (Accelrys Inc.). Two proteins with strong homologies will have a distinct diagonal line such as that seen for the comparison of two small proteoglycans, decorin and biglycan (Figure 1D). The comparisons of the various SIBLINGs show no such strong diagonal lines implying poor homologies at the amino acid level. Indeed, the results are probably no better than one would expect from a comparison of any two random protein sequences. There are a few short regions that are conserved among members of the family including the completely conserved integrin-binding tripeptide, RGD, and NXS/T motif for N-linked oligosaccharides as well as a number of casein kinase II-type phosphorylation sites.

Directly comparing the locations of these short sequences within the primary protein sequences in their entirety, however, does little to make a case for significant homology among the different proteins. The overall chemical properties of these proteins also seem to suggest that they are not related. For example BSP, DMP1, DSPP, and OPN are all acidic with predicted isoelectric points of 3.4 to 4.3 (without post-translational modifications) whereas ENAM is neutral and MEPE strongly basic (pI = 9.2). Even within the acid members, BSP is glutamic acid-rich and others are either aspartic acid-rich or a mix of the two. However, several important points of similarity within the genetic structures of these 6 proteins permit us to propose that they are all a result of an ancient gene duplication and subsequent divergence.

Five of the six genes are located within a contiguous region of chromosome 4q21.3 (Figure 2). The Human Genome Project has not completed this portion of chromosome 4 so the exact distances between the genes are not known, but currently five are thought to be within an estimated 750,000 base pair segment and four of those within a single 250,000 bp domain. The reader should be cautioned, however, that this region of chromosome 4 is based on incomplete sequences and the final orientations and locations of the gene will not be completely known until all the sequencing is complete. It is clear that the most similar five SIBLINGs are very closely spaced and this makes for a significant problem in producing double knockout mice. The typical method of producing double knockout mice by cross-breeding single KO mice cannot easily be done. The genotypes of hundreds to thousands of offspring of the breeding pairs would have to be checked to hope to detect a single cross-over event between genes as closely spaced as the SIBLING genes. Notice that MEPE, probably the most different member of the family, is located in the center of this close cluster of genes.

As of the writing of this report (2001), there is only one know gene between the DSPP and OPN (usually listed as SPP1 for secreted phosphoprotein 1 within the Human Genome Project) except the other SIBLINGs. The ABCG2 (for ATP-Binding Cassette Transporter, subfamily G, member 2, also known as Breast Cancer/Mitoxantrone Resistance Protein (BCRP/MXR) [10] gene was until recently mapped to a position outside the SIBLING cluster but the most recent build has it between OPN and MEPE. ABCG2 is structurally unrelated to the integrin-binding proteins but curiously is upregulated in placenta and many tumors, much like BSP and OPN [10–12]. The gene for enamelin, ENAM, also is on human chromosome 4 and is currently being assigned a position much closer to the centromere, ~4q13, but it is possible that this location will be refined at a later date.

A clustering of genes within a single chromosome alone, of course, is not justification for defining a family of gene products. The next evidence for the grouping of the proteins is the similarity of their intron-exon boundaries and the biochemical similarities of their corresponding exons. First, we report on our recent findings of additional exons for human MEPE gene. We performed PCR on reverse-transcribed mRNA cDNA from human brain (Invitrogen, Human Tissue Panel #1) using an oligonucleotide pair derived from the beginning and end of the coding region as defined by the original description of the MEPE mRNA [5]. The oligonucleotide pair incorporated restriction enzyme sites for subcloning into an adenovirus shuttle vector. After gel purification of the band of the approximate expected size, the PCR products were subcloned into the vector and 30 cDNA clones purified. Nine of the clones were identical to the original sequence previously described by Rowe et al. [5].

A standard BLAST analysis of this sequence against the human genome database identified three exons within the sequenced genome and a short section of 54 basepairs that have not yet been identified in the project but is very likely to represent a single exon, exon 3, rather than two or more exons. The other clones all had longer sequences within them that when compared with the human genomic sequences, were found to represent two additional exons, 4 and 5. Exon 4 was homologous

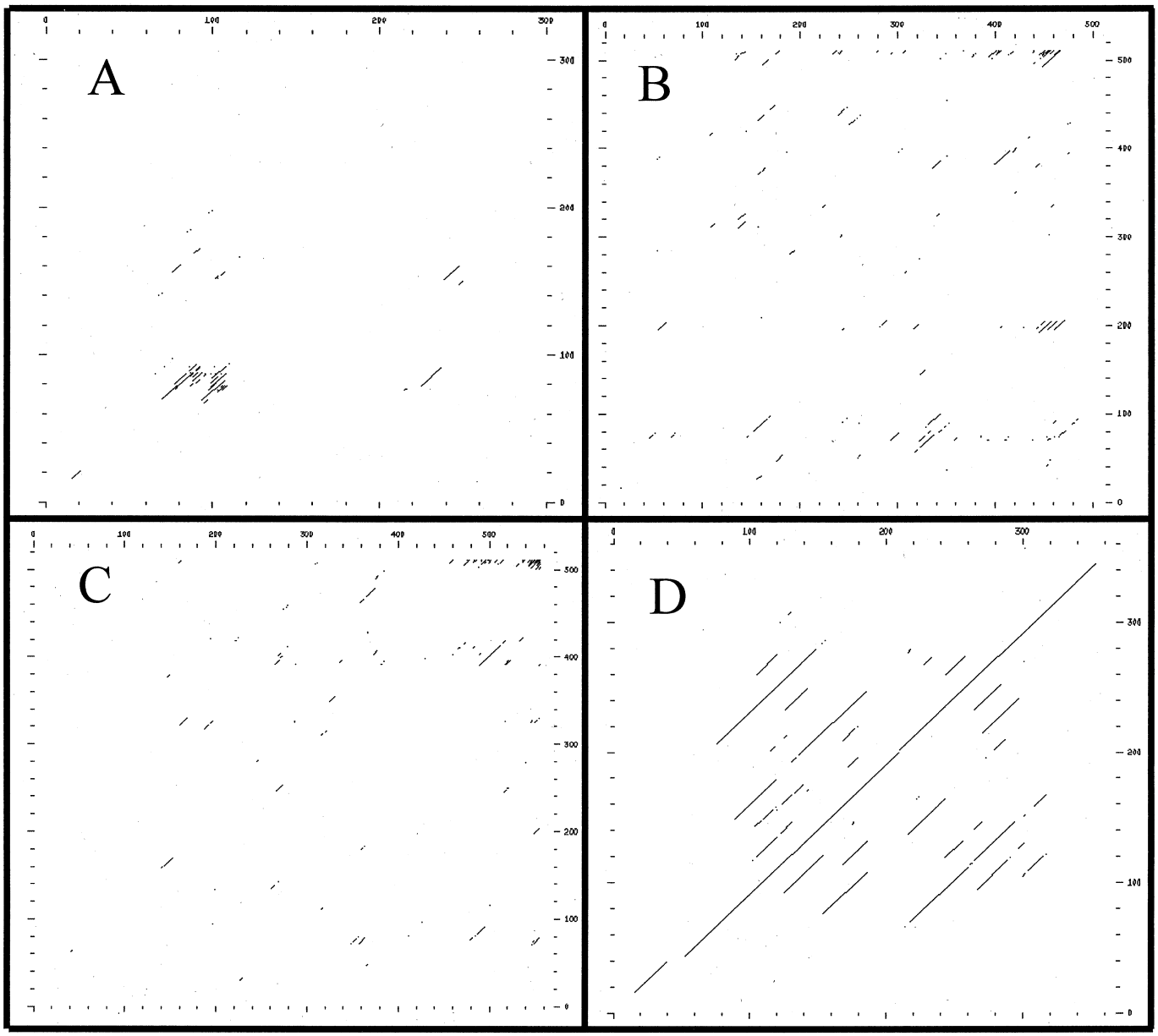

Figure 1. Graphical comparisons of paired human protein sequences using the "Compare" program of the Genetics Computer Group. (A) OPN vs. BSP; (B) MEPE vs. DSPP (with only two copies of the carboxyterminal phosphorylation repeats); (C) DMP1 vs. MEPE; and (D) Biglycan vs. Decorin. Protein pairs showing strong homology have the clear mid-panel diagonal line like that seen in the comparison of two closely related proteins, Biglycan and Decorin (panel D). Short lines off the mid-panel diagonal result from internal repeats that are shared. Notice that the SIBLING comparisons have no mid-panel diagonal lines and only short homologies throughout their lengths. This illustrates that the SIBLINGs are not very homologous at the primary sequence level.

to the extra sequences observed for monkey brain MEPE in GenBank accession number AB046056 (Osada, N et al., GenBank accession number AB046056, otherwise unpublished). Exon 5 is unique with respect to known MEPE sequences and may itself have some interesting splice variations that are currently being clarified (Fisher et al., unpublished). We have found cDNAs corresponding to mRNA containing exons 4 and 5 together as well as exon 5 alone (Figure 3). We have not yet seen the cDNA corresponding to exon 4 alone like that seen for the monkey, but additional work is being done.

Figure 3 shows the intron-exon structure of the six SIBLING family members. In each case, the full length human mRNA-derived cDNA sequence was compared with the Human Genome Project (www.ncbi.nlm.nih.gov/genome/seq/HsBlast.html) and the exons deciphered from the matches using standard intron donor/acceptor sites. Exon 1 is always a noncoding exon. ENAM is the only member that has a second noncoding exon. The next exon, exon 2 for most members, always contains the start codon, the leader sequence, and the codons for the first two amino acids of the mature proteins. The leader sequence encodes the series of

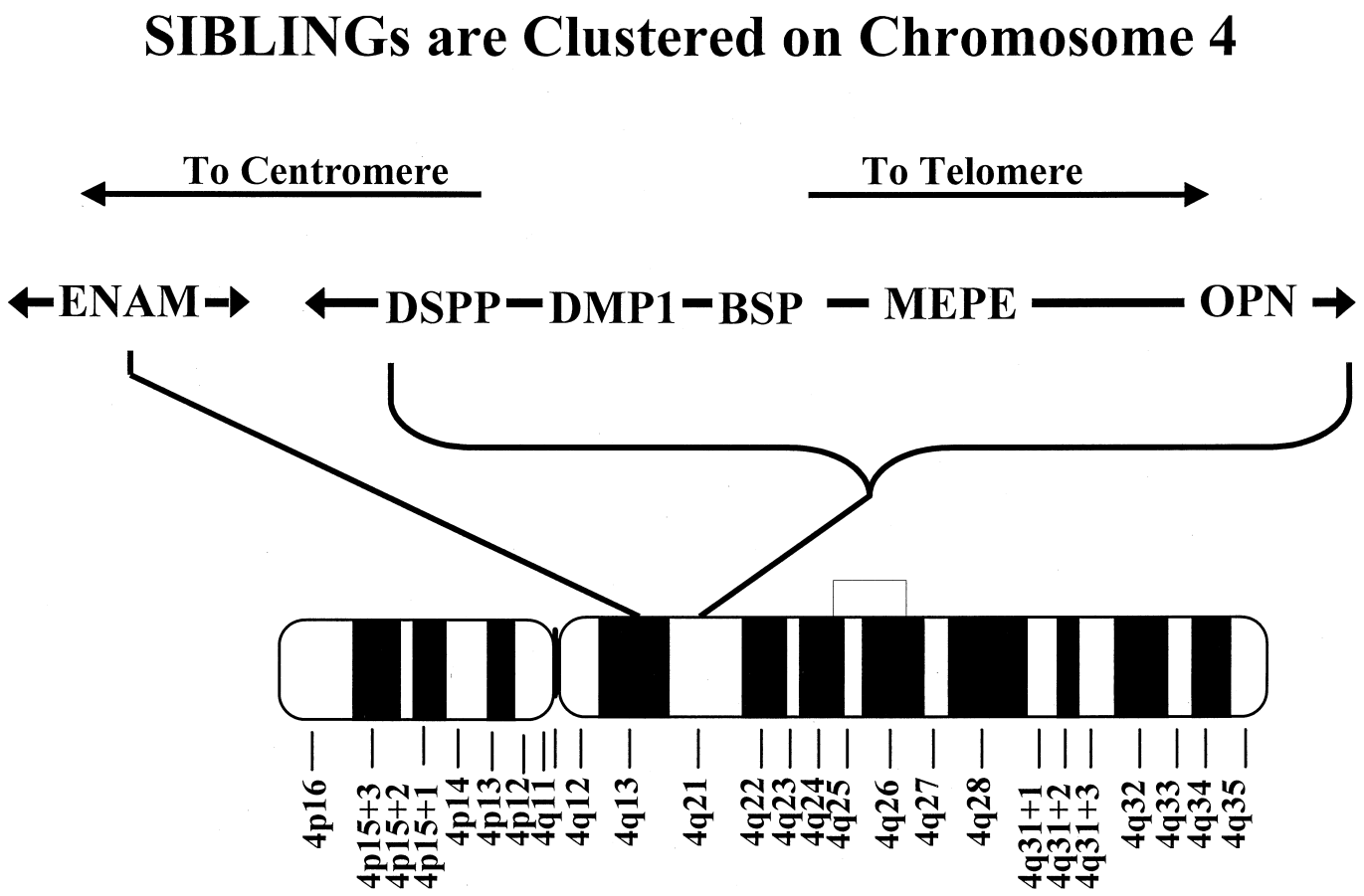

Figure 2. Five SIBLING genes cluster closely together on human chromosome 4 and a sixth candidate gene, ENAM, is located nearer the centromere. DSPP, DMP1, BSP, MEPE, and OPN are located at 4q21.3, within a region of about 750,000 basepairs. ENAM is currently assigned a position of 4q13. These locations are based on the current build (number 26) of the Human Genome Project. The sequencing of this portion of chromosome 4 is incomplete at this time, however, and the final positions may change to some small degree.

hydrophobic amino acids that directs the protein synthesis into the rough endoplasmic reticulum for post-translational modification and subsequent secretion out of the cell. Enamelin's exon 3 does not contain a classical leader sequence and may not be processed and secreted in the same way. Intron 2 and all other introns in the family interrupt the coding sequences between codons (type 0). This implies that any exon can be spliced in or out of the mRNA and not cause a frame shift. Exon 3 usually contains a casein kinase II phosphorylation site (SSEE) and exon 4 is usually relatively proline-rich (PPPP). Exon 5 usually contains another casein kinase II phosphorylation site and, like all the first four exons, is a small exon. The last one or two exons encode the vast majority of the protein (Figure 3 is not drawn to scale) and always contain the integrin-binding tripeptide, RGD. Again ENAM is more distantly related as only the human sequence encodes for the RGD. Pig [13] and mouse [14] do not contain the RGD within their reported sequences.

The exons used in the splice variants are generally conserved. As shown as gray boxes in Figure 3, splice variants missing exon 4 have been reported in OPN [15] and MEPE [5 and this Article). Splice variants missing exon 5 has been shown for OPN [15, 16], DMP1 [3] and MEPE [5 and this article]. To date, there has been no direct proof that the splice variants differ in function.

Two of the SIBLINGs, BSP and OPN, have had their structures solved by NMR. Both were found to be entirely flexible in solution [9]. Flexibility is a common property found in proteins or domains of proteins that have a number of different binding partners. Once bound to their multiple partners, the proteins often have a single conformation. For example, in isolation the protein L39e from the large subunit of ribosomes is completely flexible in solution, but its structure is well defined within the assembled ribosome and can be observed in X-ray diffraction [17]. Other ribosomal proteins (L2, L3, L4, etc.) have large domains that are completely unstructured in solution but also have single fixed structures in the assembled ribosome. None of the closely clustered five SIBLINGs has more than one cysteine within their mature sequences, so there is no chance of forming intramolecular disulfide bonds, but again ENAM is a likely exception. In contrast, most of the structured secreted proteins such as osteonectin, osteocalcin, decorin, biglycan etc. have disulfide bonds to help stabilize their three dimensional shapes in the extracellular environment. Furthermore, while the general

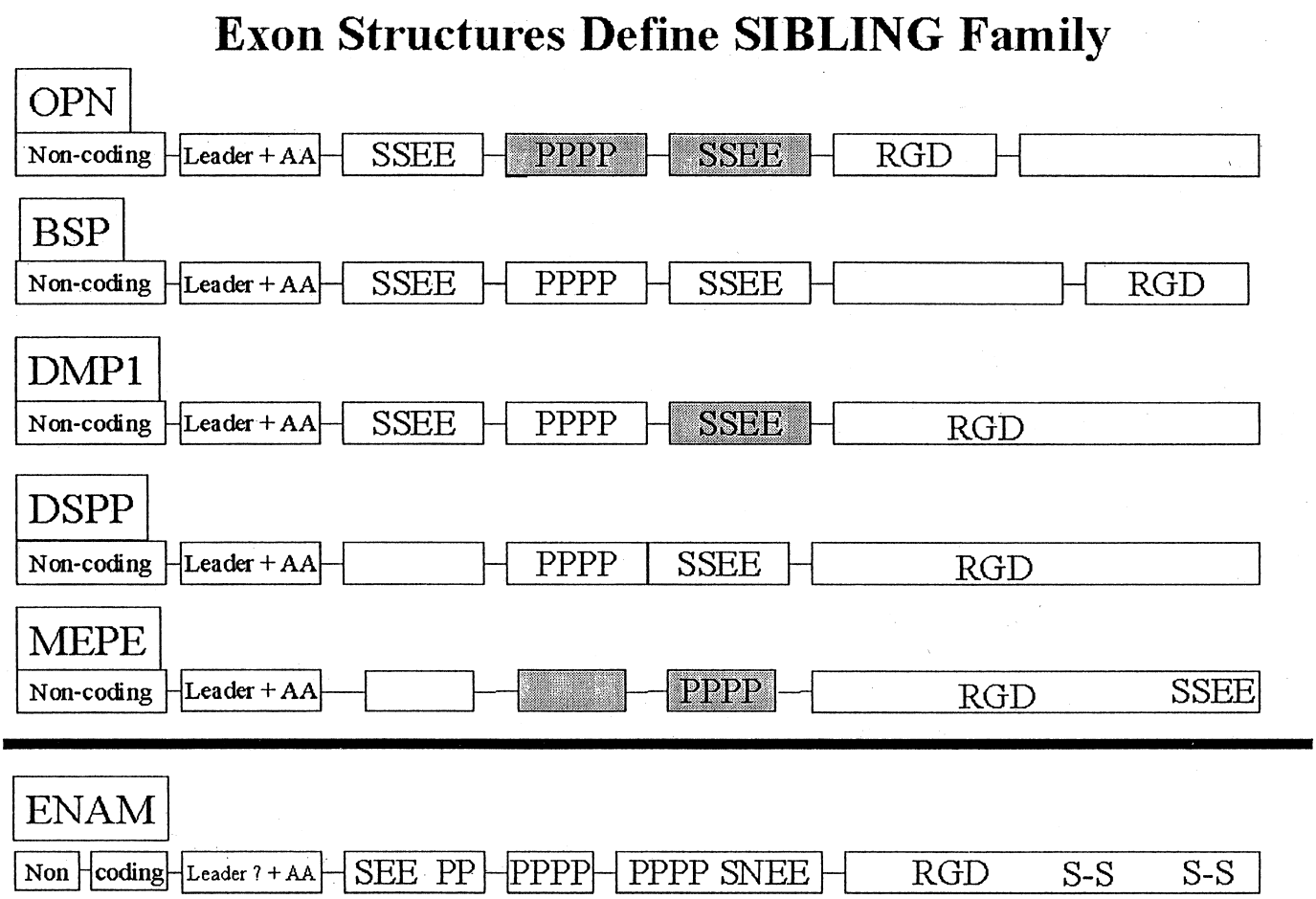

Figure 3. Exon structure defines the SIBLING family. The exon structures of the six candidate genes for the SIBLING family are illustrated. Exons are drawn as boxes and introns as connecting lines. Exon 1 is noncoding. For all but ENAM, exon 2 encodes for the leader sequence plus the first two amino acids of the mature protein. Exon 3 often contains the consensus sequences for casein kinase II phosphorylation (SSEE), as does exon 5. Exon 4 is usually relatively proline rich (PPPP). The last one or two exons encode the vast majority of the protein (figure not drawn to scale) and always contain the integrin-binding tripeptide ArgGlyAsp (RGD). The shadowing of exons illustrates those exons known to be involved in splice variants. ENAM is a more distantly related gene that has two noncoding 5′ and is also likely to contain disulfide bonds (S-S) that the other SIBLINGs do not.

chemical properties of the amino acids along each SIBLING's length are conserved across the animal species (hydrophilic and either acidic or basic, etc.), there is a great deal of divergence within each protein.

All the amino acid sequences of the SIBLINGs are only 55–73% identical between mouse and human while other noncollagenous proteins that are thought to have stable structures in solution are more highly conserved (for example, osteonectin, 96% [18]; biglycan, 91% [19, 20]; and matrix gla protein, 84% [21, 22]. It seems reasonable that proteins that encode for small conserved contact points for a number of binding partners spaced throughout their lengths could have many other regions that can mutate to other amino acids as long as they maintain their hydrophilicity and flexibility in solution. A corollary to this hypothesis is that the short stretches of amino acids that are conserved across species are likely to be directly or indirectly involved in binding other proteins. The tripeptide RGD is one example of the conservation of a short series of amino acids that is involved in binding to other protein complexes, the subfamily of integrins.

Other known binding partners of most of the acidic SIBLINGs include complement Factor H (BSP, DMP1, and OPN) and CD44 (DMP1 and OPN). A short summary of the alternate pathway of complement may be helpful at this point (Figure 4) [23]. The alternate complement pathway (ACP) is one of the most ancient of immune responses, predating the better known pathways that involve specific antibodies. The ACP involves about 20 different proteins and together they constitute approximately 5% of the serum proteins by weight. The proteins in the blood, although found in high concentration, are in conformations that do not favor interactions until an activation cascade is triggered. Briefly, the triggering event is when one component, C3 (found at ~1 mg/ml in the serum), undergoes a spontaneous rearrangement and exposes a highly reactive chemical group. If, within a few milliseconds, this activated C3 can come into contact with a free OH or NH group on a carbohydrate or

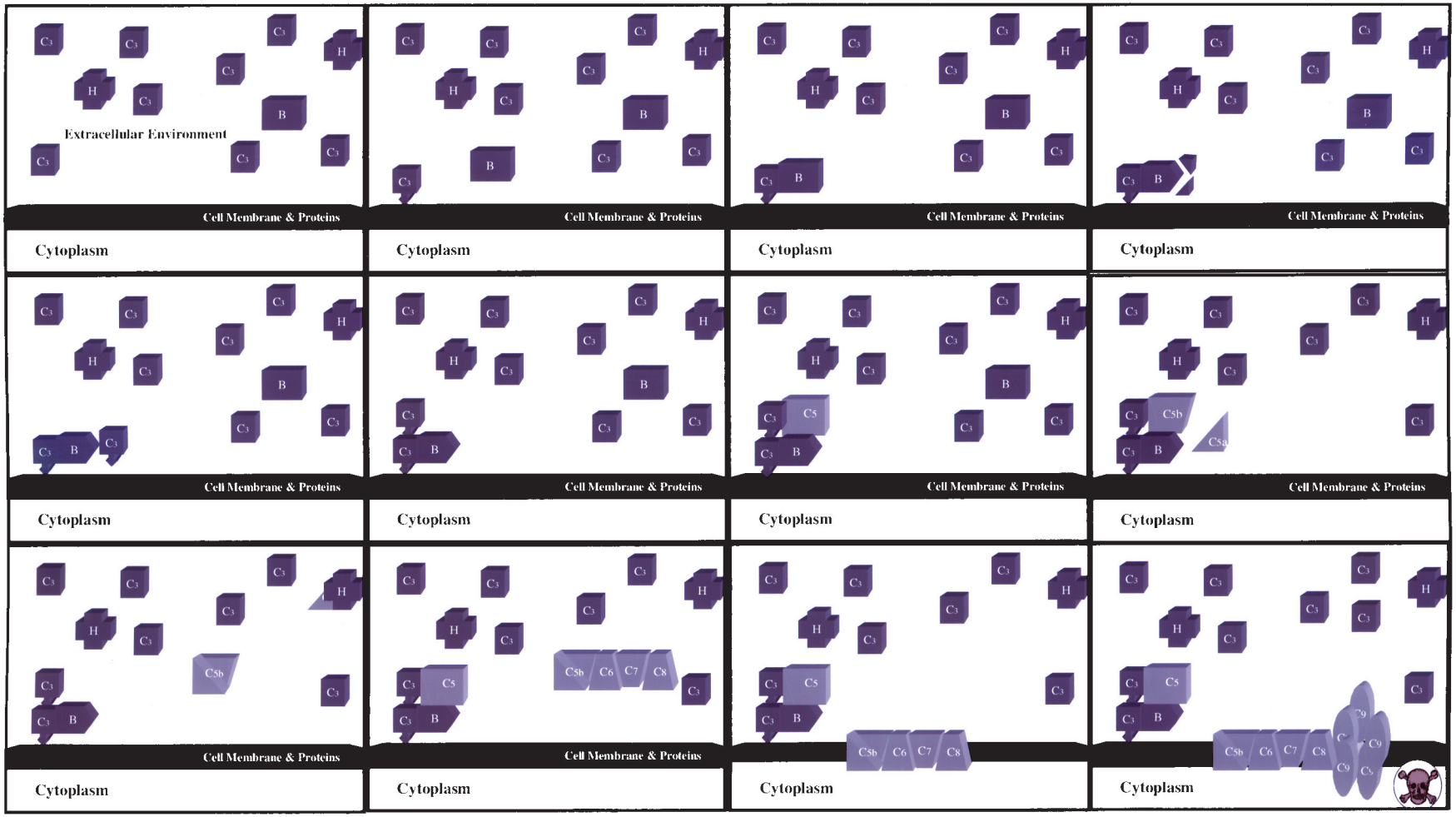

Figure 4. A cartoon description of the basic steps in the lytic process for the alternate complement pathway. See text for a brief description of the process.

protein, then the C3 will form a covalent bond with that molecule. The design is that this reactive carbohydrate or protein be on the surface of an invading bacterium or parasite, but in fact the reaction can and does occur on the surface of all cells. Furthermore, although the C3 spontaneous activation is rare, the number of C3 proteins is sufficiently high that a typical invading bacterium is likely to be bound by one or more C3 molecules within a few minutes. The bound C3 protein is in a conformation that permits the binding of the next complement protein, Factor B. Factor B itself undergoes a conformational change upon binding, and becomes a substrate for serum protease (Factor D). The digested Factor B, now designated Bb, is an activated protease that can bind C3 and cleave it into two pieces, C3b and C3a. (The C3a diffuses away and is a potent chemoattractant for various immune cells.)

The formation of the C3b exposes the chemically reactive group and, due to its proximity to the cell surface, often binds to the same cell. Because the bound C3b (and its various breakdown products) is a ligand for certain receptors on immune cells, this opsonization process can itself lead to the destruction of the labeled cell. However, a second process also occurs. Occasionally the activated C3b molecule forms the covalent bond not with the cells surface but on the C3Bb complex itself. When this happens, another complement protein, C5, can be bound into the complex and is cleaved by the Bb protease into two pieces, C5a and C5b. (The smaller C5a diffuses away and is another very potent immune activating molecule.) The C5b protein is released and now can bind C6. The induced conformation of C6 then binds C7, which then binds C8. Together the C5bC6C7C8 complex inserts into a cellular membrane and then binds a series of C9 proteins from the serum. As the number of C9 proteins increase, a pore forms in the membrane, killing the cell by depolarizing the cell and permitting an exchange of diffusible elements between the inside and outside of the cell. This is called the lytic pathway of the alternate complement process.

Most normal, healthy mammalian cells survive the continuous attack by this pathway by three mechanisms. Many cells can produce two different membrane-associated proteins that can disrupt this lytic pathway of the ACP. Decay accelerating factor (DAF, CD55) has a higher affinity for C3b than does Bb so it can displace the protease and stop the cascade. Another protein, membrane co-factor protein (MCP, CD46), can bind to complement Factor I. This binding causes a conformational change in Factor I and thereby enhances its proteolytic function. The MCP/Factor I complex can then digest the C3b and destroy its ability to promote the lytic cascade. A third mechanism involves a complement protein found at ~0.5 mg/ml in the serum, Factor H. By itself in the blood, Factor H has a real but weak affinity for C3b and can display weak DAF-like activity. Factor H also has a low affinity for Factor I and thereby can act as a poor but measurable cofactor for Factor I and display MCP-like activity. But in both cases, Factor H can itself bind to proteins or carbohydrate groups, undergo a conformational change, and acquire a higher affinity for C3b and/or Factor I. We have shown previously that at least three of the SIBLINGs have the ability to bind Factor H and confer protective activity on cells (BBRC, IADR abstract and submitted).

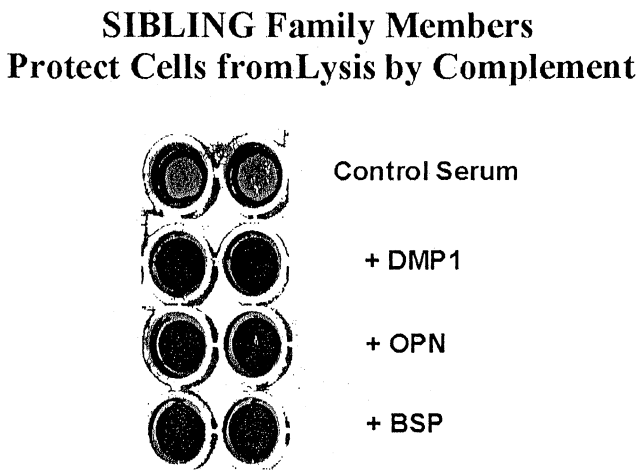

Figure 5. SIBLING family members protect cells from lysis by the alternate complement pathway. Murine erythroleukemia cells in microtiter plate wells are lysed by complement in human serum (control serum). Lysed cells cannot process the clear MTT reagent into the dark blue color and the wells remain clear. Pretreating the cells with DMP1, OPN, or BSP prior to the addition of the human serum protects these cells from the lytic pathway. The living cells process the MTT to the dark color that is seen in each of the SIBLING-treated wells.

When mouse erythroleukemia (MEL) cells are treated with dilute human serum, the cells are lysed by the ACP resulting in cells that cannot metabolize the colorless thiazolyl blue (MTT) to the characteristic blue color (Figure 5). Similar results can be

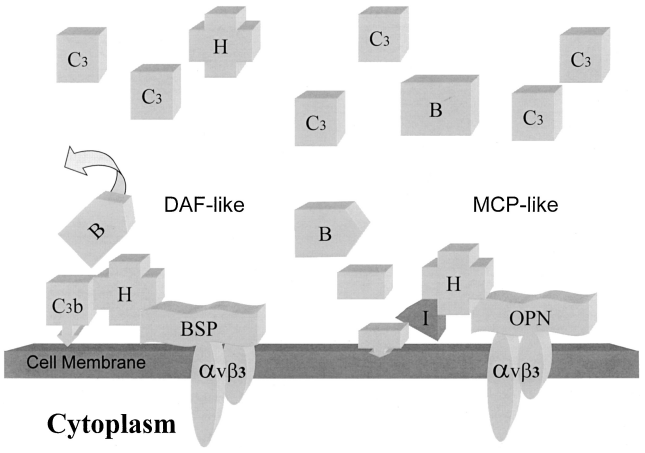

Figure 6. Two possible mechanisms for SIBLINGs to protect cells from alternate complement pathway. BSP, OPN, or DMP1 binds first to an integrin through its RGD domain (or CD44 for OPN and DMP1 but not BSP) and then bind complement Factor H. The Factor H then undergoes a conformational change and either has a higher affinity for C3b than does Bb and displaces the protease (DAF-like activity) or has a higher affinity for Factor I that then can degrade the C3b (MCP-like activity). Interestingly, if the SIBLING binds to Factor H before it encounters a cell surface receptor, the SIBLING cannot bind to the receptor and the activity is not acquired. This limits this biological activity to short distances from the site of the secretion of the SIBLING.

seen by using human cells with guinea pig serum as the source of active complement. When we treat the cells with BSP, DMP1, or OPN, and then expose them to the complement in human serum, the cells are not lysed. These three acid SIBLINGs are stopping the lytic pathway of the ACP. Blocking the ability of the SIBLINGs to bind to their cells surface receptors by mutating the RGD to KAE, using antibodies that block the receptors etc., negates the protective ability of the three SIBLINGs [9, 24, and submitted]. This shows that the protective properties of BSP, OPN, and DMP1 all work in conjunction with a cell surface receptor. Furthermore, because we have clearly shown that these proteins form a strong 1:1 complex with complement Factor H, it is reasonable to speculate that the protection provided by the three SIBLINGs is due to a simultaneous complex of Factor H, SIBLING, and cell surface receptors. We have hypothesized that these complexes likely mimic either DAF (displacing the protease, Bb, from the complex) or MCP (acting as a cofactor for Factor I) as drawn in Figure 6. Future studies will determine which of these pathways is the correct model.

CONCLUSION

There are clearly five members of the SIBLING family that cluster together on human chromosome 4, chromosome 5 in the mouse. All these are charged, possibly flexible proteins that may contain little or no secondary structure when isolated in solution but are likely to have structure induced when they interact with one or more of their binding partners. Binding partners for various members of the SIBLING family include cell surface proteins for all of them (integrins, CD44, etc.), Factor H for at least three of them, hydroxyapatite for the acid members, and likely other proteins in the future. ENAM is a more distantly related protein whose gene is found more centrally on the same chromosome and that is likely to contain secondary and tertiary structure.

REFERENCES

[1] Myllyharju, J., and Kivirikko, K.I. (2001). Collagens and collagen-related diseases. *Ann. Med.* 33:7–21.

[2] Fisher, L.W., McBride, O.W., Termine, J.D., and Young, M.F. (1990). Human bone sialoprotein: Deduced protein sequence and chromosomal localization. *J. Biol. Chem.* 265:2347–2351.

[3] Hirst, K.L., Simmons, D., Feng, J., Aplin, H., Dixon, M.J., and MacDougall, M. (1997). Elucidation of the sequence and the genomic organization of the human dentin matrix acidic phosphoprotein 1 (DMP1) gene: Exclusion of the locus from a causative role in the pathogenesis of dentinogenesis imperfecta type II. *Genomics* 42:38–45.

[4] Gu, K., Chang, S.R., Slaven, M.S., Clarkson, B.H., Rutherford, R.B. and Ritchie, H.H. (1997). Human dentin phosphophoryn nucleotide and amino acid sequence. *Eur. J. Oral Sci.* 106:1043–1047.

[5] Rowe, P.S., de Zoysa, P.A., Dong, R., Wang, H.R., White, K.E., Econs, M.J., and Oudet, C.L. (2000). MEPE, a new gene expressed in bone marrow and tumors causing osteomalacia. *Genomics* 67, 54–68.

[6] Petersen, D.N., Tkalcevic, G.T., Mansolf, A.L., Rivera-Gonzalez, R., and Brown, T.A. (2000). Identification of osteoblast/osteocyte factor 45 (OF45), a bone-specific cDNA encoding an RGD-containing protein that is highly expressed in osteoblasts and osteocytes. *J. Biol. Chem.* 17:36172–36180.

[7] Kiefer, M.C., Bauer, D.M., and Barr, P.J. (1989). The cDNA and derived amino acid sequence for human osteopontin. *Nucleic Acids Res.* 17:3306.

[8] Hu, C.C., Hart, T.C., Dupont, B.R., Chen, J.J., Sun, X., Qian, Q., Zhang, C.H., Jiang, H., Mattern, V.L., Wright, J.T., and Simmer, J.P. (2000). Cloning human enamelin cDNA, chromosomal localization, and analysis of expression during tooth development. *J. Dent. Res.* 79:912–919.

[9] Fisher, L.W., Torchia, D.A., Fohr, B., Young, M.F., and Fedarko, N.S. (2001). Flexible structures of SIBLING proteins, bone sialoprotein, and osteopontin. *Biochem. Biophys. Res. Comm.* 280:460–465.

[10] Allikmets, R., Schriml, L.M., Hutchinson, A., Romano-Spica, V., and Dean, M. (1998). A human placenta-specific ATP-binding cassette gene (ABCP) on chromosome 4q22 that is involved in multidrug resistance. *Cancer Res.* 58:5337–5339.

[11] Bianco, P., Fisher, L.W., Young, M.F., Termine, J.D., and Robey, P.G. (1991). Expression of bone sialoprotein (BSP) in developing human tissues. *Calcif. Tiss. Int.* 49:421–426.

[12] Bellahcene, A., and Castronovo, V. (1997). Expression of bone matrix proteins in human breast cancer: Potential roles in microcalcification formation and in the genesis of bone metastases. *Bull. Cancer* 84:17–24.

[13] Fukae, M., Tanabe, T., Murakami, C., Dohi, N., Uchida, T., and Shimizu, M. (1996). Primary structure of the porcine 89-kDa enamelin. *Adv. Dent. Res.* 10:111–118.

[14] Hu, C.-C., Simmer, J.P., Bartlett, J.D., Nanci, A., Qian, Q., Zhang, C., Ryu, O.H., Xue, J., Fukae, M., Uchida, T., and McDougall, M. (1998). Murine enamelin: cDNA and derived protein sequences *Connect. Tiss. Res.* 39:47–61.

[15] Saitoh, Y., Kuratsu, J., Takeshima, H., Yamamoto, S., and Ushio, Y. (1995). Expression of osteopontin in human glioma. Its correlation with the malignancy. *Lab. Invest.* 72:55–63.

[16] Young, M.F., Kerr, J.M., Termine, J.D., Wewer, U.M., Wang, M.G., McBride, O.W., and Fisher, L.W. (1990). cDNA cloning, mRNA distribution and heterogeneity, chromosomal location, and RFLP analysis of human osteopontin (OPN). *Genomics.* 7:491–502.

[17] Ban, N., Nissen, P., Hansen, J., Moore, P.B., and Steitz, T.A. (2000). The complete atomic structure of the large ribosomal subunit at 2.4 A resolution. *Science* 289:905–920.

[18] Lankat-Buttgereit, B., Mann, K., Deutzmann, R., Timpl, R., and Krieg, T. (1988). Cloning and complete amino acid sequences of human and murine basement membrane protein BM-40 (SPARC, osteonectin). *FEBS Lett.* 236:352–356.

[19] Rau, W., Just, W., Vetter, U., and Vogel, W. (1994). A dinucleotide repeat in the mouse biglycan gene (EST) on the X chromosome. *Mamm. Genome* 5:395–396.

[20] Fisher, L.W., Termine, J.D., and Young, M.F. (1989). Deduced protein sequence of bone small proteoglycan I (biglycan) shows homology with proteoglycan II (decorin) and several nonconnective tissue proteins in a variety of species. *J. Biol. Chem.* 264:4571–4576.

[21] Ikeda, T., Yamaguchi, A., Icho, T., Tsuchida, N., and Yoshiki, S. (1991). cDNA and deduced amino acid sequence of mouse matrix gla protein: One of five glutamic acid residues potentially modified to gla is not conserved in the mouse sequence. *J. Bone Miner. Res.* 6:1013–1017.

[22] Cancela, L., Hsieh, C.L., Francke, U., and Price, P.A. (1990). Molecular structure, chromosome assignment, and promoter organization of the human matrix Gla protein gene. *J. Biol. Chem.* 265:15040–15048.

[23] Rother, K., Till, G.O., and Hansch, G.M. (1998). The Complement System New York: Springer.

[24] Fedarko, N.S., Fohr, B., and Fisher, L.W. (2000). DMP1 inactivates complement by bridging Factor H to cell surface receptors. *J. Dent. Res.* 79:339.

Three small integrin binding ligand N-linked glycoproteins (SIBLINGs) bind and activate specific matrix metalloproteinases[1]

NEAL S. FEDARKO,*,†,[2] ALKA JAIN,* ABDULLAH KARADAG,† AND LARRY W. FISHER†

*Division of Geriatrics, Department of Medicine, Johns Hopkins University School of Medicine, Baltimore, Maryland, USA; and †Craniofacial and Skeletal Diseases Branch, National Institutes of Dental and Craniofacial Research, National Institutes of Health, Bethesda, Maryland, USA

SPECIFIC AIMS

Objectives were to identify proteins that co-purified with members of the small integrin-binding ligand N-linked glycoprotein (SIBLING) gene family and characterize structural and functional consequences of their binding interactions.

PRINCIPAL FINDINGS

1. Specific MMPs co-purify with SIBLINGs

Individual SIBLING family members BSP, OPN and DMP1 were subcloned into an adenovirus system and expressed in human bone marrow stromal cells. Each SIBLING was purified from the serum-free media to ≥95% purity by anion exchange chromatography under nondenaturing conditions. When purity was assessed by zymography, each HPLC purified SIBLING exhibited a single band of proteolytic activity. Bands originally visible on the zymogram did not appear in gels treated with 1,10-phenanthroline, showing that co-purifying proteolytic activity arose from metalloproteinases. Identity of proteolytic bands was determined by Western blotting and probing with specific antibodies against MMPs. MMP-2 co-purified with BSP, MMP-3 with OPN and MMP-9 with DMP1.

Specificity observed was confirmed by showing that purified SIBLINGs could be used to affinity purify their respective MMPs from conditioned media containing several different MMPs. When aliquots of eluted fractions were analyzed by zymography, positive bands for multiple MMPs were visible in the flow through peak. Fractions that eluted at ~0.3 M salt were analyzed by Western blot and immunoreactive MMP-2 (from the BSP affinity column) and immunoreactive MMP-3 (from the OPN affinity column) were identified. A DMP1 affinity column was not made due to insufficient amounts of highly purified DMP1.

2. SIBLING and MMP binding specificity

Co-purification from similar media of a single but different MMP with each SIBLING demonstrated that specific interactions were occurring between the proteins. Binding interactions between recombinant MMP-2, MMP-3 and MMP-9 and purified recombinant SIBLINGs were investigated. Relative abundance of tryptophan residues in the MMPs was exploited by carrying out intrinsic fluorescence studies of purified, authentic MMP protein binding to SIBLINGs. Titration of proMMP-2 with BSP yielded a quenching of the MMP's tryptophan emission spectra and a saturable binding curve. Addition of OPN to proMMP-3 and DMP1 to proMMP-9 also yielded fluorescent signal quenching and saturable binding functions. Stoichiometry of binding between SIBLINGs and their respective proMMPs was 1:1. Scatchard analysis indicated binding constants in the nM range. Quenching of the tryptophan fluorescent signal is consistent with a gross conformational change as a result of binding. Fluorescent binding studies were also carried out using mixed pairs of SIBLINGs and pro- and active-MMPs. SIBLINGs and MMPs showed consistent specificity in their partnering, with BSP binding to pro- and active MMP-2, OPN with pro- and active MMP-3, and DMP1 with pro- and active-MMP-9. Other combinations of SIBLINGs and MMP's exhibited either no saturable binding or binding that was orders of magnitude weaker.

3. SIBLING-MMP complexes modify the protease activity

Fluorescence spectroscopy observations suggesting that SIBLING binding induces conformational changes in their corresponding MMP partner led to an investigation of whether SIBLING binding affected MMP structure. Addition of SIBLING to pro-MMP did not appear to promote autocatalysis to the active form. An increased susceptibility of SIBLING-proMMP complexes to cleavage and activation by plasmin (a protease that is normally an inefficient activator) was seen and was

[1] To read the full text of this article, go to http://www.fasebj.org/cgi/doi/10.1096/fj.03-0966fje; doi: 10.1096/fj.03-0966fje

[2] Correspondence: Room 5B-79 JHAAC, 5501 Hopkins Bayview Circle, Baltimore, MD 21224, USA. E-mail: ndarko@jhmi.edu

0892-6638/04/0018-0734 © FASEB

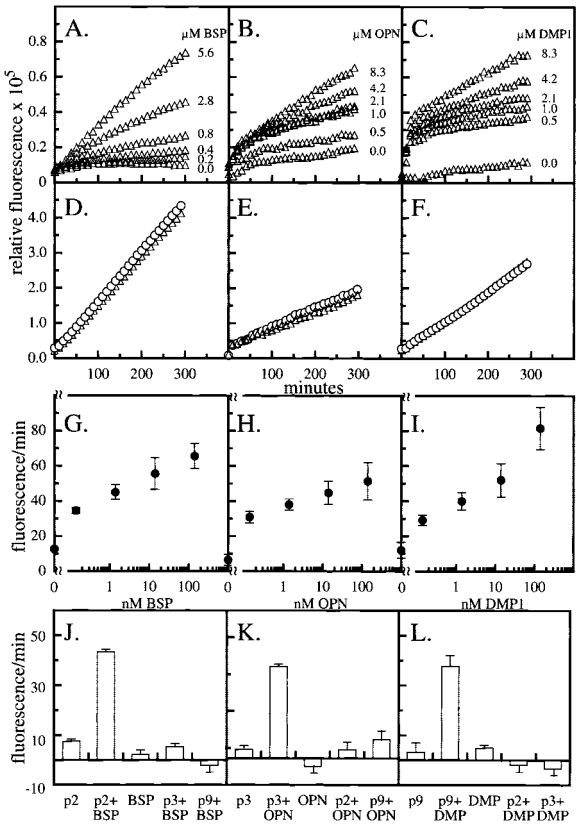

Figure 1. Modulation of MMP activity by SIBLINGs. Protease activity was followed by incubating fluorescent substrate with 1.4 nM proMMP-2 (*A*), proMMP-3 (*B*), and proMMP-9 (*C*) and increasing concentrations of BSP, OPN, or DMP1, respectively. Activity of equimolar concentrations (1.4 nM) of active MMP-2 ± BSP (*D*), MMP-3 ± OPN (*E*), and MMP-9 ± DMP1 (*F*) in the same assay showed no difference. The same assay was also employed to determine a low SIBLING concentration dose response in activity of proMMP-2 + BSP (*G*), proMMP-3 + OPN (*H*), and proMMP-9 + DMP1 (*I*). Activity of 1.4 nM BSP (*J*), OPN (*K*) and DMP1 (*L*) with correctly matched proMMPs and mismatched proMMPs as well as of proMMPs or SIBLINGs alone were analyzed by determining change in fluorescence/minute over the first 3 h of incubation. Values plotted represent the mean of three combined experiments ± SD.

consistent with SIBLING binding altering proMMP structure.

To measure potential biological effects, a fluorescent substrate assay was employed to screen SIBLING modulation of proMMP activity. Pro-MMP-2, -3, and -9 were reacted in combination with increasing concentrations of SIBLINGs (either BSP, OPN, or DMP1) and enzyme activity was measured by increased fluorescence signal. Increased proteolytic activity was observed for all three strong proMMP+SIBLING binding pairs (**Fig. 1*A–C***). When the strong binding SIBLING was added to its corresponding active MMP, enzymatic activity was not significantly changed indicating that binding of the SIBLING with its active MMP partner did not interfere with normal proteolytic activity (Fig. 1*D–F*). Properly matched SIBLING-proMMP pairs showed a dose-response increase in the rate of substrate digestion (Fig. 1*G, H, I*). Incubation of SIBLING alone with substrate was no different from pro-MMP alone or mismatched SIBLING MMP pairs, showing the increase in activity in the proMMP + SIBLING was not caused by any residual proteolytic activity that co-purified with the SIBLING (Fig. 1*J–L*). Given that there was no observed increase in the amount of propeptide-free enzyme in all of these SIBLING-proMMP pairs, it is reasonable to hypothesize that the increase in activity is due to a conformational change in the protease which allows its propeptide to be removed from the active site and thereby permit digestion of both small and large macromolecular substrates.

4. SIBLINGs restore activity to inhibited MMPs

Quenching of tryptophan fluorescence and increase in activity caused by SIBLING binding to proMMP is consistent with an alteration in the local structure near the active site. The effect of SIBLINGs on the ability of small molecular weight inhibitors to modulate MMP activity was investigated next. SIBLINGs were able to increase proMMP activity in the presence of specific small molecular weight inhibitors of MMPs, but not in the presence of 1,10 phenanthroline (which disrupts MMP activity by chelating and removing the active site required zinc ion). Active forms of MMPs also exhibited quenching of tryptophan fluorescence emission upon binding their specific SIBLING partner. The possibility that SIBLING binding also altered inhibitor interaction with active MMPs was investigated. Specific low molecular weight inhibitors were used to block active MMP activity. Addition of the corresponding SIBLING, however, rescued much of the original activity even in presence of equimolar amounts of specific inhibitor. As was the case for proMMPs, SIBLINGs were not able to restore activity to active MMPs treated with 1,10 phenanthroline. When the complex of equimolar active MMP + SIBLING was treated with increasing concentrations of the inhibitor, significant loss of activity was observed but only at substantially higher concentrations.

Because MMPs occur in vivo associated with inhibitors (tissue inhibitors of matrix metalloproteinases, TIMPs), the effect of SIBLINGs on the activity of MMP + TIMP complexes was also investigated. As expected, presence of TIMPs reduced the enzymatic activity of propeptide-free, active MMP. Addition of the correctly matched SIBLING to active MMP + TIMP complex caused a restoration of proteolytic activity. It is a reasonable hypothesis that conformational change in the active MMP upon binding its SIBLING partner lowers affinity of the TIMP (and low molecular weight inhibitors) for the active site of the MMP thereby enabling substrate access.

5. Reversal of SIBLING-induced activity by factor H

BSP, OPN and DMP1 have previously been shown to bind to factor H with high affinity, 10–100-fold higher than that just described for their partner MMPs. Gela-

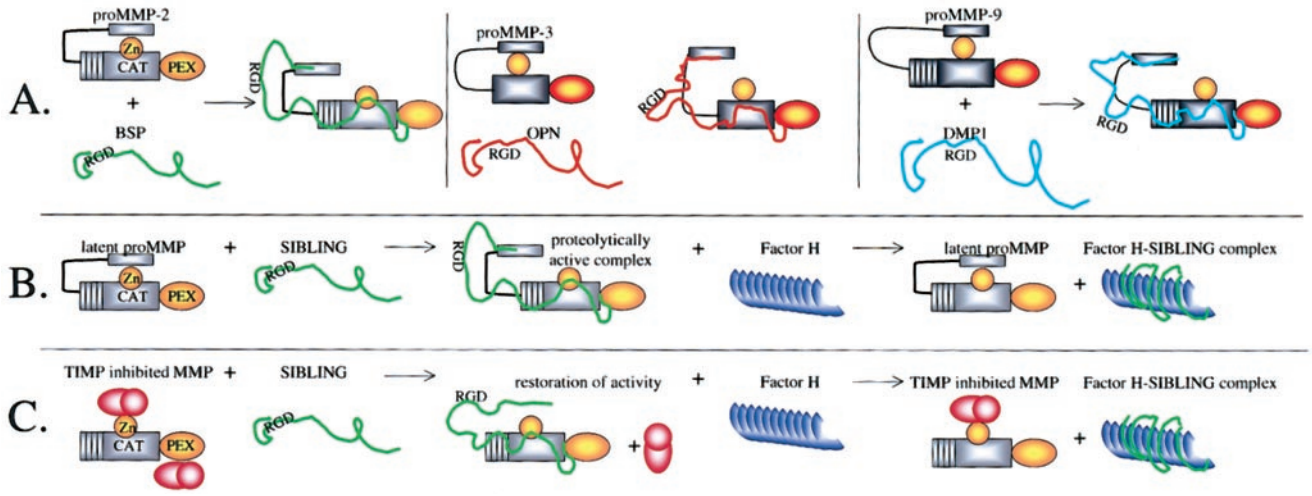

Figure 2. Schematic diagram of SIBLING-MMP interactions. *A)* Specificity of binding and activation was observed for BSP and proMMP-2, OPN and proMMP-3, and DMP1 and proMMP-9. *B)* SIBLING binding to a specific proMMP results in increased proteolytic activity in absence of propeptide cleavage. *C)* SIBLING binding to TIMP inhibited MMP leads to restoration of activity. In both cases, complement factor H, with its higher affinity for SIBLINGs may strip the SIBLING from the complex and proteolytic activity is lost.

tin and casein fluorescein conjugate assays were used to investigate whether factor H can compete with MMPs for SIBLING binding and thereby affect each SIBLING's interactions with its respective proMMP and active MMPs. TIMP-inhibited MMPs which had regained enzymatic activity by the addition of their corresponding SIBLING were treated with factor H and a significant reduction in the SIBLING-induced recovered activity for MMPs was observed. Higher affinity of factor H for SIBLING protein appears to promote removal of SIBLING from the SIBLING-MMP complex thereby permitting MMP to reverse its conformation and allow TIMP to again bind to the active site and re-inhibit the enzyme. The action of factor H on the SIBLING-mediated activation of proMMPs was also investigated. Addition of factor H caused the rate of substrate digestion by SIBLING-activated proMMP complex to decrease suggesting that removal of SIBLING from proMMP resulted in re-inactivation of catalytic activity by still-attached propeptide. These results support the hypothesis that propeptide is not removed in order to create enzymatic activity in proMMP-SIBLING pairs.

CONCLUSIONS AND SIGNIFICANCE

Results describe a novel, alternative method of MMP modulation (**Fig. 2**). SIBLING binding was associated with activation of latent pro-MMPs though this activation did not require cleavage of the propeptide. However, SIBLING binding did increase susceptibility of the propeptide to cleavage by plasmin. SIBLINGs and MMPs showed specificity in their partnering, with BSP binding to and "activating" proMMP-2, OPN with proMMP-3, and DMP1 with proMMP-9. Restoration of activity to TIMP-inhibited MMPs upon SIBLING binding demonstrates that even in presence of TIMPs, MMPs may be enzymatically active in regions of locally high concentrations of specific SIBLINGs.. The observation that complement factor H can compete with MMPs for SIBLINGs and successfully strip the SIBLING from the MMP complex suggests that activation of proMMP or reactivation of TIMP-inhibited MMPs by simple binding of their respective SIBLINGs will be limited to short distances from their sites of secretion due to abundance of factor H in the body.

SIBLING expression has been correlated with cancer progression and severity and it is interesting to consider that these proteins may be locally activating their corresponding proteases in vivo. From a clinical standpoint, SIBLINGs were found to restore activity to propeptide-free MMPs whose activity had been blocked by both natural and synthetic inhibitors. SIBLINGs are induced by neoplasms in vivo and their modulation of MMP activity might contribute to the relative lack of efficacy seen in recent clinical trials of MMP inhibitors in numerous cancers. FJ

Bone Sialoprotein, Matrix Metalloproteinase 2, and $\alpha_v\beta_3$ Integrin in Osteotropic Cancer Cell Invasion

Abdullah Karadag, Kalu U. E. Ogbureke, Neal S. Fedarko, Larry W. Fisher

Background: **Bone sialoprotein (BSP) interacts separately with both matrix metalloproteinase 2 (MMP-2) and integrin $\alpha_v\beta_3$ and is overexpressed in many metastatic tumors. Its role in tumor biology, however, remains unclear. We investigated whether BSP enhances cancer cell invasiveness by forming a trimolecular complex with MMP-2 and cell-surface integrin $\alpha_v\beta_3$. *Methods:* Invasiveness of breast, prostate, lung, and thyroid tumor cell lines was measured with a modified Boyden chamber assay. Binding and co-localization of BSP, MMP-2, and integrin $\alpha_v\beta_3$ were investigated with immunoprecipitation and *in situ* hybridization. All statistical tests were two-sided. *Results:* Treatment with BSP increased invasiveness of many breast, prostate, lung, and thyroid cancer cells through Matrigel in a dose-dependent manner. BSP at 50 n*M* increased the invasiveness of SW-579 thyroid cancer cells (95.2 units, 95% confidence interval [CI] = 90.4 to 100 units) by approximately 10-fold compared with that of untreated control SW-579 cells (9.1 units, 95% CI = 5.7 to 12.5 units) ($P<.001$). Addition of an inactive mutated BSP, in which BSP's integrin-binding RGD tripeptide was altered, or addition of integrin $\alpha_v\beta_3$-blocking antibodies resulted in invasiveness equivalent to that of untreated cells. Inhibiting cellular MMP-2 activity with chemical inhibitors or a specific antibody also blocked BSP-enhanced invasiveness. Osteopontin and dentin matrix protein 1, proteins related to BSP that also bind integrin $\alpha_v\beta_3$ and form complexes with other MMPs (but not MMP-2), did not enhance invasiveness. Immunoprecipitation showed that a complex containing BSP, integrin $\alpha_v\beta_3$, and MMP-2 formed *in vitro*. Addition of BSP increased the amount of MMP-2 bound by cells in an integrin-dependent fashion. Co-expression of BSP, integrin $\alpha_v\beta_3$, and MMP-2 in papillary thyroid carcinoma cells was shown by *in situ* hybridization. *Conclusion:* Cancer cells appear to become more invasive when BSP forms a cell-surface trimolecular complex by linking MMP-2 to integrin $\alpha_v\beta_3$. [J Natl Cancer Inst 2004;96:956–65]**

The members of the SIBLING (small integrin-binding ligand N-linked glycoprotein) family of secreted proteins contain an integrin-binding tripeptide (arginine-glycine-aspartate, or RGD) and several conserved serine/threonine (Ser/Thr) phosphorylation and N-glycosylation sites. SIBLINGs include bone sialoprotein (BSP), osteopontin, dentin matrix protein 1 (DMP1), dentin sialophosphoprotein, and matrix extracellular phosphoglycoprotein *(1)*. Genes for all of these SIBLINGs are clustered within a 375 000 base-pair (bp) region of human chromosome 4 (chromosome 5 in the mouse) *(2)*. SIBLING expression is normally restricted to skeletal tissues in adults but also includes trophoblasts during embryonic development *(3–5)*. Osteopontin is an exception, being expressed in normal kidney *(6)*, lactating breast *(7)*, and immune cells *(8)*. BSP normally interacts only with cell-surface integrins, such as integrin $\alpha_v\beta_3$ (also known as the vitronectin receptor), whereas osteopontin and DMP1 bind to both integrins and CD44 *(9–13)*.

BSP is overexpressed by many malignant tissues, including breast *(14)*, prostate *(15)*, lung *(16)*, and thyroid *(17)* cancers and

Affiliations of authors: Craniofacial and Skeletal Diseases Branch, National Institute of Dental and Craniofacial Research, National Institutes of Health, Department of Health and Human Services, Bethesda, MD (AK, KUEO, NSF, LWF); Division of Geriatrics, Department of Medicine, Johns Hopkins University School of Medicine, Baltimore, MD (NSF).

Correspondence to: Abdullah Karadag, MD, PhD, MSc, Craniofacial and Skeletal Diseases Branch, National Institute of Dental and Craniofacial Research, National Institutes of Health, Department of Health and Human Services, 9000 Rockville Pike, Bldg. 30, Rm. 228, Bethesda, MD 20892-4320 (e-mail: akaradag@dir.nidcr.nih.gov).

See "Notes" following "References."

DOI: 10.1093/jnci/djh169

melanoma *(18)*. BSP expression has been associated with clinical severity and poor survival among patients with breast cancer *(19)* or with prostate cancer *(15)*. Recently developed serum immunoassays for BSP and osteopontin show that serum from patients with breast, lung, colon, or prostate cancer had statistically significantly elevated levels of BSP and/or osteopontin *(20)*. However, the role of BSP in these cancers is unclear.

Matrix metalloproteinases (MMPs), a class of zinc-dependent endopeptidases, are collectively capable of digesting all extracellular matrix components. In addition to their role in normal tissue development and remodeling, MMPs appear to play major roles in tumor cell invasion and metastasis *(21)*. Although the mechanism by which tumors invade surrounding tissues is not completely understood, MMPs may play an important role by removing physical barriers to invasion. In particular, MMP-2 (gelatinase A) and MMP-9 (gelatinase B) degrade extracellular matrix macromolecules in basement membranes and other interstitial connective tissues *(22)*. Active MMP-2 can localize to the cell surface by binding directly to integrin $\alpha_v\beta_3$ *(23)*, and proteolytically active MMP-9 can associate with CD44 *(24)*, thereby focusing proteolytic activity on the cell membrane at the leading edge of the invasive cell.

The integrins are a family of transmembrane receptor proteins composed of heterodimeric complexes of α and β chains *(25)*. There are 18 α and eight β chains, and these chains can dimerize to form at least 25 different complexes, each binding to a specific set of ligands. For example, integrin $\alpha_v\beta_3$ binds to BSP, osteopontin, and DMP1. In addition to regulating cell adhesion to the extracellular matrix, integrins modulate many cellular processes including proliferation, apoptosis, migration, and invasiveness by activating various signaling pathways *(26)*. Some integrins are overexpressed in malignant tumors. For example, integrin $\alpha_v\beta_3$ is expressed at the invasive front of malignant melanoma cells and on angiogenic blood vessels *(27)*. The level of integrin $\alpha_v\beta_3$ expression in breast cancers is associated with the aggressiveness of the disease *(28)*.

It is generally accepted that latent pro-MMPs are enzymatically activated by removal of their inhibitory propeptide. BSP, osteopontin, and DMP1 bind with nanomolar affinity to the latent and active forms of MMP-2, MMP-3, and MMP-9, respectively. When purified SIBLINGs are incubated with their pro-MMP partners, increased proteolytic activity is detected *(29)*. Therefore, we hypothesize that one or more SIBLINGs increase the invasiveness of cancer cells by interacting with their specific MMP and integrin partners. To test this hypothesis, we used a modified Boyden chamber cell invasion assay, as described previously *(30)*, to measure the invasiveness of various cancer cell lines through a layer of Matrigel (a mixture of basement membrane components), and we determined whether BSP increases the invasiveness of cancer cells by forming a trimolecular complex in which BSP acts as a bridge to link MMP-2 to integrin $\alpha_v\beta_3$.

Materials and Methods

Materials

Human breast cancer cell lines MDA-MB-231 (HTB-26), MDA-MB-435S (HTB-29), BT-474 (HTB-20), and MCF-7 (HTB-22); human prostate cancer cell lines PC-3 (CRL-1435), LNCaP (CRL-1740), and DU-145 (HTB-81); human thyroid cancer cell line SW-579 (HTB-107); human lung cancer cell line NCI-H520 (HTB-182); and human osteosarcoma cell lines SK-ES-1 (HTB-86), SaOS-2 (HTB-85), and MG-63 (CRL-1427) were obtained from the American Type Culture Collection (Manassas, VA). The mouse fibroblastic cell line NIH 3T3 was provided by Dr. Hynda Kleinman (National Institute of Dental and Craniofacial Research, National Institutes of Health, Bethesda, MD). Fetal bovine serum was purchased from Equitech-Bio (Kerrville, TX). RPMI-1640 medium, L-glutamine, 2-mercaptoethanol, sodium pyruvate, modified Eagle medium (MEM) nonessential amino acids, Hanks' balanced salt solution (HBSS), phosphate-buffered saline (PBS), Versene (0.53 m*M* EDTA in PBS), and 10% zymogram gelatin gels were from Invitrogen (Carlsbad, CA). Matrigel was from Collaborative Research (Bedford, MA; provided by Dr. Hynda Kleinman). Transwell inserts and companion plates were purchased from BD Biosciences Discovery Labware (Bedford, MA). Calcein acetoxymethyl ester dye and the Alexa Fluor 488 protein labeling kit were purchased from Molecular Probes (Eugene, OR). Mouse anti-human vitronectin receptor monoclonal antibody immobilized on immunoaffinity gel matrix (GEM1976), vitronectin receptor complex in Triton X-100 (CC1018), and mouse anti-MMP-2 monoclonal antibody (MAB 13435) were obtained from CHEMICON International (Temecula, CA). Pro-MMP-2 and active MMP-2 were from Oncogene Research Products (Boston, MA). pBluescript II KS vector was purchased from Stratagene (La Jolla, CA). Digoxigenin labeling mixture was obtained from Roche Biochemicals (Indianapolis, IN). The *in situ* hybridization kit, which included 5-bromo-4-chloro-3-indolyl phosphate/nitroblue tetrazolium (BCIP/NBT; product SH-3018-01), was from InnoGenex (San Ramon, CA). 1,10-Phenanthroline was from Sigma Chemical Co. (St. Louis, MO). MMP-2 inhibitor I, *cis*-9-octadecenoyl-*N*-hydroxylamideleoyl-*N*-hydroxylamide, and anti-integrin $\alpha_v\beta_3$ monoclonal antibody (LM609, MAB 1976Z) were obtained from Calbiochem (San Diego, CA). Rhodamine Red–conjugated AffiniPure goat anti-rabbit immunoglobulin G (IgG; heavy- and light-chain) and Cy2-conjugated AffiniPure goat anti-mouse IgG (heavy- and light-chain) were purchased from Jackson ImmunoResearch Laboratories (West Grove, PA). Vectashield mounting medium for fluorescence microscopy with 4′,6-diamidino-2-phenylindole (DAPI; product H-1200) was obtained from Vector Laboratories (Burlingame, CA). The ProbeQuant G-50 microcolumn was from Amersham Pharmacia Biotech (Piscataway, NJ). The Microcon YM-30 centrifugal filter device was from Millipore (Bedford, MA). *In situ*-ready human thyroid papillary adenocarcinoma serial paraffin sections (product 70452-3) were purchased from Novagen, (Madison, WI).

Cell Culture

The human cancer cell lines used, as described above, were first grown in RPMI-1640 medium supplemented with 10% fetal bovine serum, 2 m*M* L-glutamine, 5 m*M* 2-mercaptoethanol, 2 m*M* sodium pyruvate, and 0.1 m*M* MEM nonessential amino acids in a humidified atmosphere of 5% CO_2/95% air at 37 °C. When the cells were approximately 80% confluent, they were used in the experiments described below or subcultured for up to 20 passages at a split ratio of 1:10.

SIBLING Production and Purification

Recombinant BSP, BSP-KAE (BSP in which the RGD sequence was replaced with the sequence KAE), osteopontin, and DMP1 with posttranslational modifications, including glycosylation, sulfation, and possibly phosphorylation, were made as described previously *(9,11)*. Briefly, adenoviral constructs containing full-length human BSP *(31)*, BSP-KAE *(9)*, osteopontin *(32)*, or bovine DMP1 *(33)* were subcloned into high-expression, replication-deficient adenovirus type 5 under the control of the elongation factor 1 (EF-1) promoter for BSP or the cytomegalovirus (CMV) promoter for BSP-KAE, osteopontin, and DMP1. The BSP-KAE constructs were made by *in situ* mutagenesis in pBluescript; the entire insert was checked for fidelity and then shuttled to the adenovirus plasmid *(34)*. The adenoviruses were selected, purified, and expressed as previously described *(9)*. Recombinant SIBLINGs were generated by infecting mid-passage subconfluent normal human bone marrow stromal fibroblasts (gift from Dr. P. Gehron Robey, National Institute of Dental and Craniofacial Research, National Institutes of Health, Bethesda, MD). Harvested serum-free medium was subjected to anion-exchange chromatography, as described *(9,11)*, to isolate SIBLINGs. The purity of each SIBLING was greater than 95%, as measured after sodium dodecyl sulfate (SDS)–polyacrylamide gel electrophoresis.

Modified Boyden Chamber Cell Invasion Assay

Invasiveness of each cancer cell line was measured by using a UV-opaque transwell polycarbonate membrane insert with a diameter of 6.4 mm and pore size of 8 μm in a modified Boyden chamber cell invasion assay. Transwell inserts were placed in a 24-well plate, precoated with Matrigel (5–10 μg in 50 μL per well), and dried overnight in a laminar airflow hood. Preconfluent cells were removed from culture dishes with 0.53 m*M* EDTA in PBS, washed twice in HBSS, and resuspended in serum-free RPMI-1640 culture medium at a final density of 4×10^5 cells per milliliter. Quadruplicate cultures of cells were briefly pretreated in a final volume of 250 μL of serum-free medium (containing 0.1% bovine serum albumin) with either buffer or SIBLINGs in 1.5-mL Eppendorf microcentrifuge tubes for 10 minutes and then placed in the upper compartment of a Boyden chamber. In some cases, cells were first treated for 20 minutes with inhibitors, blocking antibodies, or isotype control IgGs in the tube and then placed in the upper chamber. In the latter cases, buffer or recombinant SIBLING was then added directly to the chamber. To induce migration through the Matrigel layer, the lower chambers were filled with 750 μL of serum-free medium conditioned by mouse NIH 3T3 fibroblastic cells and containing 0.1% bovine serum albumin. Cells were then incubated in a humidified incubator at 37 °C for 6–24 hours, depending on the cell line. Cells that had not migrated through the barrier were removed from the top compartment, and inserts were moved to another 24-well plate in which each well contained 0.5 mL of the fluorescent dye calcein acetoxymethyl ester at 4 μg/mL. The plate was incubated at 37 °C for 45 minutes to allow the living cells to take up and activate the dye, and then the fluorescent intensity was read from the bottom of the insert with a fluorescence plate reader (Wallac 1420 VICTOR^2 Multilabel Reader; PerkinElmer Life Sciences, Boston, MA). Fluorescence intensity was proportional to the number of cells migrating to the bottom of the UV-opaque membrane.

Immunoprecipitation Experiments

Commercial mouse anti-human vitronectin receptor (integrin $\alpha_v\beta_3$) monoclonal antibody immobilized on immunoaffinity gel matrix (i.e., beads) was washed three times in ice-cold Triton buffer (TB; 20 m*M* Tris–HCl [pH 7.4], 150 m*M* NaCl, 0.2% Triton X-100, 2 m*M* $MgCl_2$, and 0.1 m*M* $CaCl_2$) and incubated in 1 mL of TB containing 1% bovine serum albumin at 4 °C for 30 minutes with gentle shaking. After washing three times with 1 mL of ice-cold TB, the beads were gently shaken with or without 10 μg of integrin $\alpha_v\beta_3$ in 50 μL of TB at 4 °C for 10 minutes. The beads were then pelleted, the liquid was carefully removed, and the beads were washed in 1 mL of TB. The beads were then resuspended in 1 mL of buffer and separated into aliquots. An aliquot was gently shaken with buffer alone or buffer containing 500 n*M* BSP or 500 n*M* BSP-KAE (in a final volume of 50 μL) at 4 °C for 10 minutes. The beads were then pelleted, washed in 1 mL of TB, and incubated in 50 μL of TB containing 1 μg of pro-MMP-2 or 1 μg of active MMP-2 at 4 °C for 10 minutes. The beads were pelleted and washed with 1 mL of TB. The MMPs were eluted from the beads with 80 μL of 1× SDS sample buffer (2.5 mL of 0.5 *M* Tris–HCl [pH 6.8], 2 mL of glycerol, 4 mL of 10% (wt/vol) SDS, and 0.5 mL of 0.1% bromophenol blue, adjusted to 20 mL with distilled water) and resolved by electrophoresis on a 10% gelatin zymogram gel.

SDS–Polyacrylamide Gel Electrophoresis and Zymography

Samples in zymogram gel sample buffer were loaded on a 10% gelatin zymogram gel, subjected to electrophoresis, and processed as recommended by the manufacturer. Resulting Coomassie-stained gels were visualized with an EagleEye II imaging system (Stratagene, La Jolla, CA) by dynamic integrated exposure with an initial integration time of 3 seconds and an increment of 3 seconds (the camera sums frames of 1/30 second for a 3-second period, sends the image to the computer, collects light for 6 seconds, sends the image to the computer, and continues in this progression until integration is stopped).

Labeling of Purified Human Active MMP-2 and Pro-MMP-2 With Alexa 488 Dye

Latent (pro-MMP-2) or active MMP-2 was fluorescently labeled with the Alexa Fluor 488 protein labeling kit according to the manufacturer's protocol but was adjusted to the smaller amounts of protein being labeled. Briefly, shipping buffer from 50 μg of pro-MMP-2 or 50 μg of active MMP-2 was exchanged for the reaction buffer (PBS) on ProbeQuant G-50 microcolumns, and the resulting mixture was concentrated to approximately 50 μL with a prewashed Microcon YM-30 centrifugal filter device. Sodium bicarbonate (0.1 *M*, 5 μL) was added to raise the pH to 7.5–8.5 for efficient labeling. All steps were performed at 4 °C. The reactive dye was dissolved in 0.5 mL of PBS containing 0.1 *M* sodium bicarbonate, 50 μL of Alexa Fluor 488 dye was added to the MMP-2 solution, and the reaction mixture was stirred at 4 °C for 2 hours. The labeled MMP-2 protein was then separated from the unreacted dye on ProbeQuant G-50 microcolumns (in PBS) and stored as aliquots at −80 °C until use.

Flow Cytometry

Cells were detached from culture dishes with PBS containing 0.53 m*M* EDTA, washed twice in HBSS, and then incubated at

2×10^6 cells per milliliter with buffer alone or buffer containing 500 n*M* BSP or 500 n*M* BSP-KAE at room temperature for 10 minutes. For the studies involving the blocking anti-integrin $\alpha_v\beta_3$ antibody, cells were incubated with buffer alone or buffer containing anti-integrin $\alpha_v\beta_3$ antibody (LM609, 4 μg/mL) or isotype control IgG_1 (4 μg/mL) at room temperature for 10 minutes, and then the mixture was incubated with 500 n*M* BSP for 10 minutes. In the final step for all samples, cells were pelleted at 225*g* for 10 minutes at room temperature, washed once in HBSS, and then incubated at room temperature with Alexa Fluor 488–labeled purified human pro-MMP-2 at 1 μg/mL or active MMP-2 at 1 μg/mL for 10 minutes. The cells were pelleted, washed once, resuspended in HBSS, and analyzed immediately with a FACSCalibur cell sorter equipped with a 488-nm argon laser and Cellquest software (BD Pharmingen, Bedford, MA).

Fluorescent Immunocytochemistry

To localize BSP, MMP-2, and integrin $\alpha_v\beta_3$ on individual cells, 1 mL containing 1×10^3 SW-579 cells was placed in each well of a two-well chamber slide and incubated at 37 °C for 24 hours. The cells were then washed with serum-free RPMI-1640 medium and incubated in this medium at 37 °C with no additions, with 100 n*M* BSP-KAE, or with 100 n*M* BSP for 24 hours. The cells were then washed and incubated at 37 °C with recombinant pro-MMP-2 (1 μg/mL per well) for 20 minutes. After three washes in PBS, the cells were fixed in absolute ethanol at 4 °C for 30 minutes, washed three times in PBS, and incubated in PBS with affinity-purified human anti-BSP polyclonal antibody (LF-84) and mouse anti-MMP-2 monoclonal antibody at the same time at 4 °C for 24 hours. The cells then were washed and incubated with Rhodamine Red–coupled AffiniPure goat anti-rabbit IgG and Cy2-coupled AffiniPure goat anti-mouse IgG secondary antibodies at room temperature for 30 minutes. The slides were detached from the chamber, washed three times with PBS, and immediately mounted in Vectashield mounting medium for fluorescence with DAPI for nuclear staining under a coverslip. The samples were analyzed with a fluorescence microscope that could simultaneously visualize both dye signals.

In Situ Hybridization

To generate strand-specific probes for *in situ* hybridization, a polymerase chain reaction–amplified human MMP-2 cDNA fragment (317 bp) was subcloned into the *Bam*HI site of pBluescript II KS vector. The oligonucleotides for amplification of the MMP-2–specific probes were 5′-ATTAGGATCCGGTCACAG CTACTTCTTCAAG-3′ (forward) and 5′-ATATGGATCCG CCTGGGAGGAGTACAG-3′ (reverse). The BSP template was the full-length human BSP cDNA B6-5g *(31)*. The human integrin α_v cDNA (1200 bp) insert originally cloned into the pUC12 vector was released with *Eco*RI and *Hin*dIII *(35)*, and human integrin β_3 cDNA (2275 bp) originally cloned into the pUC12 vector *(36)* was released with *Eco*RI. Both cDNA inserts were then subcloned in pBluescript II KS, a vector that contains the T3 and T7 RNA polymerase promoters for RNA probe synthesis. After the plasmids were linearized with the appropriate restriction enzymes, the probes were labeled with a digoxigenin-labeling mixture (1 m*M* ATP, 1 m*M* CTP, 1 m*M* GTP, 0.65 m*M* UTP, and 0.35 m*M* DIG-11-UTP [digoxigenin coupled to UTP at position 11], pH 7.5) to produce the specific digoxigenin-labeled single-stranded antisense and sense RNA fragments. *In situ* hybridization for thyroid papillary carcinoma serial sections was carried out with the InnoGenex *in situ* hybridization BCIP/NBT kit according to the manufacturer's instructions with minor modifications. Slides were deparaffinized in xylene and rehydrated through a graded ethanol series. After a 10-minute incubation in the kit's proteinase K solution, the slides were fixed in 1% formaldehyde for 10 minutes. Approximately 50 μL of hybridization buffer containing pre-titrated digoxigenin-labeled RNA probes (antisense or sense) were applied to each slide. The hybridization reaction included a 3-minute denaturation at 80 °C followed by overnight incubation at 37 °C. After hybridization, washes at room temperature consisted of rinsing with 2× PBS to remove the coverslip, followed by one 10-minute wash and two 5-minute washes in PBS. The sections were then treated with antibody-blocking solution (InnoGenex, product BS-1310-06) for 5 minutes at room temperature, and the blocking agent was gently removed. Biotinylated mouse anti-digoxigenin monoclonal antibody (InnoGenex, product AS-3000-06) was then applied to the sections for 5 minutes at 37 °C, washed for two 5-minute periods in PBS, and then incubated at 37 °C with alkaline phosphatase streptavidine conjugate (provided by the manufacturer) for 5 minutes. After washing twice with PBS, activation buffer was then applied to each section for 1 minute before incubating in BCIP/NBT substrate chromogen solution until satisfactory color reaction was observed (approximately 15 minutes). Sections were then counterstained with nuclear fast red, dehydrated through a graded series of alcohol and xylene, and mounted under a coverslip. Sections were photographed with an AxioCam MR-MRGrab camera imaging system (Carl Zeiss Vision, Munchen, Germany), which included an Axioplan2 microscope, an AxioCam MRm camera, and AxioVision 3.1 software.

Statistical Analysis

Data are the mean of quadruplicate determinations and its 95% confidence interval (CI). Each experiment was repeated at least two times. In each case, data from a single representative experiment are shown. Multiple comparisons were performed with a one-way analysis of variance followed by Dunnett's test for treatment versus control comparisons. Pairwise comparisons were carried out by performing a nonparametric Mann–Whitney *U* test. In each analysis, differences were considered statistically significant for *P* values less than .05. All statistical tests were two-sided.

Results

BSP and Invasiveness of Cancer Cells *In Vitro*

Recent reports *(14–20)* that BSP is elevated in tumors and serum from patients with breast, prostate, lung, or thyroid cancers prompted us to investigate whether BSP has a role in the invasion of cancer cells. Invasiveness was measured with a modified Boyden chamber cell invasion assay. Treatment with BSP caused dose-dependent increases in the invasiveness of the breast cancer cell lines MDA-MB-231, MDA-MB-435S, and MCF-7; prostate cancer cell lines PC-3 and DU-145; lung cancer cell line NCI-H520; and thyroid cancer cell line SW-579. Results from a representative cell line for each cancer type are shown in Fig. 1. MDA-MB-231 cells showed a clear dose-

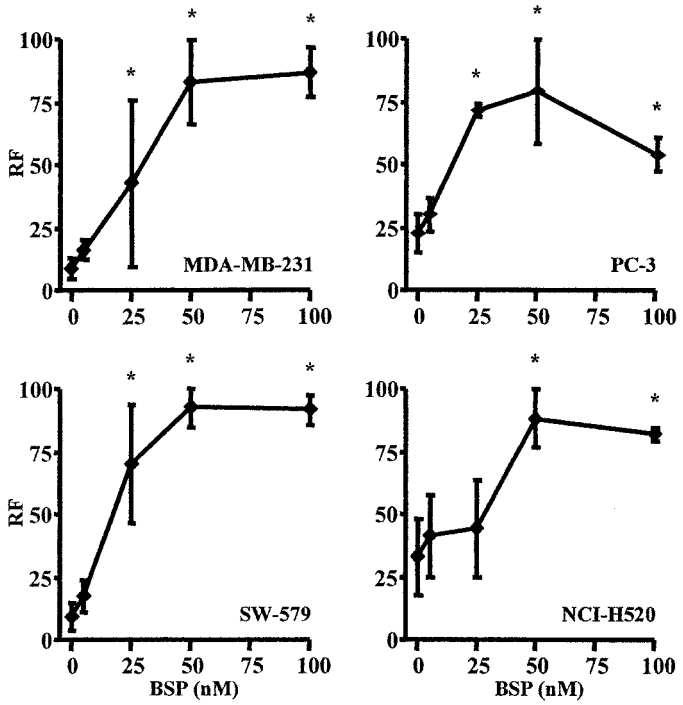

Fig. 1. Bone sialoprotein (BSP) and the invasion of selected cancer cell lines *in vitro.* BSP-treated breast (MDA-MB-231), prostate (PC-3), thyroid (SW-579), and lung (NCI-H520) cancer cells were placed in the Matrigel-coated upper chamber of a Boyden chamber with a UV-opaque transwell insert. The lower chambers contained serum-free conditioned medium as a chemoattractant. The cells were incubated at 37 °C for 6–24 hours. Invasive cells that penetrated the Matrigel artificial basement membrane into the lower chamber were detected by calcein acetoxymethyl ester (AM) fluorescent dye, which is activated by living cells. The relative fluorescence (RF) in the lower chamber corresponds directly to the number of cells that have migrated through the Matrigel. Data are the means of quadruplicate samples, and **error bars** are the 95% confidence intervals. A *P* value of <.001 was obtained for multiple comparisons within each panel, by use of one-way analysis of variance. Each treatment group was also individually compared with the control untreated group by use of Dunnett's test. **P*<.001 compared with untreated cells by Dunnett's test. All statistical tests were two-sided.

response increase in their invasiveness through a Matrigel barrier, with a maximum increase of approximately 10-fold at 100 n*M* BSP (93.1 units [U; 1 U represents 1% of the maximum number of cells invaded], 95% CI = 86.6 to 99.6 U) compared with that of untreated cells (9.5 U, 95% CI = 6.8 to 12.2 U) (*P*<.001) (Fig. 1). MDA-MB-435S cells showed an approximately twofold increase at 100 n*M* BSP (84.7 U, 95% CI = 69.4 to 100.0 U) compared with that of untreated cells (43.7 U, 95% CI = 36.8 to 50.6 U) (*P*<.001). In addition, MCF-7 cells, which are usually not aggressive in Boyden chamber cell invasion assays, showed a statistically significant approximately ninefold increased invasiveness after treatment with 100 n*M* BSP (79.5 U, 95% CI = 59.0 to 100.0 U) compared with untreated cells (8.5 U, 95% CI = 3.0 to 14.0 U) (*P*<.001).

Addition of recombinant human BSP to cultured prostate cancer cell lines PC-3 and DU-145 increased their invasiveness. The invasiveness of PC-3 cells increased more than threefold after the addition of 50 n*M* BSP (86.2 U, 95% CI = 72.4 to 100.0 U) compared with untreated cells (25.0 U, 95% CI = 19.7 to 30.3 U) (*P*<.001) (Fig. 1). Treatment with 100 n*M* BSP caused an approximately 17-fold increase in the invasiveness of DU-145 cells (84.6 U, 95% CI = 69.3 to 99.9 U) compared with untreated cells (5.0 U, 95% CI = 4.7 to 5.3 U) (*P*<.001) but caused no change in the invasiveness of another prostate cancer cell line, LNCaP (data not shown). BSP at 50 n*M* enhanced the invasiveness of the less aggressive lung squamous cell carcinoma NCI-H520 cells by approximately 2.7-fold (92.5 U, 95% CI = 85.0 to 100.0 U) compared with untreated control NCI-H520 cells (34.2 U, 95% CI = 24.4 to 44.0 U) (*P*<.001) (Fig. 1). The thyroid squamous cell carcinoma SW-579 cells responded maximally to the addition of 50 n*M* BSP with an approximately 10-fold increase in invasiveness (95.2 U, 95% CI = 90.4 to 100.0 U) compared with untreated cells (9.1 U, 95% CI = 5.7 to 12.5 U) (*P*<.001) (Fig. 1). BSP did not increase the invasiveness of the osteosarcoma cell lines SK-ES-1, SaOS-2, and MG-63 (data not shown). None of the cell lines used in these experiments expressed an appreciable level of BSP, as measured by northern blot hybridization (data not shown).

The increase in the invasiveness of these cancer cell lines was specific to BSP, because the same dose range of osteopontin and DMP1, the two other members of the SIBLING family that can support cell attachment but cannot bind to MMP-2, did not increase the invasiveness of any of the cell lines tested (data not shown).

BSP-Enhanced Invasion, Integrin $\alpha_v\beta_3$, and MMP-2

The same invasiveness studies were performed with BSP-KAE, a recombinant BSP protein whose integrin-binding RGD sequence was replaced with the chemically similar but inactive tripeptide KAE. Treatment with BSP-KAE did not increase the invasiveness of any cell line that had previously responded to BSP compared with the invasiveness of untreated cells. Results from representative breast, prostate, thyroid, and lung cancer cell lines are shown in Fig. 2.

BSP binds to the vitronectin receptor, which is also known as $\alpha_v\beta_3$ integrin *(37).* As shown in Fig. 3, when SW-579 thyroid cancer cells were pretreated with isotype control IgG_1 and then treated with BSP, their invasiveness increased about fivefold (90.3 U, 95% CI = 80.6 to 100.0 U) compared with untreated cells (19.4 U, 95% CI = 16.0 to 22.8 U). However, when cells were first incubated with the same amount of the integrin $\alpha_v\beta_3$ monoclonal antibody LM609, which blocks RGD binding, and then treated with BSP, invasiveness (21.7 U, 95% CI = 10.9 to 32.5 U) was similar to that of untreated cells (19.4 U, 95% CI = 16.0 to 22.8 U). Thus, the BSP-mediated increased invasiveness of cancer cells apparently requires BSP to have an active RGD sequence to bind to integrin $\alpha_v\beta_3$.

Integrins, particularly integrin $\alpha_v\beta_3$, modulate cancer cell invasiveness by directly interacting with MMP-2 *(23),* and BSP specifically binds to both active and pro-MMP-2 with nanomolar affinity *(29).* Because two other integrin $\alpha_v\beta_3$-binding SIBLINGs, osteopontin and DMP1, did not stimulate the invasion of cancer cells, we hypothesized that BSP increases invasiveness by interacting with both MMP-2 and integrin $\alpha_v\beta_3$. BSP-enhanced SW-579 cell invasion was completely inhibited by the addition of 10 μM 1,10-phenanthroline, a general MMP inhibitor (*P*<.001; Fig. 3). The role of MMP-2 in the BSP-enhanced cancer cell invasion was further investigated by use of a specific MMP-2 inhibitor (MMP-2 inhibitor I) and a monoclonal antibody against MMP-2. Both the specific MMP-2 inhibitor and the blocking antibody reduced the BSP-enhanced invasiveness of SW-579 cells to that of untreated control cells (*P*<.001; Fig. 3).

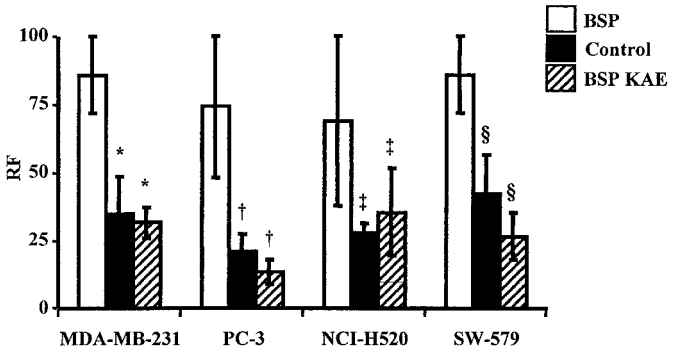

Fig. 2. Bone sialoprotein (BSP)-enhanced invasion and the RGD domain of BSP. MDA-MB-231, PC-3, NCI-H520, and SW-579 cells treated with 100 n*M* BSP or with 100 n*M* BSP-KAE (an inactive version of BSP in which the RGD domain was replaced with the chemically similar but inactive KAE tripeptide) were placed in the Matrigel-coated upper chamber of a Boyden chamber with a UV-opaque transwell insert. The lower chambers contained serum-free conditioned medium as a chemoattractant. The cells were incubated at 37 °C for 6–24 hours. Invasive cells that penetrated the Matrigel artificial basement membrane into the lower chamber were detected by calcein acetoxymethyl ester fluorescent dye, which is activated by living cells. The relative fluorescence (RF) in the lower chamber corresponds directly to the number of cells that have migrated through the Matrigel. The controls were untreated cells under the same culture conditions. The invasive activity of cells treated with BSP-KAE was similar to that of untreated cells. Relative fluorescence, which corresponds directly to the number of cells that migrated through the Matrigel, is as described in Fig. 1. Data are the means of quadruplicate samples, and **error bars** are 95% confidence intervals. A Mann–Whitney *U* test was used for the comparison of BSP-treated cells with either untreated control cells or BSP-KAE-treated cells. A *P* value of $<.01$ was obtained for MDA-MB-231 cells (*), PC-3 cells (†), NCI-H520 cells (‡), and SW-579 cells (§). All statistical tests were two-sided.

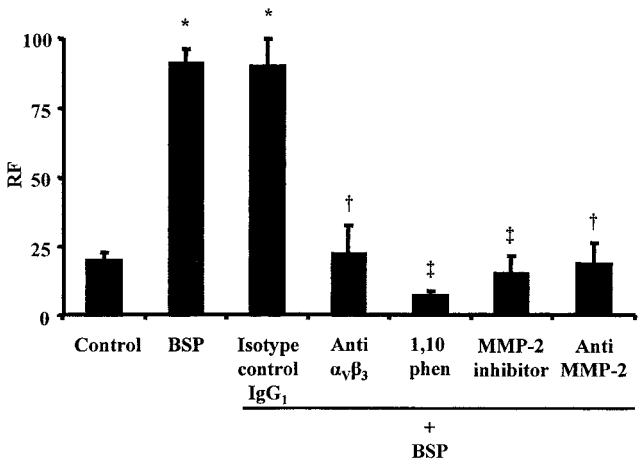

Fig. 3. Bone sialoprotein (BSP) activity and agents that block integrin $\alpha_v\beta_3$ or matrix metalloproteinase 2 (MMP-2) activities. SW-579 cells were placed in the Matrigel-coated upper chamber of a Boyden chamber with a UV-opaque transwell insert. The lower chambers contained serum-free conditioned medium as a chemoattractant. Invasive cells that penetrated the Matrigel artificial basement membrane into the lower chamber were detected by calcein acetoxymethyl ester fluorescent dye, which is activated by living cells. Cells were treated with isotype control immunoglobulin G_1 (IgG_1) (5 μg/mL), anti-integrin $\alpha_v\beta_3$ monoclonal antibody (5 μg/mL), anti-MMP-2 monoclonal antibody (5 μg/mL), the general MMP inhibitor 1,10-phenanthroline (1,10 phen) at 10 μ*M*, or the specific MMP-2 inhibitor termed MMP-2 inhibitor I at 5 μ*M* for 20 minutes, before 100 n*M* BSP was added to the inserts. The cells were incubated at 37 °C for 24 hours. Interfering with the functions of MMP or integrin negated BSP-enhanced Matrigel invasion. Relative fluorescence (RF) is as described in Fig. 1. Data are the means of quadruplicate samples from a representative experiment, and **error bars** are 95% confidence intervals. A *P* of less than .001 was obtained for multiple comparisons by use of one-way analysis of variance. Each group was also individually compared with untreated control group by use of the Dunnett test. *, $P<.001$ compared with untreated control cells; †, $P<.001$ compared with cells treated with isotype control IgG_1 and BSP; ‡, $P<.001$ compared with BSP-treated cells. All statistical tests were two-sided.

In Vitro Interaction of BSP, MMP-2, and Integrin $\alpha_v\beta_3$

Because the BSP-enhanced invasion can be blocked by interfering with the activity of either integrin $\alpha_v\beta_3$ or MMP-2 and because BSP can form a complex with integrin $\alpha_v\beta_3$ and a complex with MMP-2, we hypothesized that these three molecules form an RGD-dependent complex in which BSP acts as a bridge to link MMP-2 and integrin $\alpha_v\beta_3$. We tested this hypothesis with immunoprecipitation experiments using purified components. Integrin $\alpha_v\beta_3$ was incubated with immunoaffinity gel beads with covalently attached anti-integrin $\alpha_v\beta_3$ monoclonal antibodies to allow integrin binding. The beads were washed to remove unattached integrins, and the washed beads were then incubated with buffer alone or buffer containing recombinant BSP or recombinant BSP-KAE. After washing to remove unbound proteins, beads were incubated with soluble active MMP-2 or inactive pro-MMP-2. The beads were washed again, and then the amount of bound MMP-2 activity was measured by use of gelatin zymogram electrophoresis. No MMP activity was detected when integrin $\alpha_v\beta_3$-free beads were used, which showed that the immunoprecipitation assay had a very low background (data not shown). Beads with bound integrin $\alpha_v\beta_3$ but no BSP bound a small but reproducible amount of pro-MMP-2 and an even smaller amount of active MMP-2 (Fig. 4, lane 2). This result confirms that of Brooks et al. *(23)* and suggests that some MMP-2 can bind directly to integrin $\alpha_v\beta_3$. Addition of BSP-KAE, which lacks an active integrin-binding RGD sequence, did not increase the binding between integrin $\alpha_v\beta_3$ and either MMP-2 or pro-MMP-2 (Fig. 4, lane 4). However, addition of BSP and then of MMP-2 (active MMP-2 or pro-MMP-2) to integrin $\alpha_v\beta_3$-coated beads increased MMP activity associated with the beads, indicating that BSP stimulated the formation of a complex between integrin $\alpha_v\beta_3$ and MMP-2, presumably by linking the two proteins (Fig. 4, lane 3).

To investigate whether the complex of BSP, integrin $\alpha_v\beta_3$, and MMP-2 also occurs on living cells, we used flow cytometry, SW-579 cells, and purified active MMP-2 and pro-MMP-2 that had been covalently labeled with AlexaFluor-488. SW-579 cells were treated with anti-integrin $\alpha_v\beta_3$ monoclonal antibody or with an isotype control IgG_1 and then washed. These cells were incubated with buffer alone, buffer containing BSP, or buffer containing BSP-KAE, washed again, and then incubated with labeled pro-MMP-2. Flow cytometry was used to determine the amount of labeled pro-MMP-2 bound to these cells relative to that bound to untreated cells. Addition of BSP produced a 43% increase in the signal of labeled pro-MMP-2 bound to SW-579 cells compared with that of untreated cells (Fig. 5, A), whereas addition of BSP-KAE produced no change in this signal (Fig. 5, B). Addition of anti-integrin $\alpha_v\beta_3$ monoclonal antibodies almost completely blocked the binding of the labeled pro-MMPs to SW-579 cells compared with that of untreated control cells (Fig. 5, C) or cells treated with isotype control IgG_1 (Fig. 5, D). When labeled active MMP-2 was used for the binding analysis, BSP produced a 23% and 22% increase in signal of labeled MMP-2 bound to SW-579 cells compared with untreated control or BSP-KAE-treated cells, respectively (data not shown). Essen-

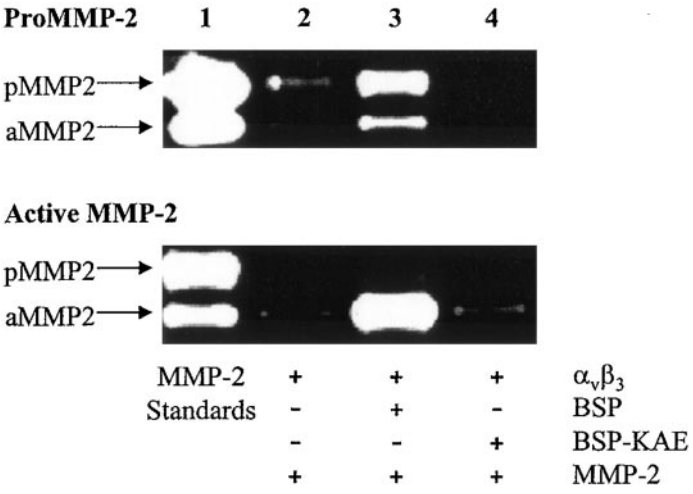

Fig. 4. Immunoprecipitation experiments and complexes of integrin $\alpha_v\beta_3$, bone sialoprotein (BSP), and matrix metalloproteinase 2 (MMP-2). Integrin $\alpha_v\beta_3$ was first bound to an anti-integrin monoclonal antibody covalently attached to immunoaffinity gel beads. After washing, the beads were incubated with buffer alone or buffer containing 500 n*M* BSP or 500 n*M* BSP-KAE, washed, and subsequently treated with recombinant pro-MMP-2 or active MMP-2. The washed samples were then separated by electrophoresis on 10% gelatin gels and examined by gelatin zymography. Note that the addition of BSP (**lane 3**) but not BSP-KAE (**lane 4**) enabled both pro-MMP-2 (**upper panel**) and active MMP-2 (**lower panel**) to be immunoprecipitated with the integrin-bound beads. Trace amounts of both pro-MMP-2 and active MMP-2 were observed without addition of BSP (**lane 2**), as described by Brooks et al. *(23)*. **Arrows** = pro-MMP-2 (pMMP2) and active MMP-2 (aMMP2) and identify the migration positions of MMP standards in **lane 1.**

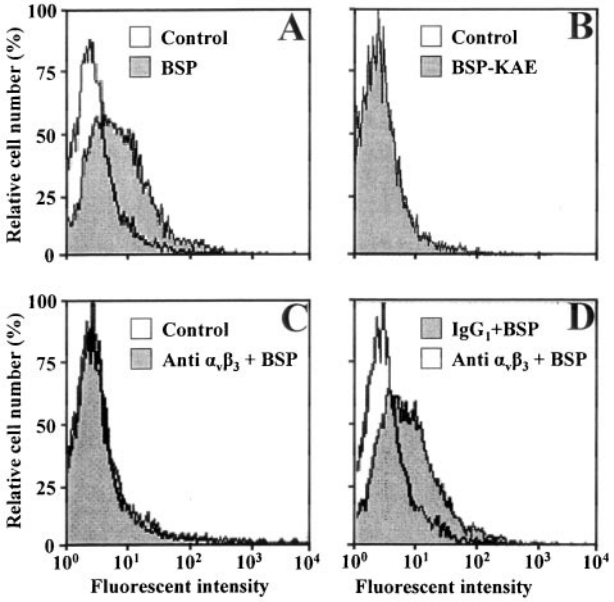

Fig. 5. Bone sialoprotein (BSP)-enhanced binding of fluorescently labeled pro-matrix metalloproteinase 2 (pro-MMP-2) to SW-579 cells. Pro-MMP-2 was labeled with Alexa Fluor-488 and incubated with cells treated as indicated or untreated cells (Control). **A**) Pretreating the cells with BSP (**shaded area**) increased the amount of labeled pro-MMP-2 bound to the living cells compared with untreated cells. **B**) Pretreating cells with BSP-KAE (**shaded area**) showed no increased binding of labeled pro-MMP-2 compared with that of untreated cells (**open area**). **C**) Blocking cell-surface integrin $\alpha_v\beta_3$ with an anti-integrin monoclonal antibody (**shaded area**) also completely blocked the BSP-enhanced binding of the labeled pro-MMP-2 (**open area**). **D**) Treating cells with a nonimmune isotype specific immunoglobulin G_1 (IgG_1) had no effect on the ability of BSP to enhance the binding of pro-MMP-2.

tially the same results for both active MMP-2 and pro-MMP-2 were obtained with PC-3 cells (data not shown).

Fluorescent immunocytochemistry experiments showed that BSP, MMP-2, and $\alpha_v\beta_3$ integrin co-localized in single cells. SW-579 cells were first treated with BSP overnight and then treated with MMP-2 for 20 minutes. BSP and MMP-2 were detected at the same locations in these cells (Fig. 6, A–C). Neither BSP nor MMP-2 was detected on untreated cells or cells treated with BSP-KAE (data not shown), suggesting that BSP rapidly localizes MMP-2 to the cell surface *in vitro* by binding to integrin $\alpha_v\beta_3$.

Finally, to verify that the complex of BSP, MMP-2, and integrin $\alpha_v\beta_3$ may occur naturally *in vivo*, *in situ* hybridization experiments were performed on serial paraffin sections of human papillary thyroid carcinomas. The purple-blue cytoplasmic staining with antisense probes verified that all four mRNAs are expressed in the same cells and/or areas of tissue (Fig. 7), showing that all the components of the complex are synthesized simultaneously by cells. Hybridization with similar amounts of the sense probes revealed no signal (data not shown).

DISCUSSION

Cellular invasion requires dynamic coordination of many cellular components, including cell adhesion molecules and proteolytic agents. MMPs and integrins participate in degradation of the basement membrane and, consequently, in the invasion of cancer cells. Several studies have reported that increased activation of MMP-2, MMP-3, MMP-9, MMP-13, MMP-14, and/or MMP-15 is associated with tumor cell invasion *(23,38–44)*. Two studies have demonstrated that the progression of various cancers is also associated with the overexpression of integrins $\alpha_v\beta_3$, $\alpha_3\beta_1$, $\alpha_4\beta_1$, and/or $\alpha_2\beta_3$ *(23,45)*. Finally, several co-localization studies have reported that integrin $\alpha_v\beta_3$ may function not only as an adhesion and/or migration receptor but may also activate and properly distribute proteases that degrade the extracellular matrix during invasion *(23,46,47)*.

Because it is overexpressed in malignant tissues, BSP may play a role in the progression and invasion of a number of

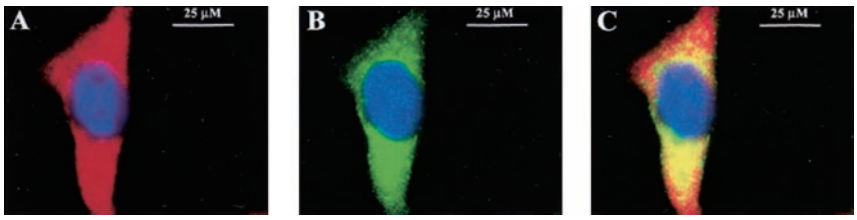

Fig. 6. Localization of bone sialoprotein (BSP) and matrix metalloproteinase 2 (MMP-2) on SW-579 thyroid cancer cells. Cells were treated first with BSP and then with pro-MMP-2. The cells were incubated with a polyclonal antibody against BSP and a monoclonal antibody against MMP-2, and both proteins were detected by indirect immunofluorescence with Rhodamine Red–conjugated AffiniPure goat anti-rabbit immunoglobulin G (IgG) for BSP and Cy2-conjugated AffiniPure goat anti-mouse IgG for MMP-2. The red color in **panel A** shows the location of BSP, the green color in **panel B** shows the location of MMP-2, and the yellow color in **panel C** shows that the two proteins co-localize. 4′,6-Diamidino-2-phenylindole (DAPI) was used as a nuclear counterstain (blue color). **Scale bar** = 25 μm.

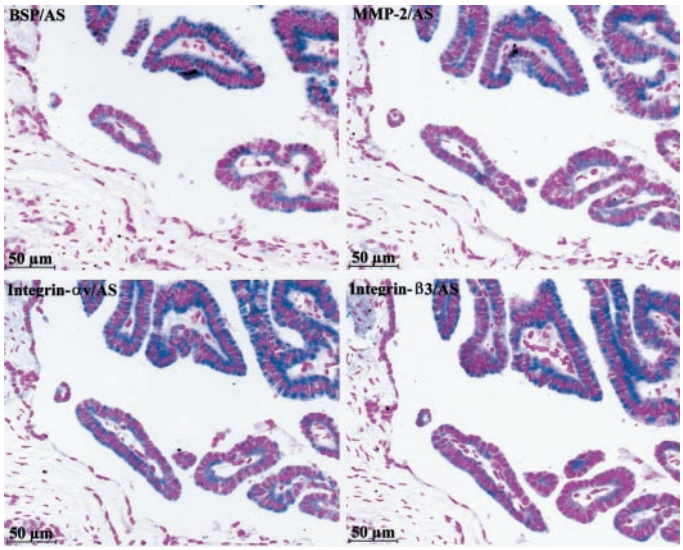

Fig. 7. mRNA for bone sialoprotein (BSP), matrix metalloproteinase 2 (MMP-2), and both chains of integrin $\alpha_v\beta_3$ in sections of an invasive thyroid papillary carcinoma. Deparaffinized sections of an invasive thyroid papillary carcinoma were incubated with digoxigenin-labeled antisense probes specific for BSP, MMP-2, the α_v chain, and the β_3 chain. Indirect localization of the probes was determined with anti-digoxigenin antibodies and colorimetric staining. Cytoplasmic purple-blue color indicates that mRNAs for BSP (**upper left**), MMP-2 (**upper right**), α_v chain (**lower left**), and β_3 chain (**lower right**) are in the same cells, suggesting that all proteins required for formation of complexes of integrin $\alpha_v\beta_3$, BSP, and MMP-2 are likely to be expressed in the same cells. Fast red was used as a nuclear counterstain (nuclear red color). **Scale bar** = 50 μm.

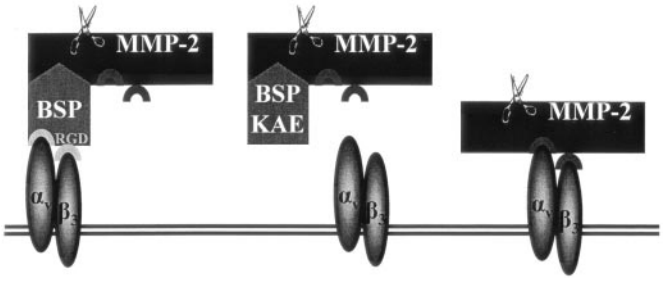

Fig. 8. Proposed trimolecular complex of bone sialoprotein (BSP), matrix metalloproteinase 2 (MMP-2), and integrin $\alpha_v\beta_3$. (**Left**) BSP with an intact RGD domain acts as a bridge between MMP-2 and integrin $\alpha_v\beta_3$. (**Middle**) BSP-KAE, mutant BSP in which the RGD is replaced with KAE, can bind to MMP-2, but the complex does not interact with the integrin $\alpha_v\beta_3$ heterodimer. (**Right**) As shown in Fig. 4 and by others *(23)*, some MMP-2 may also interact with integrin $\alpha_v\beta_3$ even in the absence of BSP. **Double line** = cell membrane; **scissors** = active site of MMP-2.

osteotropic cancers, including breast, prostate, lung, and thyroid cancers *(14–17,20)*. Addition of BSP stimulates the *in vitro* migration of breast cancer cells via a mechanism involving integrin $\alpha_v\beta_3$ *(48,49)*. Strong and specific *in vitro* interactions (with nanomolar affinity) have been described *(29)* between three members of the SIBLING family (BSP, osteopontin, and DMP1) and specific MMPs (MMP-2, MMP-3, and MMP-9, respectively). Thus, the combination of BSP, MMP-2, and integrin $\alpha_v\beta_3$ appears to play an important role in cancer cell invasion. This study demonstrated that BSP, but not osteopontin or DMP1, increased the Matrigel invasiveness of a large subset of breast, prostate, lung, and thyroid cancer cell lines. Addition of BSP-KAE, a recombinant form of BSP in which the RGD sequence was replaced with KAE, or addition of an antibody that blocks BSP binding to integrin $\alpha_v\beta_3$ through RGD sequence blocked all BSP-enhanced invasive activity, suggesting that BSP acts through this integrin. The BSP-enhanced invasion by these cells was also inhibited by specific chemical inhibitors of MMP-2 and by an antibody for MMP-2. Formation of a complex containing BSP, integrin $\alpha_v\beta_3$, and MMP-2 was demonstrated by immunoprecipitation experiments, immunofluorescence experiments, and flow cytometry. These results suggest that cells use BSP as a bridge to link MMP-2 to its cell surface receptor, integrin $\alpha_v\beta_3$, which thereby increases their ability to invade basement membranes and other connective tissues. Fig. 8 shows BSP with an intact RGD bridging MMP-2 to its cell-surface receptor, integrin $\alpha_v\beta_3$. When the integrin-binding RGD sequence is replaced with the chemically similar but inactive KAE sequence, MMP-2 may still bind to the BSP-KAE protein, but the complex between MMP-2 and BSP-KAE does not interact with cell-surface integrin.

Because BSP enhances the attachment and migration of several cancer cell lines, we also tested the effect of two other members of the SIBLING family, osteopontin and DMP1, that support cell attachment. Osteopontin also supports migration *(50)*. For all 16 cell lines tested, neither osteopontin nor DMP1 increased the invasiveness of these cells through Matrigel, even though the increased expression of these proteins in various cancers has been reported *(20,51–53)*. We have recently shown *in vitro* that osteopontin and DMP1 bind specifically to MMP-3 and MMP-9, respectively, with nanomolar affinity but do not bind to MMP-2 *(29)*. Because the Boyden chamber cell invasion assay can detect differences only in those functions that result in a net change in rate-limiting steps in the *in vitro* invasion process *(54)*, it is reasonable to conclude that the binding and possible activation of MMP-2 by BSP overcomes such a rate-limiting step for the cell lines tested, whereas cell attachment alone or the binding and activation of MMP-3 by osteopontin or MMP-9 by DMP1 does not overcome such a step.

In conclusion, we have shown that recombinant BSP can enhance the invasiveness of some, but not all, breast, prostate, lung, and thyroid cancer cell lines in a modified Boyden chamber assay through formation of an RGD-dependent complex with MMP-2 and integrin $\alpha_v\beta_3$.

REFERENCES

(1) Fisher LW, Torchia DA, Fohr B, Young MF, Fedarko NS. Flexible structures of SIBLING proteins, bone sialoprotein, and osteopontin. Biochem Biophys Res Commun 2001;280:460–5.

(2) Fisher LW, Fedarko NS. Six genes expressed in bones and teeth encode the current members of the SIBLING family of proteins: special issue: 7th International Conference on the Chemistry and Biology of Mineralized Tissues. Connect Tissue Res 2003;44 Suppl 1:33–40.

(3) Bianco P, Fisher LW, Young MF, Termine JD, Robey PG. Expression of bone sialoprotein (BSP) in developing human tissues. Calcif Tissue Int 1991;49:421–6.

(4) MacDougall M. Refined mapping of the human dentin sialophosphoprotein (DSPP) gene within the critical dentinogenesis imperfecta type II and dentin dysplasia type II loci. Eur J Oral Sci 1998;106 Suppl 1:227–33.

(5) Omigbodun A, Daiter E, Walinsky D, Fisher L, Young M, Hoyer J, et al. Regulated expression of osteopontin in human trophoblasts. Ann N Y Acad Sci 1995;760:346–9.

(6) Hampel DJ, Sansome C, Romanov VI, Kowalski AJ, Denhardt DT, Goligorsky MS. Osteopontin traffic in hypoxic renal epithelial cells. Nephron Exp Nephrol 2003;94:e66–76.

(7) Dhanireddy R, Senger D, Mukherjee BB, Mukherjee AB. Osteopontin in human milk from mothers of premature infants. Acta Paediatr 1993;82: 821–2.

(8) Gravallese EM. Osteopontin: a bridge between bone and the immune system. J Clin Invest 2003;112:147–9.

(9) Fedarko NS, Fohr B, Robey PG, Young MF, Fisher LW. Factor H binding to bone sialoprotein and osteopontin enables tumor cell evasion of complement-mediated attack. J Biol Chem 2000;275:16666–72.

(10) Weber GF, Ashkar S, Glimcher MJ, Cantor H. Receptor-ligand interaction between CD44 and osteopontin (Eta-1). Science 1996;271:509–12.

(11) Jain A, Karadag A, Fohr B, Fisher LW, Fedarko NS. Three SIBLINGs (small integrin-binding ligand, N-linked glycoproteins) enhance factor H's cofactor activity enabling MCP-like cellular evasion of complement-mediated attack. J Biol Chem 2002;277:13700–8.

(12) Ue T, Yokozaki H, Kitadai Y, Yamamoto S, Yasui W, Ishikawa T, et al. Co-expression of osteopontin and CD44v9 in gastric cancer. Int J Cancer 1998;79:127–32.

(13) Zohar R, Suzuki N, Suzuki K, Arora P, Glogauer M, McCulloch CA, et al. Intracellular osteopontin is an integral component of the CD44-ERM complex involved in cell migration. J Cell Physiol 2000;184:118–30.

(14) Bellahcene A, Merville MP, Castronovo V. Expression of bone sialoprotein, a bone matrix protein, in human breast cancer. Cancer Res 1994;54: 2823–6.

(15) Waltregny D, Bellahcene A, Van Riet I, Fisher LW, Young M, Fernandez P, et al. Prognostic value of bone sialoprotein expression in clinically localized human prostate cancer. J Natl Cancer Inst 1998;90: 1000–8.

(16) Bellahcene A, Maloujahmoum N, Fisher LW, Pastorino H, Tagliabue E, Menard S, et al. Expression of bone sialoprotein in human lung cancer. Calcif Tissue Int 1997;61:183–8.

(17) Bellahcene A, Albert V, Pollina L, Basolo F, Fisher LW, Castronovo V. Ectopic expression of bone sialoprotein in human thyroid cancer. Thyroid 1998;8:637–41.

(18) Riminucci M, Corsi A, Peris K, Fisher LW, Chimenti S, Bianco P. Coexpression of bone sialoprotein (BSP) and the pivotal transcriptional regulator of osteogenesis, Cbfa1/Runx2, in malignant melanoma. Calcif Tissue Int 2003.

(19) Bellahcene A, Menard S, Bufalino R, Moreau L, Castronovo V. Expression of bone sialoprotein in primary human breast cancer is associated with poor survival. Int J Cancer 1996;69:350–3.

(20) Fedarko NS, Jain A, Karadag A, Van Eman MR, Fisher LW. Elevated serum bone sialoprotein and osteopontin in colon, breast, prostate, and lung cancer. Clin Cancer Res 2001;7:4060–6.

(21) Matrisian LM. Cancer biology: extracellular proteinases in malignancy. Curr Biol 1999;9:R776–8.

(22) Kleiner DE, Stetler-Stevenson WG. Matrix metalloproteinases and metastasis. Cancer Chemother Pharmacol 1999;43 Suppl:S42–51.

(23) Brooks PC, Stromblad S, Sanders LC, von Schalscha TL, Aimes RT, Stetler-Stevenson WG, et al. Localization of matrix metalloproteinase MMP-2 to the surface of invasive cells by interaction with integrin alpha v beta 3. Cell 1996;85:683–93.

(24) Yu Q, Stamenkovic I. Localization of matrix metalloproteinase 9 to the cell surface provides a mechanism for CD44-mediated tumor invasion. Genes Dev 1999;13:35–48.

(25) Hynes RO. Integrins: versatility, modulation, and signaling in cell adhesion. Cell 1992;69:11–25.

(26) Aplin AE, Howe AK, Juliano RL. Cell adhesion molecules, signal transduction and cell growth. Curr Opin Cell Biol 1999;11:737–44.

(27) Hood JD, Cheresh DA. Role of integrins in cell migration and invasion. Nature Rev Cancer 2002;2:91–100.

(28) Gasparini G, Brooks PC, Biganzoli E, Vermeulen PB, Bonoldi E, Dirix LY, et al. Vascular integrin alpha(v)beta3: a new prognostic indicator in breast cancer. Clin Cancer Res 1998;4:2625–34.

(29) Fedarko NS, Jain A, Karadag A, Fisher LW. Three small integrin binding ligand N-linked glycoproteins (SIBLINGs) bind and activate specific matrix metalloproteinases. FASEB J 2004;18:734–6.

(30) Albini A, Iwamoto Y, Kleinman HK, Martin GR, Aaronson SA, Kozlowski JM, et al. A rapid in vitro assay for quantitating the invasive potential of tumor cells. Cancer Res 1987;47:3239–45.

(31) Fisher LW, McBride OW, Termine JD, Young MF. Human bone sialoprotein. Deduced protein sequence and chromosomal localization. J Biol Chem 1990;265:2347–51.

(32) Kiefer MC, Bauer DM, Barr PJ. The cDNA and derived amino acid sequence for human osteopontin. Nucleic Acids Res 1989;17:3306.

(33) Hirst KL, Ibaraki-O'Connor K, Young MF, Dixon MJ. Cloning and expression analysis of the bovine dentin matrix acidic phosphoprotein gene. J Dent Res 1997;76:754–60.

(34) Becker TC, Noel RJ, Coats WS, Gomez-Foix AM, Alam T, Gerard RD, et al. Use of recombinant adenovirus for metabolic engineering of mammalian cells. Methods Cell Biol 1994;43:161–89.

(35) Fitzgerald LA, Poncz M, Steiner B, Rall SC Jr, Bennett JS, Phillips DR. Comparison of cDNA-derived protein sequences of the human fibronectin and vitronectin receptor alpha-subunits and platelet glycoprotein IIb. Biochemistry 1987;26:8158–65.

(36) Fitzgerald LA, Steiner B, Rall SC Jr, Lo SS, Phillips DR. Protein sequence of endothelial glycoprotein IIIa derived from a cDNA clone. Identity with platelet glycoprotein IIIa and similarity to "integrin". J Biol Chem 1987; 262:3936–9.

(37) Oldberg A, Franzen A, Heinegard D, Pierschbacher M, Ruoslahti E. Identification of a bone sialoprotein receptor in osteosarcoma cells. J Biol Chem 1988;263:19433–6.

(38) Collier IE, Wilhelm SM, Eisen AZ, Marmer BL, Grant GA, Seltzer JL, et al. H-ras oncogene-transformed human bronchial epithelial cells (TBE-1) secrete a single metalloprotease capable of degrading basement membrane collagen. J Biol Chem 1988;263:6579–87.

(39) Pyke C, Ralfkiaer E, Huhtala P, Hurskainen T, Dano K, Tryggvason K. Localization of messenger RNA for Mr 72,000 and 92,000 type IV collagenases in human skin cancers by in situ hybridization. Cancer Res 1992; 52:1336–41.

(40) Monteagudo C, Merino MJ, San-Juan J, Liotta LA, Stetler-Stevenson WG. Immunohistochemical distribution of type IV collagenase in normal, benign, and malignant breast tissue. Am J Pathol 1990;136:585–92.

(41) Lochter A, Galosy S, Muschler J, Freedman N, Werb Z, Bissell MJ. Matrix metalloproteinase stromelysin-1 triggers a cascade of molecular alterations that leads to stable epithelial-to-mesenchymal conversion and a premalignant phenotype in mammary epithelial cells. J Cell Biol 1997;139:1861–72.

(42) Belien AT, Paganetti PA, Schwab ME. Membrane-type 1 matrix metalloprotease (MT1-MMP) enables invasive migration of glioma cells in central nervous system white matter. J Cell Biol 1999;144:373–84.

(43) Ala-Aho R, Johansson N, Baker AH, Kahari VM. Expression of collagenase-3 (MMP-13) enhances invasion of human fibrosarcoma HT-1080 cells. Int J Cancer 2002;97:283–9.

(44) Hotary K, Allen E, Punturieri A, Yana I, Weiss SJ. Regulation of cell invasion and morphogenesis in a three-dimensional type I collagen matrix by membrane-type matrix metalloproteinases 1, 2, and 3. J Cell Biol 2000;149:1309–23.

(45) Klein CE, Steinmayer T, Kaufmann D, Weber L, Brocker EB. Identification of a melanoma progression antigen as integrin VLA-2. J Invest Dermatol 1991;96:281–4.

(46) Deryugina EI, Bourdon MA, Luo GX, Reisfeld RA, Strongin A. Matrix metalloproteinase-2 activation modulates glioma cell migration. J Cell Sci 1997;110:2473–82.

(47) Deryugina EI, Bourdon MA, Jungwirth K, Smith JW, Strongin AY. Functional activation of integrin alpha V beta 3 in tumor cells expressing membrane-type 1 matrix metalloproteinase. Int J Cancer 2000;86:15–23.

(48) Sung V, Stubbs JT 3rd, Fisher L, Aaron AD, Thompson EW. Bone sialoprotein supports breast cancer cell adhesion proliferation and migration through differential usage of the alpha(v)beta3 and alpha(v)beta5 integrins. J Cell Physiol 1998;176:482–94.

(49) Byzova TV, Kim W, Midura RJ, Plow EF. Activation of integrin alpha (V)beta(3) regulates cell adhesion and migration to bone sialoprotein. Exp Cell Res 2000;254:299–308.

(50) Xuan JW, Hota C, Shigeyama Y, D'Errico JA, Somerman MJ, Chambers AF. Site-directed mutagenesis of the arginine-glycine-aspartic acid sequence in osteopontin destroys cell adhesion and migration functions. J Cell Biochem 1995;57:680–90.

(51) Chambers AF, Wilson SM, Kerkvliet N, O'Malley FP, Harris JF, Casson AG. Osteopontin expression in lung cancer. Lung Cancer 1996; 15:311–23.
(52) Tuck AB, O'Malley FP, Singhal H, Harris JF, Tonkin KS, Kerkvliet N, et al. Osteopontin expression in a group of lymph node negative breast cancer patients. Int J Cancer 1998;79:502–8.
(53) Chaplet M, De Leval L, Waltregny D, Detry C, Fornaciari G, Bevilacqua G, et al. Dentin matrix protein 1 is expressed in human lung cancer. J Bone Miner Res 2003;18:1506–12.
(54) Albini A. Tumor and endothelial cell invasion of basement membranes. The matrigel chemoinvasion assay as a tool for dissecting molecular mechanisms. Pathol Oncol Res 1998;4:230–41.

NOTES

We thank Dr. Albert Kingman (Division of Intramural Research, National Institute of Dental and Craniofacial Research, National Institutes of Health, Bethesda, MD) for assistance with statistical analysis.

Manuscript received October 16, 2003; revised April 19, 2004; accepted April 28, 2004.

0021-972X/04/$15.00/0
Printed in U.S.A.

The Journal of Clinical Endocrinology & Metabolism 89(8):4158–4161

doi: 10.1210/jc.2003-032031

Serum Levels of Matrix Extracellular Phosphoglycoprotein (MEPE) in Normal Humans Correlate with Serum Phosphorus, Parathyroid Hormone and Bone Mineral Density.

A. JAIN, N.S. FEDARKO, M.T. COLLINS, R. GELMAN, M.A. ANKROM, M. TAYBACK AND L.W. FISHER

Division of Geriatric Medicine, Department of Medicine, Johns Hopkins University, Baltimore, MD 21224 (A.J., N.S.F., M.A.A.); General Clinical Research Center, Johns Hopkins Bayview Medical Center, Baltimore, MD 21224 (N.S.F., R.G., M.T.); Craniofacial and Skeletal Diseases Branch, National Institute of Dental and Craniofacial Research, National Institutes of Health, DHHS, Bethesda, MD 20892 (M.T.C., L.W.F.).

ABSTRACT. Matrix extracellular phosphoglycoprotein (MEPE), a member of the Small Integrin Binding Ligand N-linked Glycoprotein (SIBLING) family, is primarily expressed in normal bone and has been proposed as a phosphaturic factor because of high expression and secretion in oncogenic hypophosphatemic osteomalacia tumors. In order to begin to address the role of MEPE in normal human physiology, we developed a competitive ELISA to measure serum levels of MEPE. The ELISA was used to characterize the distribution pattern in a population consisting of 114 normal adult subjects. The mean value of MEPE was 476 ± 247 ng/ml and levels decreased significantly with increasing age. MEPE levels were also significantly correlated with serum phosphorus and parathyroid hormone (PTH). In addition, MEPE levels correlated significantly with measures of bone mineral density in the femoral neck and total hip in a subset of 60 elderly subjects. The results are consistent with MEPE being involved in phosphate and bone metabolism in a normal population.

Introduction

Matrix extracellular phosphoglycoprotein (MEPE), is a member of the SIBLING gene family (1, 2). Other family members include bone sialoprotein (BSP), osteopontin (OPN), dentin matrix protein-1 (DMP1), and dentin sialophosphoprotein. The family shares the RGD integrin-binding motif, several conserved phosphorylation and N-glycosylation sites, a common gene structure and chromosomal localization (4q21).

Normal MEPE expression has been described primarily in bone marrow, brain (3) and bone (4), while tumors which cause hypophosphatemic osteomalacia exhibit high expression and secretion (3). MEPE has consistently been linked with mineralization and bone formation associated with bone mineral (3-6). Whether MEPE plays a role as a positive or negative regulator of bone formation in humans remains unclear. The current study was undertaken to determine the distribution of MEPE in normal donors and to correlate the values with other biomarkers of bone metabolism as well as measures of bone mineral density (BMD).

Methods

Subjects. Sera from clinically defined normal patients were obtained under IRB approved protocols from a commercial serum bank (East Coast Biologicals, Inc., North Burwick, ME) as well as from the Johns Hopkins Bayview Medical Center General Clinical Research Center (JHBMC). The JHBMC normal group was obtained from an existing serum bank using samples from which all patient identifiers were removed.

Received 11/25/03. Accepted 3/22/04.

Cloning and expression of MEPE. The last exon of human MEPE constitutes 95% of the mature protein as defined by Rowe et al. (3). The last exon was amplified by PCR from human genomic DNA using a 5' oligonucleotide with a NdeI restriction site engineered in (AGTACCCATATGAAAGACAATA-TTGGTTTTCACCAT) and a 3' oligonucleotide with a BamHI site (CTGATGGGATCCCTAGTCACCAT-CGCTCTCAC). The ~1.5 kbp PCR product was gel purified, digested with NdeI plus BamHI, ligated into pET15b expression vector (Novagen, Madison, WI) digested with the same restriction enzymes. After transfection into BL-21 (DE3) E. coli cells, a high expression colony was selected and used to produce the MEPE protein by stimulation with IPTG. The MEPE protein in the apparent inclusion bodies was purified in 6 M urea on a HisBind resin column (Novagen) following the manufacturer's instructions. The eluted fraction was dialyzed exhaustively against 0.1 M ammonium acetate at 4°C and freeze-dried. Four ~200 μg aliquots of the highly purified MEPE were injected into a New Zealand white rabbit to make antiserum LF-155.

Serum sample preparation and competitive ELISA procedure. The SIBLINGs BSP, OPN and DMP1 are complexed with complement Factor H in human serum (7, 8). We have developed competitive ELISAs for measuring the BSP and OPN that requires disruption of the serum complex between the SIBLING and complement Factor H (9). For the current study, serum samples for use in ELISA analyses were processed in a chaotropic buffer exactly as described (9). The MEPE competitive ELISA developed utilized the same plates, buffers, and protein standard concentrations, secondary antibody concentrations, as well as substrate color reagents as

previously described (9). The only changes to the ELISA steps were that plates were coated with 10 ng/well recombinant MEPE and the primary antibody, LF-155, was employed at a 1:200,000 dilution.

Western blotting. Samples diluted in gel sample buffer were resolved by Tris/glycine SDS 12% polyacrylamide gels (Invitrogen, Inc., Carlsbad, CA) and transferred to nitrocellulose following standard conditions (10). Nitrocellulose membranes were rinsed with Tris-buffered saline-Tween (TBS-Tween, 0.05 M Tris-HCl, pH 7.5, 0.15 M NaCl containing 0.05% Tween 20). After a 1 h incubation in TBS-Tween + 5% non-fat powdered milk at room temperature, a 1:20,000 primary antibody (polyclonal antibody LF-155) was incubated overnight at 4 ^{O}C. The blot was washed in TBS-Tween four times for 5 min with TBS-Tween and then HRP-conjugated goat anti-rabbit IgG (1:2,000) in TBS-Tween + 5% milk was added and incubated for 2 h at room temperature. After washing, enhanced chemiluminescence reagents were employed for signal detection (Pierce Chemical Co., Chicago, IL) with x-ray film.

DEXA measurements. BMD was measured in the hip, spine and proximal femur using the Hologic QDR 1000 scanner (Hologic Corp., Waltham MA). The precision of this machine is 1.8% ± 0.05%. Mean values for total hip and spine were obtained, as were BMD values for neck and trochanter in the left proximal femur.

Serum and urine biochemical measures. Blood samples were drawn in the morning after an overnight fast. Serum bone biochemical measurements included bone-specific alkaline phosphatase (Hybritech, San Diego, CA), osteocalcin (Immunotopics, San Clemente, CA), procollagen type I carboxy-terminal propeptide (DiaSorin Stillwater, MN), intact PTH (Nichols Institute, San Juan Capistrano, CA), and 25 hydroxy vitamin D (DiaSorin). The excretion of deoxypyridinoline crosslinks (Quidel Corp. San Diego, CA) and cross-linked amino-terminal telopeptides (OSTEX International, Seattle, WA) were assayed in 2-hour, second-void morning urine specimens. The values for cross-links were normalized to urinary creatinine assayed using the Jaffe Rate method and a Beckman Creatinine Analyzer 2 (11). Serum inorganic phosphorus was measured using standard clinical methods (12). The performance characteristics of the immmunoassays as carried out in our laboratory are given in Table I.

Results

Previous work has demonstrated that the SIBLINGs BSP, DMP1 and OPN were bound to complement Factor H in serum (7, 8). Disruption of the serum complex required heating in a chaotropic buffer containing reducing agent, followed by a column step to clean up the sample (9). The same disruption procedure was used on serum samples from elderly and young adult donors and MEPE was detected by western blot. Immunoreactive bands shifted in migration with reduction and younger donors appeared to have more MEPE present (Fig. 1a and b). The amount of MEPE present in sera from 114 different normal subjects was analyzed. A reproducible standard curve profile combining 34 different analyses performed over the past two years was obtained (Fig. 1c). MEPE values quantified by ELISA paralleled semi-quantitative results obtained from western blots (Fig/ 1c, inset).

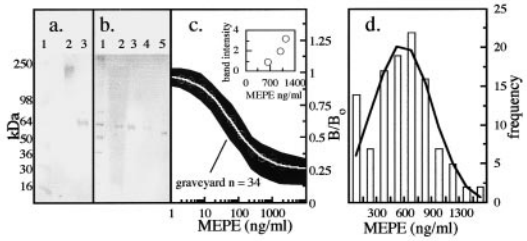

Figure 1. MEPE is present in human serum. (a) Unreduced (lane 2) and reduced (lane 3) serum samples from normal donors were analyzed for the presence of MEPE by western blot. Molecular weight standards were run in lane 1. (b) Samples derived from different age donors analyzed by western blot. Lane 1, standards; lanes 2, 3 & 4 contained 60, 24 and 78-year-old normal donor serum, lane 5, recombinant MEPE (lacking glycosylation). (c) Competitive ELISA profile; inset, representative correlation of western blot band intensity with ELISA results. (d) The distribution of MEPE (bars) in 114 normal subjects. Solid line represents the normal Gaussian distribution.

Addition of recombinant MEPE to serum samples prior to reduction, column chromatography and competitive ELISA yielded an average recovery of 88 % based on three different trials. The inter-assay coefficient of variance for repetitive measurements on the same serum sample was 19.4% (n = 6), while the intra-assay coefficient of variance was 12.6% (n = 12). The major source of this variance was tracked to the column chromatography step. Repeated measures of post-reduction and column samples gave rise to a coefficient of variance of 7.9%. The measure of MEPE levels in normal subject-derived sera revealed a distribution with a slight hook at the low end (Fig. 1d).

When MEPE levels were plotted versus the age of the subject, the reason for the low end hook to the distribution of normal values became apparent. MEPE exhibited a significant age-related decrease in level, (Fig. 2a). The population analyzed possessed a sufficient number of subjects > 60 years of age, where MEPE levels are 1/2 to 1/3 those of younger adults, to account for the increased distribution at low MEPE levels. Serum measures of markers of bone metabolism were also performed on normal subjects. Comparing MEPE levels with serum values of bone-specific alkaline phosphatase, procollagen type I carboxy-terminal propeptide, 25-hydroxy vitamin D, osteocalcin, and urine levels of collagen cross-link markers revealed no significant correlation (data not shown).

Table I. Immunoassay Performance and Study Population Characteristics.

Analyte		mean ± s.d.	units	range	%CV intra-assay	%CV inter-assay
bone-specific alkaline phosphatase		11.2 ± 4.2	ng/ml	5.0 – 28	5.49	5.83
deoxypyridinoline crosslinks		5.1 ± 2.0	nM/mM Cr	1.7 – 13	6.00	4.16
N-terminal telopeptides		31.3 ±13.3	BCE/mM Cr	5.2 – 64.2	8.25	4.00
osteocalcin		5.2 ± 1.9	ng/ml	2.1 – 10.2	4.55	6.10
procollagen type I C-terminal propeptide		133.9 ±45	ng/ml	10.7 – 289	2.24	4.38
intact parathyroid hormone		33.7 ± 14.5	pg/ml	3.2 – 94.2	2.40	5.95
25-hydroxy vitamin D		34.5 ± 9.3	ng/ml	14.6 – 62.6	5.19	7.90
MEPE		476.0 ± 247	ng/ml	19.0 – 1269	12.60	19.40
study population	male (n = 64)	60 ± 20	years	21 - 87		
	female (n = 54)	55 ± 12	years	35 - 62		
	BMD group (n = 60)	65 ± 11	years	50 - 82		

Because MEPE has been proposed to play a role in phosphate metabolism, we next investigated serum levels of PTH and inorganic phosphorus. Using a third generation commercial intact PTH assay, the PTH levels were found to be significantly negatively correlated with serum MEPE values (Fig. 2b). The serum levels of intact PTH showed no correlation with donor age (data not shown), suggesting that the association of MEPE and PTH was age-independent. The levels of serum phosphate in the same donors was significantly positively correlated ($r^2 = 0.35$, $p \leq 0.0001$) with serum MEPE values (Figure 2b, inset).

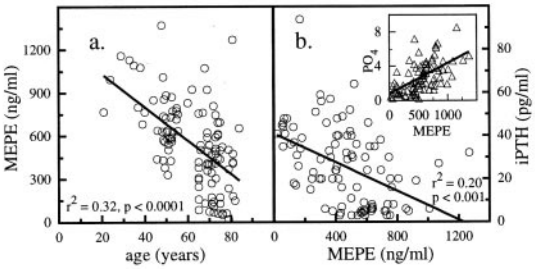

Figure 2. MEPE levels in serum correlate with age (a) and parathyroid hormone levels (b). Serum inorganic phosphorus levels were also determined (inset).

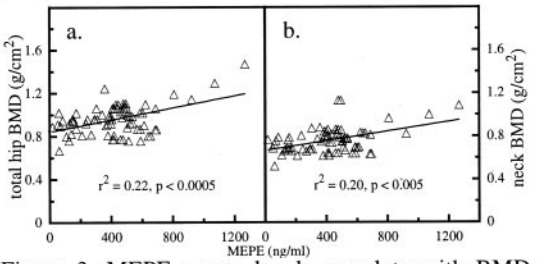

Figure 3. MEPE serum levels correlate with BMD values for total hip (a) and femur neck (b).

In addition to serum and urine markers of bone metabolism, BMD measurements were obtained on a subset of normal subjects (n = 60). The BMD values (g/cm^2) determined were analyzed for correlation with MEPE levels in the corresponding subject's serum (Fig. 3). MEPE levels were significantly positively correlated with bone mineral density values for total hip and femur neck. MEPE levels were also correlated with femur trochanter BMD ($r^2 = 0.13$, $p \leq 0.01$), while the correlation with total spine BMD did not reach statistical significance (data not shown). The correlation of serum MEPE levels with BMD was still significant when adjusted for subject age using multiple regression analysis and StatView software (SAS Institute, Inc.)

Discussion

MEPE and its rodent homologue, OF45, have been implicated in bone and mineral metabolism (3, 4, 13). The increase in bone density found in the OF45 knockout mouse in the presence of normal serum phosphorus and calcium without evidence of a mineralization defect, suggests that it may have a direct effect on bone formation (6). In that report, the MEPE knockout animal had, what is for a gene knockout model, a relatively subtle increase in the amount of bone. While histomorphometric analysis was performed, there were no data on the parameters of mineralization (osteoid thickness, etc.), only formation and resorption. Elevated levels of MEPE mRNA expression by tumors from patients with hypophosphatemia and osteomalacia suggested that it may be involved in mineral homeostasis. The control of systemic phosphate homeostasis is incompletely understood. Key modulators include PTH, calcium, phosphorus, vitamin D, as well as novel phosphatonin(s), and the bone and kidney organs. Candidate phosphaturic factors include MEPE; PHEX, a putative endopeptidase believed to process factors regulating bone mineralization and renal phosphate reabsorption (5); FGF23, a phosphaturic factor in fibrous dysplasia (14), tumor-induced osteomalacia and autosomal-dominant hypophosphatemic rickets (15, 16) and secreted frizzled-related protein 4, an antagonist of renal Wnt-signaling (17). These phosphate regulators remain to be fully characterized both individually, and in their interactions which will lead to the description of a new hormonal pathway.

Demonstration of significant levels of MEPE in the serum of normal humans, as well as a clear age-related decrease suggest that MEPE may be an interesting marker of normal human bone and mineral metabolism. While the positive correlation between MEPE and phosphorus might suggest an anti-phosphaturic effect, it may represent a secondary response to higher serum phosphorus levels. This idea is supported by the significant correlation of serum MEPE levels with the important constituents of mineral metabolism serum, PTH and phosphorus. The relationships between serum MEPE and PTH, MEPE and phosphorus, and phosphorus and PTH are all internally consistent, and the relationship between phosphorus and PTH is consistent with established

physiology. The correlation of MEPE levels with BMD suggests that it may be involved in mineralization in the human. The finding that MEPE is low in aged patients, when BMD is lower, and that MEPE levels are higher when BMD is high is corroborative, and suggests that these findings in humans are of physiologic significance. Two recent studies have provided contrasting data on the biological activity of MEPE. Recombinant MEPE promoted renal phosphate excretion in mice and inhibited BMP2-mediated mineralization in a mouse osteoblasts cell line (18). The inhibitory action was mapped to the carboxy terminal region of the molecule. In a second study, a peptide fragment corresponding to the RGD-containing mid region stimulated new bone formation in neonatal mouse calvarial organ culture and increased osteoblast proliferation and alkaline phosphatase activity (19). Our current study demonstrates the association of serum MEPE levels with serum phosphate, PTH and bone mineral density but does not address causality.

Acknowledgements

This research was supported by CA 87311 (N.S.F.), DAMD17-02-0684 (N.S.F.) and the Johns Hopkins Bayview Medical Center General Clinical Research Center, NIH/NCRR grant M01RR02719.

References

1. **Fisher LW, Torchia DA, Fohr B, Young MF, Fedarko NS** 2001 The solution structures of two SIBLING proteins, bone sialoprotein and osteopontin, by NMR. Biochem Bophys Res Comm 280:460-465
2. **Fisher LW, Fedarko NS** 2003 Six genes expressed in bones and teeth constitute the current members of the SIBLING family of proteins. Connective Tissue Res. 44:1-8
3. **Rowe PS, de Zoysa PA, Dong R, Wang HR, White KE, Econs MJ, Oudet CL** 2000 MEPE, a new gene expressed in bone marrow and tumors causing osteomalacia. Genomics 67:54-68
4. **Argiro L, Desbarats M, Glorieux FH, Ecarot B** 2001 Mepe, the gene encoding a tumor-secreted protein in oncogenic hypophosphatemic osteomalacia, is expressed in bone. Genomics 74:342-51
5. **Quarles LD** 2003 FGF23, PHEX, and MEPE regulation of phosphate homeostasis and skeletal mineralization. Am J Physiol Endocrinol Metab 285:E1-9
6. **Gowen LC, Petersen DN, Mansolf AL, Qi H, Stock JL, Tkalcevic GT, Simmons HA, Crawford DT, Chidsey-Frink KL, Ke HZ, McNeish JD, Brown TA** 2003 Targeted disruption of the osteoblast/osteocyte factor 45 gene (OF45) results in increased bone formation and bone mass. J Biol Chem 278:1998-2007
7. **Fedarko NS, Fohr B, Gehron Robey P, Young MF, Fisher LW** 2000 Factor H binding to bone sialoprotein and osteopontin enables molecular cloaking of tumor cells from complement-mediated attack. J Biol Chem 275:16666-16672
8. **Jain A, Karadag A, Fohr B, Fisher LW, Fedarko NS** 2002 Three Small Integrin Binding LIgands N-linked Glycoproteins (SIBLINGs) enhance Factor H's cofactor activity enabling MCP-like cellular evasion of complement-mediated attack. J Biol Chem 277:13700-13708
9. **Fedarko NS, Jain A, Karadag A, Van Eman MR, Fisher LW** 2001 Elevated serum bone sialoprotein and osteopontin in colon, breast, prostate, and lung cancer. Clin Cancer Res 7:4060-6
10. **Towbin H, Staehelin T, Gordon J** 1979 Electrophoretic transfer of proteins from polyacrylamide gels to nitrocellulose sheets: procedure and some applications. Proc Natl Acad Sci U S A 76:4350-4
11. **Mazzachi BC, Peake MJ, Ehrhardt V** 2000 Reference range and method comparison studies for enzymatic and Jaffe creatinine assays in plasma and serum and early morning urine. Clin Lab 46:53-55
12. **Daly JA, Ertingshausen G** 1972 Direct method for determining inorganic phosphate in serum with the "CentrifiChem". Clin Chem 18:263-5
13. **Petersen DN, Tkalcevic GT, Mansolf AL, Rivera-Gonzalez R, Brown TA** 2000 Identification of osteoblast/osteocyte factor 45 (OF45), a bone- specific cDNA encoding an RGD-containing protein that is highly expressed in osteoblasts and osteocytes. J Biol Chem 275:36172-80
14. **Riminucci M, Collins MT, Fedarko NS, Cherman N, Corsi A, White KE, Waguespack S, Gupta A, Hannon T, Econs MJ, Bianco P, Gehron Robey P** 2003 FGF-23 in fibrous dysplasia of bone and its relationship to renal phosphate wasting. J Clin Invest 112:683-92
15. **Shimada T, Mizutani S, Muto T, Yoneya T, Hino R, Takeda S, Takeuchi Y, Fujita T, Fukumoto S, Yamashita T** 2001 Cloning and characterization of FGF23 as a causative factor of tumor-induced osteomalacia. Proc Natl Acad Sci U S A 98:6500-5
16. **White KE, Carn G, Lorenz-Depiereux B, Benet-Pages A, Strom TM, Econs MJ** 2001 Autosomal-dominant hypophosphatemic rickets (ADHR) mutations stabilize FGF-23. Kidney Int 60:2079-86
17. **Berndt T, Craig TA, Bowe AE, Vassiliadis J, Reczek D, Finnegan R, Jan De Beur SM, Schiavi SC, Kumar R** 2003 Secreted frizzled-related protein 4 is a potent tumor-derived phosphaturic agent. J Clin Invest 112:785-94
18. **Rowe PS, Kumagai Y, Gutierrez G, Garrett IR, Blacher R, Rosen D, Cundy J, Navvab S, Chen D, Drezner MK, Quarles LD, Mundy GR** 2004 MEPE has the properties of an osteoblastic phosphatonin and minhibin. Bone 34:303-19
19. **Hayashibara T, Hiraga T, Yi B, Nomizu M, Kumagai Y, Nishimura R, Yoneda T** 2004 A synthetic peptide fragment of human MEPE stimulates new bone formation in vitro and in vivo. J Bone Miner Res 19:455-62

Small Integrin Binding Ligand *N*-Linked Glycoprotein Gene Family Expression in Different Cancers

Larry W. Fisher,[1] Alka Jain,[2] Matt Tayback,[2] and Neal S. Fedarko[2]

[1]Craniofacial and Skeletal Diseases Branch, National Institute of Dental and Craniofacial Research, National Institutes of Health, Department of Health and Human Services, Bethesda, Maryland; and [2]Division of Geriatric Medicine, Department of Medicine, Johns Hopkins University, Baltimore, Maryland

ABSTRACT

Purpose: **Members of the small integrin binding ligand *N*-linked glycoprotein (SIBLING) gene family have the capacity to bind and modulate the activity of matrix metalloproteinases (MMPs). The expression levels of five SIBLING gene family members [bone sialoprotein (BSP), osteopontin (OPN), dentin matrix protein 1 (DMP1), matrix extracellular phosphoglycoprotein (MEPE), and dentin sialophosphoprotein (DSPP)] and certain MMPs were determined using a commercial cancer array.**

Experimental Design: **Cancer profiling arrays containing normalized cDNA from both tumor and corresponding normal tissues from 241 individual patients were used to screen for SIBLING and MMP expression in nine distinct cancer types.**

Results: **Significantly elevated expression levels were observed for BSP in cancer of the breast, colon, stomach, rectum, thyroid, and kidney; OPN in cancer of the breast, uterus, colon, ovary, lung, rectum, and thyroid; DMP1 in cancer of the breast, uterus, colon, and lung; and dentin sialophosphoprotein in breast and lung cancer. The degree of correlation between a SIBLING and its partner MMP was found to be significant within a given cancer type (*e.g.,* BSP and MMP-2 in colon cancer, OPN and MMP-3 in ovarian cancer; DMP1 and MMP-9 in lung cancer). The expression levels of SIBLINGs were distinct within subtypes of cancer (*e.g.,* breast ductal tumors compared with lobular tumors). In general, SIBLING expression increased with cancer stage for breast, colon, lung, and rectal cancer.**

Conclusions: **These results suggest SIBLINGs as potential markers of early disease progression in a number of different cancer types, some of which currently lack vigorous clinical markers.**

INTRODUCTION

The small integrin-binding ligand *N*-linked glycoprotein (SIBLING) gene family is clustered on human chromosome 4, and its members include bone sialoprotein (BSP), osteopontin (OPN), dentin matrix protein 1 (DMP1), matrix extracellular phosphoglycoprotein (MEPE), and dentin sialophosphoprotein (DSPP; ref. 1). SIBLINGs are normally thought to be restricted in expression to mineralizing tissue such as bones and teeth (1). Retrospective studies using pathological specimens have shown that OPN expression occurs in cancer of the breast, colon, stomach, ovary, lung, thyroid, kidney, prostate, and pancreas (2, 3). The expression of other SIBLING members in cancer has not been extensively studied. BSP expression was been reported in breast (4, 5), prostate (6), lung (7), and thyroid cancer (8). DMP1 has been shown to be strongly up-regulated in lung cancer (9). Elevated levels of MEPE mRNA expression by tumors from patients with hypophosphatemia and osteomalacia have been reported (10). The neoplastic expression pattern of DSPP has not been defined.

Matrix metalloproteinases (MMPs) are critical for development, wound healing, and the progression of cancer. We have recently shown that BSP, OPN, and DMP1 specifically bind to pro–MMP-2, pro–MMP-3, and pro–MMP-9, respectively, thereby activating the latent proteolytic activity (11). Furthermore, it was shown that active MMPs inhibited by either tissue inhibitors of MMPs or low molecular weight synthetic inhibitors were reactivated by their corresponding SIBLING. The current study was undertaken to determine the mRNA expression patterns of SIBLINGs in nine different types of cancer. An additional goal was to determine whether SIBLINGs exhibited expression levels that correlated with their MMP partners as well as various measures of tumor progression.

MATERIALS AND METHODS

Cancer Array Analysis. A cancer profiling array (product 7841-1; Clontech, Palo Alto, CA) containing normalized cDNA from tumor and corresponding normal tissues from 241 individual patients was used to screen for SIBLING and MMP expression (12). Several cancer profiling arrays were hybridized in ExpressHyb hybridization solution (Clontech) with ^{32}P-labeled cDNA probes as per the manufacturer's instructions. Briefly, 1 to 2 $\times$ 10^7 cpm of random-prime labeled cDNA was made single stranded by heating to 95°C for 5 minutes and allowed to hybridize with the prepared membrane overnight at 65°C. Membranes were washed in a series of high stringency washes as recommended by the manufacturer. The washed membranes were quantified by exposure to PhosphorImager screens for 1 to 24 hours, and the exposed screen was analyzed on a PhosphorImager (Amersham Biosciences, Piscataway, NJ)

Received 6/1/04; revised 9/10/04; accepted 9/17/04.
Grant support: Grants CA 87311 (N. Fedarko) and DAMD17-02-0684 (N. Fedarko).
The costs of publication of this article were defrayed in part by the payment of page charges. This article must therefore be hereby marked *advertisement* in accordance with 18 U.S.C. Section 1734 solely to indicate this fact.
Requests for reprints: Neal S. Fedarko, Room 5A-64 JHAAC, 5501 Hopkins Bayview Circle, Baltimore, MD 21224. Phone: 410-550-2632; Fax: 410-550-1007; E-mail: ndarko@jhmi.edu.

using the manufacturer's ImageQuant program. All polymerase chain reaction (PCR) products were subcloned into a shuttle plasmid, cloned, and sequenced, and the inserts were gel-purified before ^{32}P labeling by random priming. Unincorporated label was removed before hybridization.

SIBLING Probes. The labeled DNA used for probing was obtained as follows. Human BSP and OPN were cDNA inserts released from OP-10 and B6-5g plasmids, respectively (13, 14). Human DMP1 insert was the ~1.4-kb coding region of exon 6 (15) amplified from human genomic DNA subcloned into pBluescript at the *Eco*RI and *Bam*HI sites using oligonucleotides ATTATAGAATTCAAATGAAGACCCCAGTGACAG (forward) and TAATTAGGATCCAATAGCCGTCTTGGCAGTC (reverse). The MEPE probe was a 1.45-kb, exon 5, cDNA insert corresponding to the last exon of human MEPE, which constitutes 95% of the mature protein as defined by Rowe *et al.* (10). The exon was amplified by PCR from human genomic DNA using a 5′ oligonucleotide with a *Nde*I restriction site engineered in AGTACCCATATGAAAGACAATATTGGTTTTCACCAT and a 3′ oligonucleotide with a *Bam*HI site (CTGATGGGATCCCTAGTCACCATCGCTCTCAC). The PCRproduct was subcloned into pBluescript and sequenced, and the ~1.5-kb insert was released with *Nde*I plus *Bam*HI and labeled. The DSPP probe corresponding to the last exon was similarly amplified using a 5′ oligonucleotide with a *Hind*III restriction site engineered in CTGTTGGTACCGATATCGAAATCAAGGGTCCCAGCAG and a 3′ oligonucleotide with a *Kpn*I restriction site (GTGCAAAGCTTCTAATCATCACTGGTTGAGTGG), subcloned, and sequenced, and the released ~2.6-kb insert was labeled.

Matrix Metalloproteinase Probes. Specific probes of ~300 bp each for human MMP-2, MMP-3, and MMP-9 were made by PCR using human genomic DNA as template and the following oligonucleotides: MMP-2, ATTAGGATCCGGTCACAGCTACTTCTTCAAG (forward with *Bam*HI site added for subcloning) and ATATGGATCCGCCTGGGAGGAGTACAG (reverse with *Bam*HI site); MMP-3, ATATGGATCCAGCTGGCTTAATTGTTGAAAG (forward with *Bam*HI) and TAATGGATCCAACTGACAAATCGTCTTTATTA (reverse with *Bam*HI); and MMP-9, AATTGAATTCAGAGAAAGCCTATTTCTGCCAG (forward with *Eco*RI) and TAATGAATTCGGTTAGAGAATCCAAGTTTATTAG (reverse with *Eco*RI). In each case, the PCR products were subcloned into pBluescript and verified by sequencing, and the ~0.3-kb inserts were released and labeled. Membranes were used up to three times, each time removing the previous probe according to the manufacturer's instructions. The stripped membranes were reimaged by PhosphorImager to verify the removal of the previous probe.

Statistical Analysis. Clinical data linked to samples spotted on the cancer profiling array were accessed through the manufacturer's World Wide Web-based database.[3] Comparisons between normal and tumor tissue (derived from the same subject) were performed using a paired *t* test. The coordinated expression of SIBLINGs with MMP binding partners in tumors was tested by regression analysis. Significant differences in tumor subtype expression of SIBLINGs was tested by Student's *t* test. The association of SIBLING expression levels with tumor stage was investigated using a conservative statistical approach. The nonparametric Spearman rank order correlation was used to examine the correlation of tumor stage and SIBLING expression. The analysis was performed on untransformed data, and the adjusted Spearman correlation coefficient (r_S) is reported. All statistical calculations were carried out using StatView software (SAS Institute, Inc., Cary, NC).

RESULTS

SIBLINGs Are Elevated in Multiple Cancer Types. Because BSP and OPN protein expression have been found to be greatly increased in many separate, often immunohistochemistry-based studies of different neoplasms, the expression levels of five SIBLING gene family members were determined using a commercial cancer array. The array included normalized cDNA from tumor and corresponding normal tissues from 241 individual patients, as well as certain internal controls (Fig. 1). Because the sample sizes were too small for some tumor types on the array, the tissues reported for this study include only breast, uterus, colon, stomach, ovary, lung, kidney, rectum, and thyroid. In each array experiment, the patient's normal and tumor cDNA was separately hybridized with ^{32}P-labeled probes for BSP, OPN, DMP1, MEPE, and DSPP, and the array was digitized by PhosphorImager. Whereas BSP, DMP1, and DSPP exhibited minimal normal tissue expression, significant OPN expression by normal tissues was observed. In fact, the highest levels of expression of OPN were seen in normal kidney. Because MEPE expression was minimal in both normal and tumor tissue, its expression was not analyzed further (data not shown). The amount of hybridized probe was quantified, and the average expression values of BSP, OPN, DMP1, and DSPP in normal and tumor tissue were compared (Fig. 2). The expression levels of BSP were significantly elevated (from 2- to 6-fold) in cancer of the breast, colon, rectum, thyroid, and kidney. OPN expression was significantly elevated (2- to 4-fold) in cancer of the breast, uterus, colon, ovary, lung, rectum, and thyroid. DMP1 exhibited significant (1.7- to 3-fold) elevated expression in cancer of the breast, uterus, colon, and lung, whereas DSPP exhibited significant (2-fold) increase in cancer of the breast and lung. Elevated SIBLING family expression was greatest in breast cancer, in which expression of four different family members was increased. Colon, lung, and thyroid cancer had significantly elevated expression of three different SIBLING family members. Of the nine different types of tumors quantified, each one had a significantly high expression of at least one SIBLING.

Matrix Metalloproteinases Are Elevated in Multiple Cancer Types. We have recently shown that three members of the SIBLING family can specifically bind and modulate the activity of three different MMPs (11). The SIBLINGs BSP, OPN, and DMP1 were found to bind to and modulate the activity of MMP-2, MMP-3, and MMP-9, respectively. Corresponding MMP partners for DSPP and MEPE, if any, have yet to be identified. Because MMPs have been postulated to play major roles in tumor cell progression and metastasis (16), the expression levels of SIBLING-matched MMPs were screened in

[3] http://bioinfo.clonetech.com/dparray/array-list-action.do.

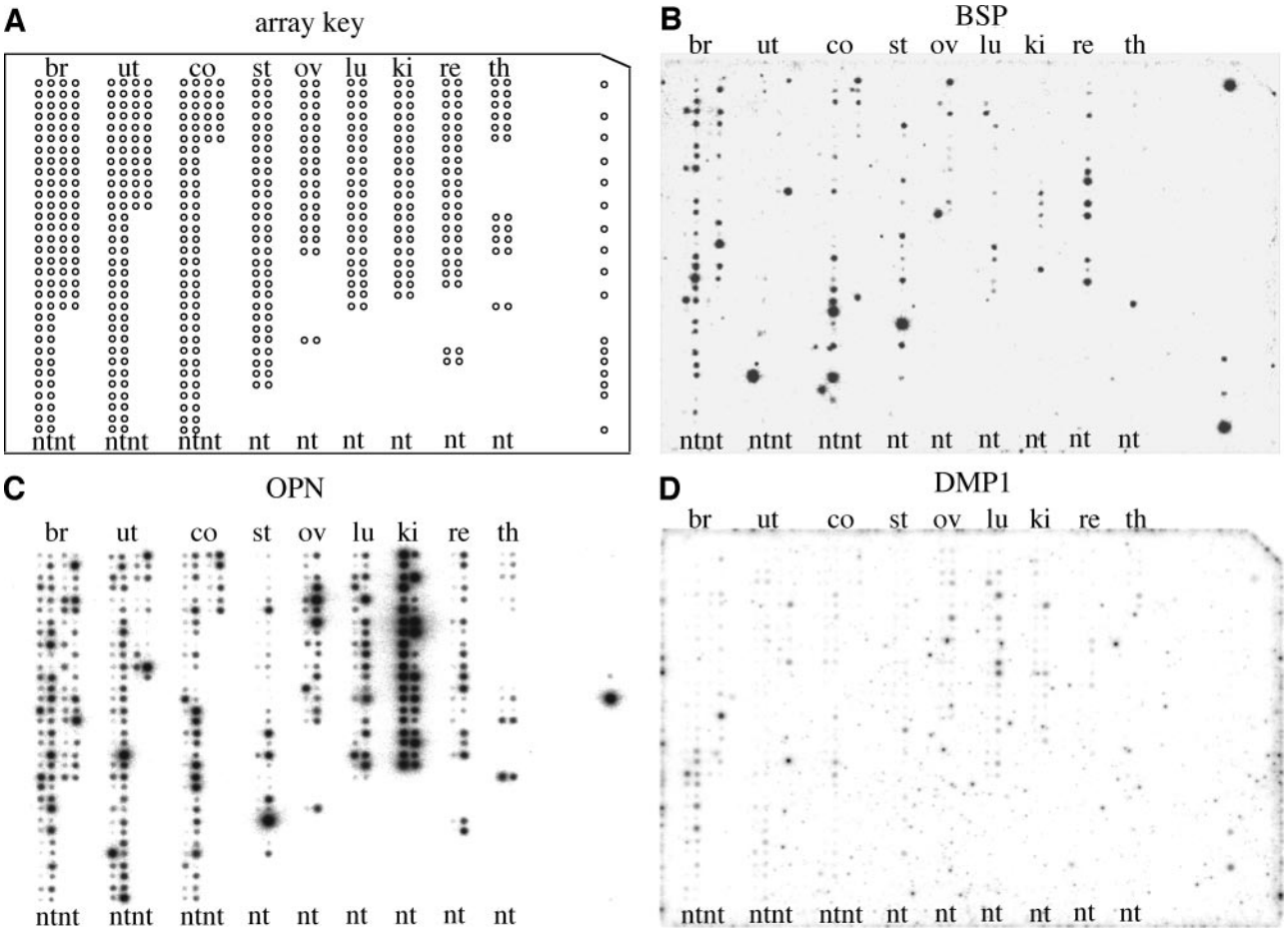

Fig. 1 SIBLING expression in different cancer types. A cancer profiling array was hybridized with cDNA probes for SIBLINGs. The arrays contained samples from 13 different types of cancer with paired normal and tumor tissue mRNA from individual subjects (*A*). The amount of hybridized probe for BSP (*B*), OPN (*C*), and DMP1 (*D*) was visualized by PhosphorImager. *br*, breast cancer; *ut*, uterine cancer; *co*, colon cancer; *st*, stomach cancer; *ov*, ovarian cancer; *lu*, lung cancer; *ki*, kidney cancer; *re*, rectal cancer; *th*, thyroid cancer; *n*, normal tissue; *t*, tumor tissue. Those hybridization spots that are not contiguous with the identified tumor types represent patient samples with tumor types too few in number to be statistically useful.

different cancer types. The cancer arrays were separately hybridized with probes for MMP-2, MMP-3, and MMP-9, and the expression values between normal tissue and the corresponding tumor sample for each patient were compared (Fig. 3). MMP-2 expression was significantly elevated in cancer of the colon, stomach, lung, and rectum. MMP-3 expression exhibited significant elevation in cancer of the breast, colon, stomach, and rectum. MMP-9 expression levels were significantly elevated in cancer of the breast, uterus, colon, stomach, ovary, lung, rectum, and kidney. The increases in expression ranged from 2- to 3-fold higher for MMP-2 and MMP-3, whereas expression levels were increased 2- to 7-fold for MMP-9.

Correlated Expression of SIBLINGs and Their Partner Matrix Metalloproteinases. Given the observed binding and activation specificity seen with SIBLINGs and their partner MMPs [BSP with MMP-2, OPN with MMP-3, and DMP1 with MMP-9 (11)], it was reasonable to postulate that SIBLINGs and their paired MMPs might exhibit correlated expression levels. When the levels of SIBLING and matched MMP expressed by individual tumors were analyzed by regression analysis, significant correlation was seen within different cancer types (Fig. 4). The expression of BSP and MMP-2 was significantly correlated in breast and colon cancer [$r^2 = 0.40$ ($P \leq 0.0001$) and $r^2 = 0.36$ ($P \leq 0.0001$), respectively]. OPN pairing with MMP-3 showed a significant correlation in stomach and ovarian cancer [$r^2 = 0.52$ ($P \leq 0.0001$) and $r^2 = 0.45$ ($P \leq 0.005$), respectively]. DMP1 and MMP-9 expression was significantly correlated in lung and kidney cancer [$r^2 = 0.60$ ($P \leq 0.001$) and $r^2 = 0.39$ ($P \leq 0.05$), respectively]. Mismatched pairs of BSP with MMP-3, OPN with MMP-2, or DMP1 with MMP-2, for example, showed no significant correlation (data not shown).

SIBLING Expression Is Distinct in Different Cancer Subtypes. Within cancers arising from a given tissue/organ, there are histopathologically defined subtypes that are often used in assessing disease course and treatment. There were sufficient numbers of breast cancer array samples to permit segregation by clinically defined subtypes of ductal *versus* lobular tumors. The results of microarray screening of SIBLING

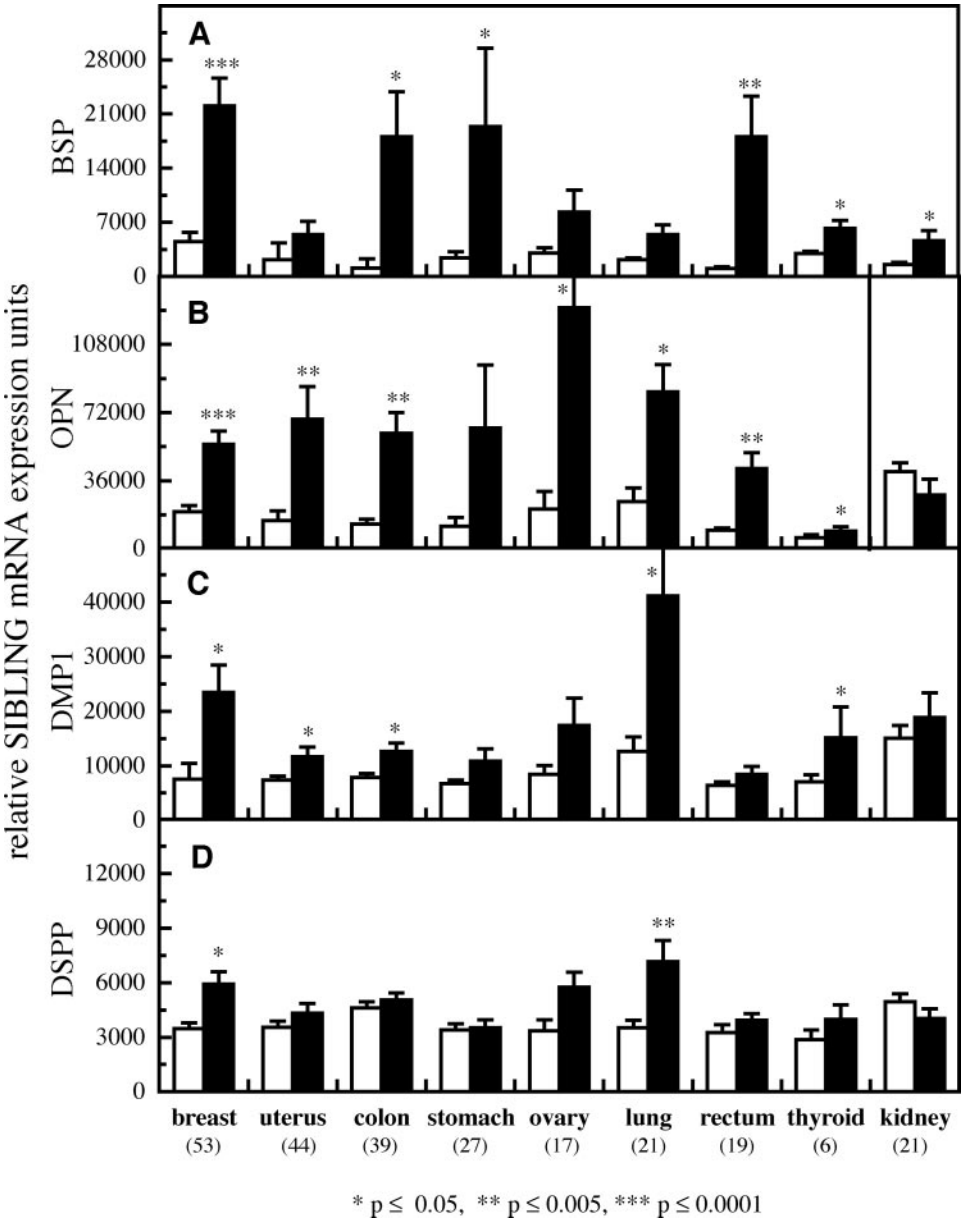

Fig. 2 SIBLING mRNAs are induced in multiple cancer types. Digitized exposures from Fig. 1 were quantified using ImageQuant software, and the mean values of relative expression of BSP (*A*), OPN (*B*), DMP1 (*C*), and DSPP (*D*) in normal tissue (□) and tumor tissue (■) were determined for each of nine different cancer types. *Asterisks* denote the statistical significance as determined by paired *t* tests. *, $P \leq 0.05$; **, $P \leq 0.005$; ***, $P \leq 0.0001$. *Error bars* represent the SE, and *numbers in parentheses* represent the number of subjects. OPN expression in both normal and tumor tissue from kidney is shown at one-tenth the actual mean values.

expression in breast cancer tissue were segregated by the pathological classification, and the average values of each group were compared (Fig. 5*A*). SIBLING mRNA levels were significantly higher in the ductal cancer groups, whereas the levels in the lobular group were intermediate between normal and ductal levels.

A similar analysis was carried out on uterine cancer samples, where there were sufficient numbers to permit segregation into clinically defined subtypes of adenocarcinoma, squamous cell, and benign tumors (Fig. 5*B*). OPN expression was significantly different between the two subtypes of malignant uterine tumors ($P \leq 0.005$) and between malignant and benign tumors ($P \leq 0.05$). The adenocarcinoma subtype expressed higher levels than the squamous cell subtype.

SIBLING Expression and Tumor Stage. Defined cancer stages represent how large the tumor is and how far it may have spread. The association of SIBLING expression levels with tumor progression was investigated by identifying tumor types with sufficient clinical detail to stratify into different tumor stages. Tumors from colon, rectal, and lung cancer were grouped by stage, and the distribution of SIBLINGs was compared (Fig. 6). In general, cancer stages mark tumors that were either localized and had a relatively small size (stage I), localized and larger in size (stage II), metastasized to lymph nodes (stage III), or metastasized to distant sites (stage IV). Colon cancer tumors exhibited mean values of BSP, OPN, DMP1, and DSPP that increased between stage I and stage III. Colon tumors with distant metastases exhibited SIBLING values with a sim-

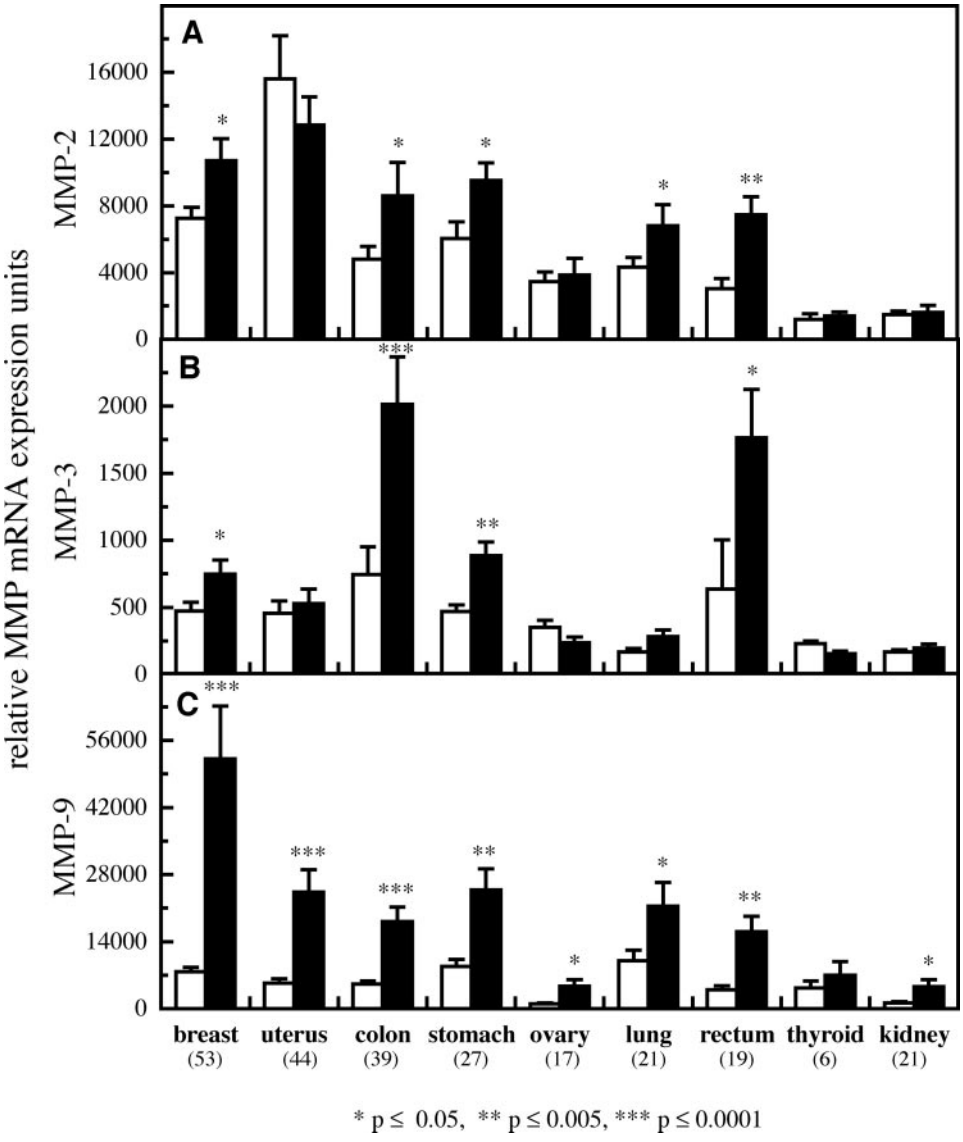

Fig. 3 MMP mRNAs are induced in multiple cancer types. Cancer profiling arrays were hybridized with cDNA probes for different MMPs, the amount of hybridized probe was quantified using ImageQuant software, and the mean values of expression of MMP-2 (*A*), MMP-3 (*B*), and MMP-9 (*C*) in normal tissue (□) and tumor tissue (■) were determined for each of nine different cancer types. *Asterisks* denote the statistical significance as determined by paired *t* tests. *, $P \leq 0.05$; **, $P \leq 0.005$; ***, $P \leq 0.0001$. *Error bars* represent the SE, and *numbers in parentheses* represent the number of subjects.

ilar or lower pattern of distribution than that of stage III tumors. Rectal cancer tumors showed increasing BSP, OPN, and DMP1 levels from stage I to stage IV, whereas DSPP values were unchanged across different stages. In lung cancer, BSP, OPN, and DSPP levels increased with increasing stage. When the association of SIBLING expression and tumor stage in colon cancer was analyzed by Spearman rank order correlation analysis, only BSP was significantly correlated (Table 1). In rectal tumors, BSP, OPN, and DMP1 levels correlated with stage, whereas for lung cancer, BSP, OPN, and DSPP levels correlated with stage.

Breast cancer tumors were stratified into tumor-node-metastasis (TNM) stages, which reflect tumor size (T), lymph node involvement (N), and metastatic state (M). Enough breast tumor samples were analyzed to enable the analysis of SIBLING expression and tumor progression. Tumors were grouped by TNM stage, and the stages were ordered in sequence of increasing progression. The sequence of tumors ranged from those with no nodal involvement or metastasis state (N_0M_0) that increased in size as well as N_1M_0 tumors that increased in size. For BSP, OPN, DMP1, and DSPP, significant differences were observed in the expression pattern as a function of tumor progression (Fig. 7; Table 1). Spearman rank order correlation analysis of SIBLING values and TNM stage yielded significant correlation for all four SIBLINGs.

DISCUSSION

Microarray technology has been typically used to screen the simultaneous expression of many genes using an array spotted with thousands of genes and measuring hybridization of target cDNA generated from a given tissue or cell type. In contrast, the cancer profiling array used in the current study was developed to enable the quantification of expression of a single

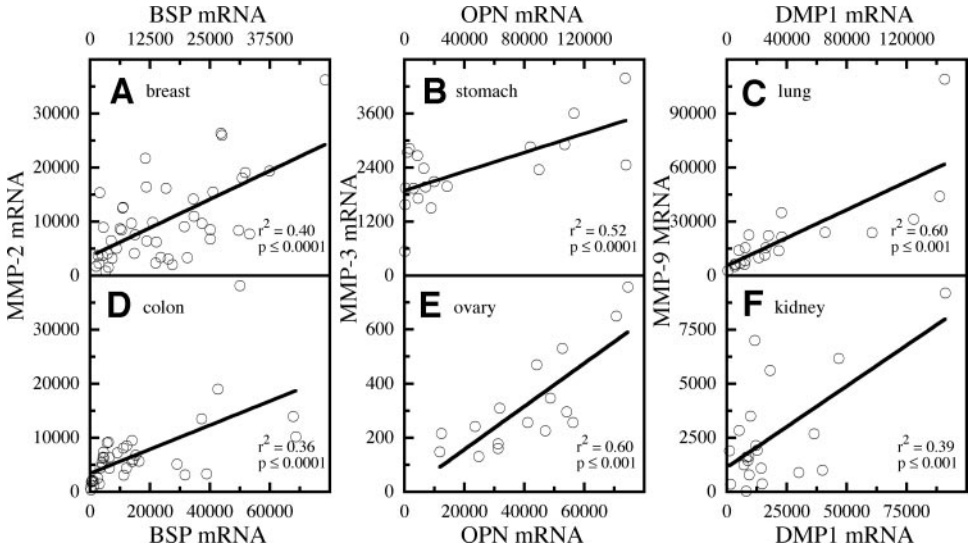

Fig. 4 Paired SIBLING and MMP expression is correlated in specific cancers. The expression levels of SIBLINGs and their respective binding partner MMPs were analyzed by regression analysis. BSP and MMP-2 levels in breast (*A*) and colon cancer (*D*), OPN and MMP-3 levels in stomach (*B*) and ovarian cancer (*E*), as well as DMP1 and MMP-9 levels in lung (*C*) and rectal cancer (*F*) were paired by subject and analyzed by regression analysis.

gene across multiple tissue types and tumor stages. The cancer profiling array contained multiple cDNA pairs from normal and tumor tissues including breast, uterus, colon, stomach, ovary, lung, kidney, rectum, thyroid, prostate, small intestine, pancreas, and cervix. Complementary DNA was generated by an efficient cDNA amplification technique that is based on the switching mechanism at the 5′ end of mRNA templates (17). This methodology has been shown to yield a high representation of mRNA transcripts, avoidance of biased amplification, linearity of signal, and recapitulation of the complexity of the original mRNA (12). Because the expression of individual housekeeping genes varies between normal and tumor tissue (18–20), the

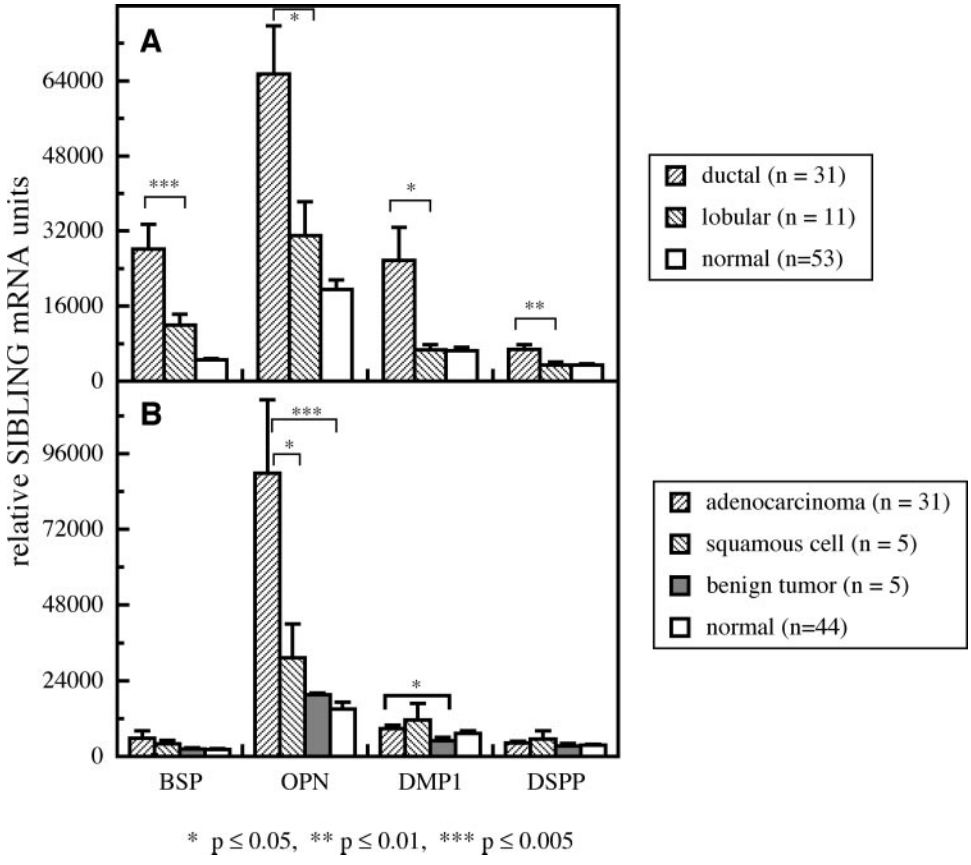

Fig. 5 SIBLING expression distinguishes cancer subtypes for breast and uterine tumors. The expression values of BSP, OPN, DMP1, and DSPP by breast cancer tumors were stratified by pathological classification (ductal *versus* lobular), and the average values were compared (*A*). Similarly, the expression of SIBLINGs by uterine tumors stratified into groups defined as adenocarcinoma, squamous cell, or benign tumor were averaged and compared (*B*). *Asterisks* denote the statistical significance as determined by *t* test. *, $P \leq 0.05$; **, $P \leq 0.01$; ***, $P \leq 0.005$. *Error bars* represent the SE.

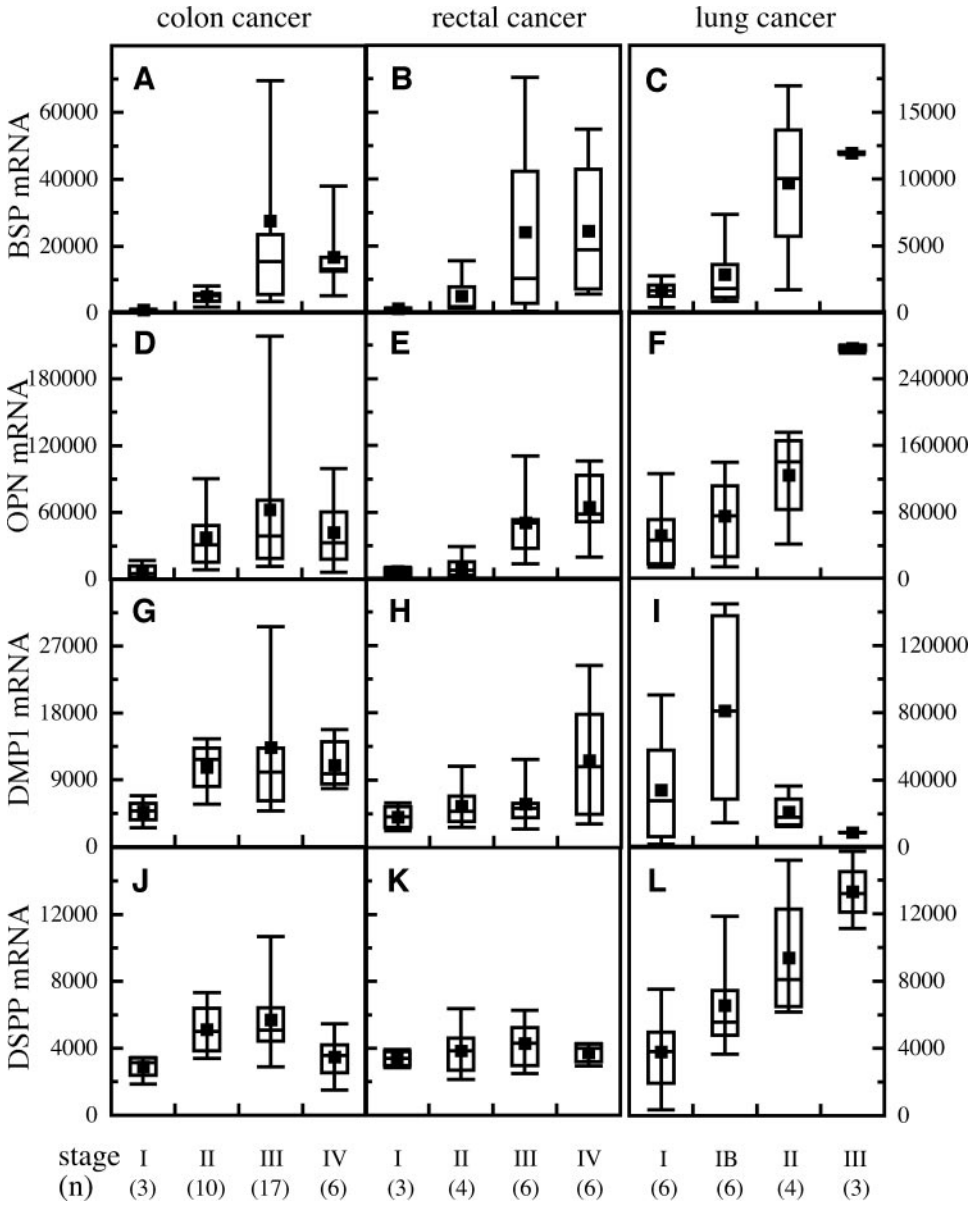

Fig. 6 Comparison of SIBLING mRNA levels with tumor stage in colon, rectal, and lung cancer. The expression values of BSP (*A*−*C*), OPN (*D*−*F*), DMP1 (*G*−*I*), and DSPP (*J*−*L*) by colon cancer tumors (*A*, *D*, *G*, and *J*), rectal cancer tumors (*B*, *E*, *H*, and *K*), and lung cancer tumors (*C*, *F*, *I*, and *L*) were stratified by pathological classification (stage), and the average values were compared. *Top line*, *bottom line*, and *line through the middle* correspond to 75th percentile, 25th percentile, and 50th percentile (median), respectively. *Error bar whiskers* represent the 10th and 90th percentile, whereas ■ indicates the arithmetic mean. Rectal and colon cancer stages were as follows: I, tumor invaded submucosa; II, tumor invaded through muscularis propia; III, invasive tumor with metastasis in one to three pericolic or perirectal lymph nodes; and IV, invasive tumor with metastasis in pericolic or perirectal lymph nodes and distant metastasis. Lung cancer stages were as follows: I, tumor $<$ 3 cm in greatest dimension; IB, tumor $>$ 3 cm in greatest dimension, involved main bronchus, associated with atelectasis or obstructive pneumonitis; II, metastasis to ipsilateral peribronchial and/or ipsolateral lymph nodes; and III, metastasis to ipsilateral mediastinal, and/or subcarinal lymph nodes. The number of subjects (*n*) for each group is shown at the *bottom*.

equal loading of cDNA onto the array membrane was carried out by normalizing to the average expression of three housekeeping genes: ubiquitin, β-actin, and M_r 23,000 highly basic protein (12, 21). The array has recently been used to profile a number of genes that exhibited either up- or down-regulation in cancer including gelsolin and glutathione peroxidase (12), netrin 1 (22), thiamin transporter THTR2 (23), PAGE 4 (24), and XAGE-1 (25). Strong correlation between tumor tissue expression by the current cDNA microarray and by *in situ* hybridization (24, 25) as well as reverse transcription-PCR and immunohistochemical staining (26, 27) has been observed.

The microarray design pairing normalized cDNA from an individual subject's tumor and normal tissue enabled differences in expression to be analyzed by paired *t* test, which provided a greater power to detect significant differences. Another method of evaluating the significance of biomarker elevation is to compare target tissue measures to a cut point of the mean of normal levels plus twice the SD (m + 2 SD). A value of $>m$ + 2 SD translates to a $<$5% probability that the elevation is due to chance (95% of normal values will lie within the m + 2 SD range). The overall significance of the microarray results was assessed by comparing concordance between these two methods of analysis, as well as comparison with the published results of other studies (Table 2). Elevated BSP expression was identified in two tissues (breast and thyroid), in agreement with previous studies. The current results for BSP did not replicate previous reports on elevated expression in cancer of the uterus or lung. Novel expression was identified in four different cancer types (colon, stomach, rectum, and kidney). Elevated OPN expression was observed in the current study in four different cancer types

Table 1 SIBLING expression and tumor staging

Spearman rank order correlation	BSP	OPN	DMP1	DSPP
Colon cancer*				
Spearman coefficient (r_S)	0.61	0.29	0.26	0.20
P	<0.001	>0.05	>0.05	>0.05
Rectal cancer*				
Spearman coefficient (r_S)	0.61	0.72	0.49	0.28
P	<0.005	<0.001	<0.05	>0.05
Lung cancer*				
Spearman coefficient (r_S)	0.70	0.70	−0.18	0.77
P	<0.001	<0.001	>0.05	<0.0005
Breast cancer†				
Spearman coefficient (r_S)	0.62	0.38	0.37	0.47
P	<0.0005	<0.05	<0.05	<0.005

* Spearman rank order correlation between mean SIBLING values and tumor stage. The Spearman coefficient value (r_S) is an adjusted value (corrected for ties). Tumor stages for colon, rectal, and lung cancer were defined as stated in the Fig. 5 legend.

† Correlation between mean SIBLING values and breast tumor progression. Spearman rank order correlation was performed on breast tumor SIBLING expression levels grouped by TNM stage and ordered across increasing progression ($T_1N_0M_0$, $T_2N_0M_0$, $T_3N_0M_0$, $T_1N_1M_0$, $T_2N_1M_0$, $T_3N_1M_0$). Breast tumor T stages were defined as stated in the Fig. 6 legend.

(breast, colon, ovary, and lung) in agreement with other published studies. For cancer of the stomach, thyroid, and kidney, the OPN expression levels and published literature were not in concordance. Novel expression of OPN in cancer of the uterus and rectum was identified. Elevated DMP1 expression was confirmed in lung cancer and newly identified in breast cancer. DMP1 levels in cancer of the uterus and colon, although significantly elevated by paired *t* test, did not satisfy the $>m + 2$

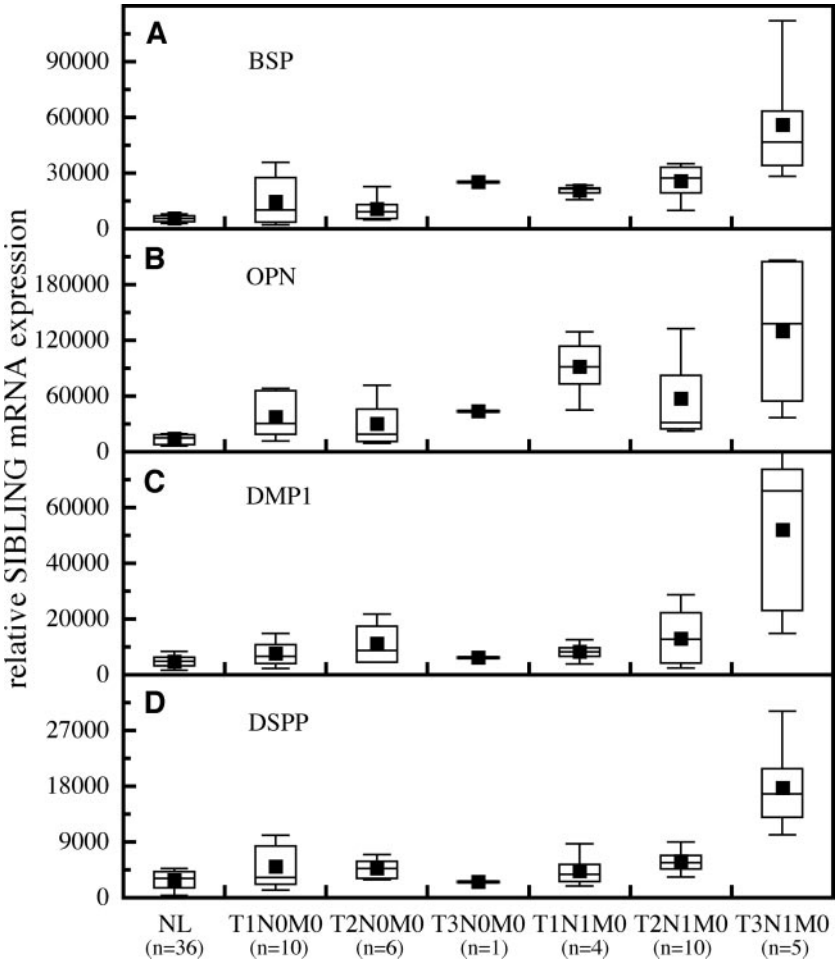

Fig. 7 Comparison of SIBLING mRNA levels and tumor stage in breast cancer. The expression values of BSP (*A*), OPN (*B*), DMP1 (*C*), and DSPP (*D*) by breast cancer tumors were stratified by increasing TNM stage, and the values were compared. *Top line*, *bottom line*, and *line through the middle* correspond to 75th percentile, 25th percentile, and 50th percentile (median), respectively. *Error bar whiskers* represent the 10th and 90th percentile, whereas ■ indicates the arithmetic mean. Breast cancer TNM staging was as follows: T_1, tumor ≤ 2 cm in greatest dimension; T_2, 2 cm < tumor < 5 cm; T_3, tumor > 5 cm; N_0, no regional lymph node metastasis; N_1, metastasis to movable ipsilateral axillary lymph node(s); N_2, metastasis to movable ipsilateral axillary lymph node(s) fixed to one another or to other structure; M_0, no distant metastasis; and M_1, distant metastasis. The number of subjects (*n*) for each group is shown at the *bottom*. The normal group consisted of the 36 normal breast tissue samples corresponding to the 36 paired tumor tissues with well-defined TNM stage.

Table 2 SIBLING expression in different cancer types

	Breast cancer	Uterine cancer	Colon cancer	Stomach cancer	Ovarian cancer	Lung cancer	Rectal cancer	Thyroid cancer	Kidney cancer
BSP									
t test*	Yes	No	Yes	Yes	No	No	Yes	Yes	Yes
$>m + 2$ SD†	Yes	No	Yes	Yes	Yes	Yes	Yes	Yes	Yes
Other studies (ref. no.)‡	4 and 28	29				7		8	
OPN									
t test*	Yes	Yes	Yes	No	Yes	Yes	Yes	Yes	No
$>m + 2$ SD†	Yes	Yes	Yes	Yes	Yes	Yes	Yes	No	No
Other studies (ref. no.)‡	30 and 31		32 and 33	34 and 35	36 and 37	38 and 39		40	2
DMP1									
t test*	Yes	Yes	Yes	No	No	Yes	No	No	No
$>m + 2$ SD†	Yes	No	No	No	No	Yes	No	No	No
Other studies (ref. no.)‡						9			
DSPP									
t test*	Yes	No	No	No	No	Yes	No	No	No
$>m + 2$ SD†	No	No	No	No	No	Yes	No	No	No
Other studies (ref. no.)‡									

* Significant elevation defined by a paired *t* test pairing individual subject's normal and tumor tissue expression levels.
† Significant elevation defined by a mean cancer tissue level of expression $>m + 2$SD.
‡ Published studies finding increased expression of SIBLINGs in a given tumor type.

SD criteria. DSPP expression was elevated significantly by both criteria in lung cancer, but only by paired *t* test in breast cancer. Cancers for which the two analysis methods were not in accordance are obvious targets for further, more extensive studies.

The observed increase in MMP-2 expression observed in tumor samples is consistent with previous studies of breast (41, 42), colon (43–47), stomach (48, 49), lung (50–53), rectal (43, 54), and kidney cancer (55–57). Whereas a strong association of increased MMP-3 has been found in breast cancer (41, 58–61), the increased expression levels observed in other tumor types are not as well supported by published literature. Altered MMP-3 levels have been observed in colon (62–64), stomach (65–67), and rectal (68) cancer, although in some cases, the increases were relatively small. In addition, studies have indicated that the MMP-3 source was not necessarily tumor cell but stromal cell or another infiltrating cell type, distinct from the tumor. The observed increases in MMP-9 expression are consistent with published studies of breast (41, 69), uterine (70, 71), colon (46, 53, 72), stomach (73–75), ovarian (76, 77), lung (50, 78), rectal (43, 79), and kidney cancer (56, 80).

A correlation of SIBLING message expression levels with MMP message levels of their partners (BSP with MMP-2, OPN with MMP-3, and DMP1 with MMP-9) was observed. That, in association with the recently described ability of these SIBLINGs to bind to and modulate the activity of specific MMPs, suggests that the same factors that activate SIBLING genes in tumor progression may be the same ones that can activate the corresponding MMP genes. It is also possible that the expression of one SIBLING member in a tumor may induce the production of its corresponding MMP partner, or *vice versa*. Interestingly, SIBLING production by tumors could facilitate angiogenesis because both BSP and OPN have been shown to possess angiogenesis activity *in vivo* (81, 82).

SIBLING expression was different between different subtypes of cancer. Whereas the historical basis for the distinction between the main two types of breast cancer (the belief that ductal carcinomas arose from ducts and lobular carcinomas from lobules) is subject to debate (both can arise from the terminal duct lobular unit), there is evidence that the two classes as used clinically refer to disease entities that differ in tumor size, shape, dissemination, and proliferation rates (83). The most common hallmark associated with the lobular classification is multifocality. Lobular tumors tend to be more slowly proliferating than ductal tumors. They also tend to frequently exhibit hormone receptor positivity and show distinct chromosomal changes (84, 85). The more rapidly progressing ductal tumors had an associated higher level of SIBLING expression. OPN was recently identified by microarray analysis as a discriminating marker between ductal and lobular cancer (86). In our current study, OPN, as well as BSP, DMP1, and DSPP were significantly different between lobular and ductal tumors. Similarly, the association of higher OPN expression with adenocarcinomas as opposed to squamous cell carcinomas in uterine cancer may be associated with different size, shape, and progression rates.

SIBLING expression correlated with tumor stages associated with changing size and lymph node involvement. These observations are consistent with SIBLING expression coupled with MMP activity modulation having an effect on early tumor progression. These results suggest SIBLINGs as potential markers of early disease progression in a number of different cancers. Future studies of SIBLING expression and serum levels will address the degree to which these tumor biomarkers can be correlated with disease progression.

REFERENCES

1. Fisher LW, Fedarko NS. Six genes expressed in bones and teeth encode the current members of the SIBLING family of proteins. Connect Tissue Res 2003;44(Suppl 1):33–40.

2. Brown LF, Papadopoulos-Sergiou A, Berse B, et al. Osteopontin expression and distribution in human carcinomas. Am J Pathol 1994; 145:610–23.

3. Coppola D, Szabo M, Boulware D, et al. Correlation of osteopontin protein expression and pathological stage across a wide variety of tumor histologies. Clin Cancer Res 2004;10:184–90.

4. Bellahcene A, Merville MP, Castronovo V. Expression of bone sialoprotein, a bone matrix protein, in human breast cancer. Cancer Res 1994;54:2823–6.

5. Waltregny D, Bellahcene A, de Leval X, et al. Increased expression of bone sialoprotein in bone metastases compared with visceral metastases in human breast and prostate cancers. J Bone Miner Res 2000;15: 834–43.

6. Waltregny D, Bellahcene A, Van Riet I, et al. Prognostic value of bone sialoprotein expression in clinically localized human prostate cancer. J Natl Cancer Inst (Bethesda) 1998;90:1000–8.

7. Bellahcene A, Maloujahmoum N, Fisher LW, et al. Expression of bone sialoprotein in human lung cancer. Calcif Tissue Int 1997;61: 183–8.

8. Bellahcene A, Albert V, Pollina L, et al. Ectopic expression of bone sialoprotein in human thyroid cancer. Thyroid 1998;8:637–41.

9. Chaplet M, De Leval L, Waltregny D, et al. Dentin matrix protein 1 is expressed in human lung cancer. J Bone Miner Res 2003;18:1506–12.

10. Rowe PS, de Zoysa PA, Dong R, et al. MEPE, a new gene expressed in bone marrow and tumors causing osteomalacia. Genomics 2000;67:54–68.

11. Fedarko NS, Jain A, Karadag A, Fisher LW. Three small integrin binding ligand N-linked glycoproteins (SIBLINGs) bind and activate specific matrix metalloproteinases. FASEB J 2004;18:734–6.

12. Zhumabayeva B, Diatchenko L, Chenchik A, Siebert PD. Use of SMART-generated cDNA for gene expression studies in multiple human tumors. Biotechniques 2001;30:158–63.

13. Fisher LW, McBride OW, Termine JD, Young MF. Human bone sialoprotein. Deduced protein sequence and chromosomal localization. J Biol Chem 1990;265:2347–51.

14. Oldberg A, Franzen A, Heinegard D. Cloning and sequence analysis of rat bone sialoprotein (osteopontin) cDNA reveals an Arg-Gly-Asp cell-binding sequence. Proc Natl Acad Sci USA 1986;83:8819–23.

15. Hirst KL, Simmons D, Feng J, et al. Elucidation of the sequence and the genomic organization of the human dentin matrix acidic phosphoprotein 1 (DMP1) gene: exclusion of the locus from a causative role in the pathogenesis of dentinogenesis imperfecta type II. Genomics 1997; 42:38–45.

16. Freije JM, Balbin M, Pendas AM, et al. Matrix metalloproteinases and tumor progression. Adv Exp Med Biol 2003;532:91–107.

17. Chenchik A, Zhu YY, Diatchenko L, Li R, Hill J, Siebert PD. Generation and use of high-quality cDNA from small amounts of total RNA by SMART PCR. In: Siebert P, Larrick J, editors. Gene Cloning and Analysis by RT-PCR. Natick, MA: Eaton Publishing; 1998. p. 305–19.

18. Blanquicett C, Johnson MR, Heslin M, Diasio RB. Housekeeping gene variability in normal and carcinomatous colorectal and liver tissues: applications in pharmacogenomic gene expression studies. Anal Biochem 2002;303:209–14.

19. Rondinelli RH, Epner DE, Tricoli JV. Increased glyceraldehyde-3-phosphate dehydrogenase gene expression in late pathological stage human prostate cancer. Prostate Cancer Prostatic Dis 1997;1:66–72.

20. Aerts JL, Gonzales MI, Topalian SL. Selection of appropriate control genes to assess expression of tumor antigens using real-time RT-PCR. Biotechniques 2004;36:84–6, 88, 90–1.

21. Zhumabayeva B, Chenchik A, Siebert PD, Herrler M. Disease profiling arrays: reverse format cDNA arrays complimentary to microarrays. Adv Biochem Eng Biotechnol 2004;86:191–213.

22. Thiebault K, Mazelin L, Pays L, et al. The netrin-1 receptors UNC5H are putative tumor suppressors controlling cell death commitment. Proc Natl Acad Sci USA 2003;100:4173–8.

23. Liu S, Huang H, Lu X, et al. Down-regulation of thiamine transporter THTR2 gene expression in breast cancer and its association with resistance to apoptosis. Mol Cancer Res 2003;1:665–73.

24. Iavarone C, Wolfgang C, Kumar V, et al. PAGE4 is a cytoplasmic protein that is expressed in normal prostate and in prostate cancers. Mol Cancer Ther 2002;1:329–35.

25. Egland KA, Kumar V, Duray P, Pastan I. Characterization of overlapping XAGE-1 transcripts encoding a cancer testis antigen expressed in lung, breast, and other types of cancers. Mol Cancer Ther 2002;1:441–50.

26. Sers C, Husmann K, Nazarenko I, et al. The class II tumour suppressor gene H-REV107-1 is a target of interferon-regulatory factor-1 and is involved in IFNgamma-induced cell death in human ovarian carcinoma cells. Oncogene 2002;21:2829–39.

27. Wiechen K, Diatchenko L, Agoulnik A, et al. Caveolin-1 is down-regulated in human ovarian carcinoma and acts as a candidate tumor suppressor gene. Am J Pathol 2001;159:1635–43.

28. Bellahcene A, Menard S, Bufalino R, Moreau L, Castronovo V. Expression of bone sialoprotein in primary human breast cancer is associated with poor survival. Int J Cancer 1996;69:350–3.

29. Detry C, Waltregny D, Quatresooz P, et al. Detection of bone sialoprotein in human (pre)neoplastic lesions of the uterine cervix. Calcif Tissue Int 2003;73:9–14.

30. Gillespie MT, Thomas RJ, Pu ZY, et al. Calcitonin receptors, bone sialoprotein and osteopontin are expressed in primary breast cancers. Int J Cancer 1997;73:812–5.

31. Tuck AB, O'Malley FP, Singhal H, et al. Osteopontin expression in a group of lymph node negative breast cancer patients. Int J Cancer 1998;79:502–8.

32. Yeatman TJ, Chambers AF. Osteopontin and colon cancer progression. Clin Exp Metastasis 2003;20:85–90.

33. Agrawal D, Chen T, Irby R, et al. Osteopontin identified as lead marker of colon cancer progression, using pooled sample expression profiling. J Natl Cancer Inst (Bethesda) 2002;94:513–21.

34. Maeng HY, Choi DK, Takeuchi M, et al. Appearance of osteonectin-expressing fibroblastic cells in early rat stomach carcinogenesis and stomach tumors induced with N-methyl-N′-nitro-N-nitrosoguanidine. Jpn J Cancer Res 2002;93:960–7.

35. Ue T, Yokozaki H, Kitadai Y, et al. Co-expression of osteopontin and CD44v9 in gastric cancer. Int J Cancer 1998;79:127–32.

36. Kim JH, Skates SJ, Uede T, et al. Osteopontin as a potential diagnostic biomarker for ovarian cancer. JAMA 2002;287:1671–9.

37. Tiniakos DG, Yu H, Liapis H. Osteopontin expression in ovarian carcinomas and tumors of low malignant potential (LMP). Hum Pathol 1998;29:1250–4.

38. Zhang J, Takahashi K, Takahashi F, et al. Differential osteopontin expression in lung cancer. Cancer Lett 2001;171:215–22.

39. Chambers AF, Wilson SM, Kerkvliet N, et al. Osteopontin expression in lung cancer. Lung Cancer 1996;15:311–23.

40. Tunio GM, Hirota S, Nomura S, Kitamura Y. Possible relation of osteopontin to development of psammoma bodies in human papillary thyroid cancer. Arch Pathol Lab Med 1998;122:1087–90.

41. Lebeau A, Nerlich AG, Sauer U, Lichtinghagen R, Lohrs U. Tissue distribution of major matrix metalloproteinases and their transcripts in human breast carcinomas. Anticancer Res 1999;19:4257–64.

42. Onisto M, Riccio MP, Scannapieco P, et al. Gelatinase A/TIMP-2 imbalance in lymph-node-positive breast carcinomas, as measured by RT-PCR. Int J Cancer 1995;63:621–6.

43. Liabakk NB, Talbot I, Smith RA, Wilkinson K, Balkwill F. Matrix metalloprotease 2 (MMP-2) and matrix metalloprotease 9 (MMP-9) type IV collagenases in colorectal cancer. Cancer Res 1996;56:190–6.

44. Ornstein DL, MacNab J, Cohn KH. Evidence for tumor-host cooperation in regulating MMP-2 expression in human colon cancer. Clin Exp Metastasis 1999;17:205–12.

45. Karakiulakis G, Papanikolaou C, Jankovic SM, et al. Increased type IV collagen-degrading activity in metastases originating from primary tumors of the human colon. Invasion Metastasis 1997;17:158–68.

46. Collins HM, Morris TM, Watson SA. Spectrum of matrix metalloproteinase expression in primary and metastatic colon cancer: relationship to the tissue inhibitors of metalloproteinases and membrane type-1-matrix metalloproteinase. Br J Cancer 2001;84:1664–70.

47. Papadopoulou S, Scorilas A, Arnogianaki N, et al. Expression of gelatinase-A (MMP-2) in human colon cancer and normal colon mucosa. Tumour Biol 2001;22:383–9.

48. Mori M, Mimori K, Shiraishi T, et al. Analysis of MT1-MMP and MMP2 expression in human gastric cancers. Int J Cancer 1997;74: 316–21.

49. Ohtani H, Nagai T, Nagura H. Similarities of in situ mRNA expression between gelatinase A (MMP-2) and type I procollagen in human gastrointestinal carcinoma: comparison with granulation tissue reaction. Jpn J Cancer Res 1995;86:833–9.

50. Nakagawa H, Yagihashi S. Expression of type IV collagen and its degrading enzymes in squamous cell carcinoma of lung. Jpn J Cancer Res 1994;85:934–8.

51. Yamamoto M, Mohanam S, Sawaya R, et al. Differential expression of membrane-type matrix metalloproteinase and its correlation with gelatinase A activation in human malignant brain tumors in vivo and in vitro. Cancer Res 1996;56:384–92.

52. Suzuki M, Iizasa T, Fujisawa T, et al. Expression of matrix metalloproteinases and tissue inhibitor of matrix metalloproteinases in non-small-cell lung cancer. Invasion Metastasis 1998;18:134–41.

53. Creighton C, Hanash S. Expression of matrix metalloproteinase 9 (MMP-9/gelatinase B) in adenocarcinomas strongly correlated with expression of immune response genes. In Silico Biol 2003;3:301–11.

54. Chan CC, Menges M, Orzechowski HD, et al. Increased matrix metalloproteinase 2 concentration and transcript expression in advanced colorectal carcinomas. Int J Colorectal Dis 2001;16:133–40.

55. Kitagawa Y, Kunimi K, Uchibayashi T, Sato H, Namiki M. Expression of messenger RNAs for membrane-type 1, 2, and 3 matrix metalloproteinases in human renal cell carcinomas. J Urol 1999;162: 905–9.

56. Hagemann T, Gunawan B, Schulz M, Fuzesi L, Binder C. mRNA expression of matrix metalloproteases and their inhibitors differs in subtypes of renal cell carcinomas. Eur J Cancer 2001;37:1839–46.

57. Slaton JW, Inoue K, Perrotte P, et al. Expression levels of genes that regulate metastasis and angiogenesis correlate with advanced pathological stage of renal cell carcinoma. Am J Pathol 2001;158:735–43.

58. Freije JM, Diez-Itza I, Balbin M, et al. Molecular cloning and expression of collagenase-3, a novel human matrix metalloproteinase produced by breast carcinomas. J Biol Chem 1994;269:16766–73.

59. Basset P, Bellocq JP, Anglard P, et al. Stromelysin-3 and other stromelysins in breast cancer: importance of epithelialstromal interactions during tumor progression. Cancer Treat Res 1996;83:353–67.

60. Iwata H, Kobayashi S, Iwase H, et al. Production of matrix metalloproteinases and tissue inhibitors of metalloproteinases in human breast carcinomas. Jpn J Cancer Res 1996;87:602–11.

61. Chenard MP, O'Siorain L, Shering S, et al. High levels of stromelysin-3 correlate with poor prognosis in patients with breast carcinoma. Int J Cancer 1996;69:448–51.

62. Baker EA, Bergin FG, Leaper DJ. Matrix metalloproteinases, their tissue inhibitors and colorectal cancer staging. Br J Surg 2000;87: 1215–21.

63. Gallegos NC, Smales C, Savage FJ, Hembry RM, Boulos PB. The distribution of matrix metalloproteinases and tissue inhibitor of metalloproteinases in colorectal cancer. Surg Oncol 1995;4:21–9.

64. Matrisian LM, Wright J, Newell K, Witty JP. Matrix-degrading metalloproteinases in tumor progression. Princess Takamatsu Symp 1994;24:152–61.

65. Murray GI, Duncan ME, Arbuckle E, Melvin WT, Fothergill JE. Matrix metalloproteinases and their inhibitors in gastric cancer. Gut 1998;43:791–7.

66. Nomura H, Fujimoto N, Seiki M, Mai M, Okada Y. Enhanced production of matrix metalloproteinases and activation of matrix metalloproteinase 2 (gelatinase A) in human gastric carcinomas. Int J Cancer 1996;69:9–16.

67. Saarialho-Kere UK, Vaalamo M, Puolakkainen P, et al. Enhanced expression of matrilysin, collagenase, and stromelysin-1 in gastrointestinal ulcers. Am J Pathol 1996;148:519–26.

68. Imai K, Yokohama Y, Nakanishi I, et al. Matrix metalloproteinase 7 (matrilysin) from human rectal carcinoma cells. Activation of the precursor, interaction with other matrix metalloproteinases and enzymic properties. J Biol Chem 1995;270:6691–7.

69. Pacheco MM, Mourao M, Mantovani EB, Nishimoto IN, Brentani MM. Expression of gelatinases A and B, stromelysin-3 and matrilysin genes in breast carcinomas: clinico-pathological correlations. Clin Exp Metastasis 1998;16:577–85.

70. Davidson B, Goldberg I, Liokumovich P, et al. Expression of metalloproteinases and their inhibitors in adenocarcinoma of the uterine cervix. Int J Gynecol Pathol 1998;17:295–301.

71. Davidson B, Goldberg I, Kopolovic J, et al. Expression of matrix metalloproteinase-9 in squamous cell carcinoma of the uterine cervix-clinicopathologic study using immunohistochemistry and mRNA in situ hybridization. Gynecol Oncol 1999;72:380–6.

72. Takeha S, Fujiyama Y, Bamba T, et al. Stromal expression of MMP-9 and urokinase receptor is inversely associated with liver metastasis and with infiltrating growth in human colorectal cancer: a novel approach from immune/inflammatory aspect. Jpn J Cancer Res 1997; 88:72–81.

73. Parsons SL, Watson SA, Collins HM, et al. Gelatinase (MMP-2 and -9) expression in gastrointestinal malignancy. Br J Cancer 1998;78: 1495–502.

74. Torii A, Kodera Y, Ito M, et al. Matrix metalloproteinase 9 in mucosally invasive gastric cancer. Gastric Cancer 1998;1:142–5.

75. Wang L, Zhang LH, Li YL, Liu Z. Expression of MMP-9 and MMP-9 mRNA in gastric carcinoma and its correlation with angiogenesis [in Chinese]. Zhonghua Yi Xue Za Zhi 2003;83:782–6.

76. Sakata K, Shigemasa K, Nagai N, Ohama K. Expression of matrix metalloproteinases (MMP-2, MMP-9, MT1-MMP) and their inhibitors (TIMP-1, TIMP-2) in common epithelial tumors of the ovary. Int J Oncol 2000;17:673–81.

77. Davidson B, Goldberg I, Gotlieb WH, et al. High levels of MMP-2, MMP-9, MT1-MMP and TIMP-2 mRNA correlate with poor survival in ovarian carcinoma. Clin Exp Metastasis 1999;17:799–808.

78. Kremer EA, Chen Y, Suzuki K, Nagase H, Gorski JP. Hydroxyapatite induces autolytic degradation and inactivation of matrix metalloproteinase-1 and -3. J Bone Miner Res 1998;13:1890–902.

79. Roeb E, Dietrich CG, Winograd R, et al. Activity and cellular origin of gelatinases in patients with colon and rectal carcinoma differential activity of matrix metalloproteinase-9. Cancer (Phila) 2001;92: 2680–91.

80. Inoue K, Kamada M, Slaton JW, et al. The prognostic value of angiogenesis and metastasis-related genes for progression of transitional cell carcinoma of the renal pelvis and ureter. Clin Cancer Res 2002;8: 1863–70.

81. Hirama M, Takahashi F, Takahashi K, et al. Osteopontin overproduced by tumor cells acts as a potent angiogenic factor contributing to tumor growth. Cancer Lett 2003;198:107–17.

82. Bellahcene A, Bonjean K, Fohr B, et al. Bone sialoprotein mediates human endothelial cell attachment and migration and promotes angiogenesis. Circ Res 2000;86:885–91.

83. Sainsbury JRC, Anderson TJ, Morgan DAL. Breast cancer. Br Med J 2000;321:745–50.

84. Coradini D, Pellizzaro C, Veneroni S, Ventura L, Daidone MG. Infiltrating ductal and lobular breast carcinomas are characterized by different interrelationships among markers related to angiogenesis and hormone dependence. Br J Cancer 2002;87:1105–11.

85. Gunther K, Merkelbach-Bruse S, Amo-Takyi BK, et al. Differences in genetic alterations between primary lobular and ductal breast cancers detected by comparative genomic hybridization. J Pathol 2001;193: 40–7.

86. Korkola JE, DeVries S, Fridlyand J, et al. Differentiation of lobular versus ductal breast carcinomas by expression microarray analysis. Cancer Res 2003;63:7167–75.

Dentin Matrix Protein 1 Enhances Invasion Potential of Colon Cancer Cells by Bridging Matrix Metalloproteinase-9 to Integrins and CD44

Abdullah Karadag,[1] Neal S. Fedarko,[1,2] and Larry W. Fisher[1]

[1]Craniofacial and Skeletal Diseases Branch, National Institute of Dental and Craniofacial Research, NIH, Department of Health and Human Services, Bethesda, Maryland and [2]Division of Geriatrics, Department of Medicine, Johns Hopkins University School of Medicine, Baltimore, Maryland

Abstract

The up-regulation of various matrix metalloproteinases (MMP), certain cell receptors such as integrins and CD44, and the SIBLING family of integrin-binding glycophosphoproteins have been reported separately and in various combinations for many types of tumors. The mechanisms by which these different proteins may be interacting and enhancing the ability of a cancer cell to survive and metastasize have become an interesting issue in cancer biology. Dentin matrix protein 1 (DMP1) has been known for a number of years to bind to CD44 and ArgGlyAsp sequence–dependent integrins. This SIBLING was recently shown to be able to specifically bind and activate proMMP-9 and to make MMP-9 much less sensitive to inhibition by tissue inhibitors of metalloproteinases and synthetic inhibitors. In this study, we used a modified Boyden chamber assay to show that DMP1 enhanced the invasiveness of the MMP-9 expressing colon cancer cell line, SW480, through Matrigel in a dose-dependant manner. DMP1 (100 nmol/L) increased invasion 4-fold over controls (86.1 $\pm$ 13.9 versus 22.3 $\pm$ 9.8, $P < 0.001$). The enhanced invasive potential required the presence of MMP-9 and at least one of the cell surface receptors, CD44, $\alpha_v\beta_3$, or $\alpha_v\beta_5$ integrin. The bridging of MMP-9 to the cell surface receptors was shown by both pull-down and fluorescence activated cell sorting experiments. Because all of these proteins were also shown by immunohistochemistry to be expressed in serial sections of a colon adenocarcinoma, we have hypothesized that the MMP-9/DMP1/cell surface complexes observed to enhance cell invasion *in vitro* may be aiding metastatic events *in vivo*. (Cancer Res 2005; 65(24): 11545-52)

Introduction

Dentin matrix protein 1 (DMP1) is an acidic phosphoglycoprotein and member of the integrin-binding SIBLING protein family (1). All of the SIBLINGs have been shown over the years to be up-regulated in many different primary tumors but curiously are often not expressed in high-passage cell lines derived from these tumors. DMP1, historically thought to be expressed in only bones and teeth, has recently been shown to be made in some normal ductal epithelial tissues as well (2, 3). Although the precise functions of the protein have not been explicated, it has been associated with the regulation of postnatal chondrogenesis and subsequent osteogenesis and matrix mineralization (2, 4–6). DMP1 has been shown to bind both $\alpha_v\beta_3$ integrin and CD44 cell surface molecules (7). Several studies have shown significantly elevated expression of DMP1 in a number of cancerous tissues, including lung (8), breast, uterus, thyroid, and colon (9). DMP1 has been shown to bind with nanomolar affinity and to activate latent matrix metalloproteinase-9 (proMMP-9) apparently without removal of its propeptide. It can bind active MMP-9 without changing the ability of protease to digest natural substrates and causes the protease to remain active in the presence of normally inhibitory amounts of tissue inhibitors of metalloproteinase 1 (TIMP1) *in vitro* (10). Up-regulation of MMP-9 has been described for many types of cancers, including colon cancer (11), and it has been used in a portal blood assay to determine colorectal metastases in liver (12). Furthermore, the increased expression of MMP-9 in primary colon tumors has been associated with liver metastases (13) and was increased in biopsy samples from patients with colon cancer (14). We have recently shown by array analysis that there is a coordinate increase in MMP-9 and DMP1 expression in lung and kidney cancer (9). The $\alpha_v\beta_3$ and $\alpha_v\beta_5$ integrins have also been associated with colon cancer metastasizing to liver in an orthotopic murine model (15). CD44 expression has been linked to transendothelial migration of colon cancer cell lines (16) and to the invasion of colorectal cancer cell lines that also showed increased MMP-9 expression (17). Another member of the SIBLING family, bone sialoprotein (BSP), promotes invasion of several osteotropic cancer cell lines by localizing MMP-2 on the cell surface through $\alpha_v\beta_3$ integrin (18). DMP1 had no effect on the invasion of the recombinant BSP-responsive cancer cell lines, suggesting that MMP-2 was the rate-limiting protease for those particular cell lines in the modified Boyden chamber assay.

MMPs are a class of zinc-dependent endopeptidases that are collectively capable of digesting all extracellular matrix components. These proteases play an important role in remodeling the extracellular matrix and their regulation is implicated in a variety of diseases, including cancer invasion and metastasis (19). The regulation of MMP activity in tumor cell invasion and metastasis involves selective expression as well as a balance of activators, inhibitors, and regulators. The first step in invasion generally requires digestion of basement membrane proteins, including type IV collagen. MMP-2, MMP-3, MMP-7, MMP-9, and MMP-10 are all able to degrade this collagen (20). MMP-2 (gelatinase A) and MMP-9 (gelatinase B) have long been known to degrade extracellular matrix macromolecules in basement membranes and other interstitial connective tissues (21). It has been shown that the localization of active MMP-9 on the cell membrane of the invasive cell through association with CD44 can be critical for tumor cell invasion and metastasis (22). Similarly, MMP-2 localization on the cancer cell surfaces through $\alpha_v\beta_3$ integrin has been reported to be important in the initiation of invasion of several cancer cells (18, 23, 24). Therefore, understanding the interaction of MMPs, cell adhesion molecules, and any modifying proteins could offer insight into cancer biology.

Requests for reprints: Larry W. Fisher, Craniofacial and Skeletal Diseases Branch, National Institute of Dental and Craniofacial Research, NIH, Department of Health and Human Services, Room 228, Building 30, 9000 Rockville Pike, Bethesda, MD 20892-4320. Phone: 301-496-5769; Fax: 301-402-0824; E-mail: lfisher@dir.nidcr.nih.gov.

doi:10.1158/0008-5472.CAN-05-2861

We hypothesized that DMP1 may play a role in cancer metastasis by bridging MMP-9 to the cell surface through $\alpha_v\beta_3$ integrin, $\alpha_v\beta_5$ integrin, and/or CD44. To test this hypothesis, both fluorescence-activated cell sorting (FACS) analysis and a previously described modified Boyden chamber invasion assay were used (25) to measure the enhancement of invasion by DMP1 for the colon cancer cell line, SW480, cells known to expresses significant amounts of MMP-9 *in vitro*.

Materials and Methods

Materials. The human colon cancer cell line SW480 (CCL-228) was obtained from the American Type Culture Collection (Manassas, VA). Fetal bovine serum (FBS) was purchased from Equitech-Bio, Inc. (Kerrville, TX). RPMI 1640, L-glutamine, 2-mercaptoethanol, sodium pyruvate, modified Eagle's medium (MEM) nonessential amino acids, HBSS, PBS, Versene (0.53 mmol/L EDTA in PBS), and 10% zymogram gelatin gels were from Invitrogen, Inc. (Carlsbad, CA). Matrigel was from Collaborative Research, Inc. (Bedford, MA). Transwell inserts and companion plates were purchased from BD Biosciences Discovery Labware (Bedford, MA). Calcein acetoxymethyl ester dye and the Alexa Fluor 488 protein-labeling kit were purchased from Molecular Probes, Inc. (Eugene, OR). Mouse anti-human $\alpha_v\beta_3$ integrin monoclonal antibody (mAb) immobilized on immunoaffinity gel matrix (GEM1976), mouse antihuman $\alpha_v\beta_5$ integrin mAb immobilized on immunoaffinity gel matrix (GEM1961), antihuman $\alpha_v\beta_3$ integrin mAb (LM609, MAB1976Z), antihuman $\alpha_v\beta_5$ integrin mAb (P1F6, MAB1961Z), recombinant $\alpha_v\beta_3$ integrin in Triton X-100 (CC1018), and recombinant $\alpha_v\beta_5$ integrin in Triton X-100 (CC1025) were obtained from Chemicon International, Inc. (Temecula, CA). Antihuman CD44 mAb (BU75) was purchased from Ancell Corporation (Bayport, MN). ProMMP-9 was from Oncogene Research Products (Boston, MA). ProbeQuant G-50 microcolumns were from Amersham Pharmacia Biotech, Inc. (Piscataway, NJ). Microcon YM-30 centrifugal filter devices were from Millipore Corporation (Bedford, MA).

Cell culture. The SW480 cells were first grown in RPMI 1640 supplemented with 10% FBS, 2 mmol/L L-glutamine, 5 mmol/L 2-mercaptoethanol, 2 mmol/L sodium pyruvate, and 0.1 mmol/L MEM nonessential amino acids in a humidified atmosphere of 5% CO_2/95% air at 37°C. When the cells were ~80% confluent, they were either used in the experiments as described in appropriate sections below or subcultured with the split ratio of 1:10 for up to 20 passages.

SIBLING production and purification. Recombinant DMP1 with good posttranslational modifications (including glycosylation, sulfation and, possibly phosphorylation) was made as described previously (7). Briefly, full-length bovine DMP1 cDNA (26) was subcloned into a high-expression, replication-deficient adenovirus type 5 with transcription under the control of the cytomegalovirus promoter. The DMP1-LysAlaGlu (KAE) construct was made by *in situ* mutagenesis of the ArgGlyAsp (RGD) domain into KAE while in pBluescript. The entire insert was checked for fidelity and then shuttled to the adenovirus plasmid (27). The adenoviruses were selected, purified, and expressed as previously described (28). Recombinant SIBLINGs were generated by infecting mid-passage, subconfluent normal human bone marrow stromal cells (a gift of Dr. Pamela Gehron Robey, National Institute of Dental and Craniofacial Research, NIH, Bethesda, MD). Harvested serum-free medium was subjected to anion-exchange chromatography, as described (7, 28), to isolate SIBLINGs. Purity of each SIBLING was >95%, as measured after SDS-PAGE.

Preparation of Matrigel-coated inserts. Matrigel-coated inserts placed in 24-well plates were prepared as described previously (18). Briefly, Matrigel was diluted with ice-cold sterile H_2O and mixed well. The solution was dispensed as 5 μg/50 μL/insert/well. The plates were left in a laminar flow tissue culture hood overnight to dry. The inserts were then rinsed with sterile HBSS to rehydrate films and the plates were immediately used as described below.

Modified Boyden chamber cell invasion assay. Invasiveness of each cancer cell line was measured by using an UV-opaque transwell polycarbonate membrane (diameter of 6.4 mm and pore size of 8 μm) in a modified Boyden chamber cell invasion assay. Transwell inserts precoated with Matrigel as described above were placed in a 24-well plate. Preconfluent cells were removed from culture dishes with 0.53 mmol/L EDTA in PBS, washed twice in HBSS, and resuspended in serum-free RPMI 1640 at a final density of 4×10^5 cells/mL. Quadruplicate cultures of cells were briefly pretreated in a final volume of 250 μL of serum-free medium [containing 0.1% bovine serum albumin (BSA)] with either buffer or SIBLINGs in sterile 1.5 mL microcentrifuge tubes for 10 minutes and then placed in the upper compartment of a Boyden chamber. In some cases, cells were first treated for 20 minutes with blocking antibodies or control IgGs in the tube and then placed in the upper chamber. In the latter cases, buffer or recombinant SIBLING was then added directly to the chamber. To induce migration through the Matrigel layer, the lower chambers were filled with 750 μL of serum-free medium conditioned by mouse NIH 3T3 fibroblastic cells and containing 0.1% BSA. Cells were then incubated in humidified incubator at 37°C for 24 hours. Cells that had not migrated through the barrier were removed from the top compartment and inserts were moved to another 24-well plate in which each well contained 0.5 mL of the fluorescent dye, calcein acetoxymethyl ester, at 4 μg/mL. The plate was incubated at 37°C for 45 minutes to allow the living cells to take up and activate the dye before the fluorescent intensity was read from the bottom of the insert with a fluorescence plate reader (Wallac 1420 VICTOR^2 Multilabel Reader, Perkin-Elmer Life Sciences, Inc., Boston, MA). Fluorescence intensity was proportional to the number of cells having migrated to the bottom of the UV-opaque membrane.

Pull-down experiments. Commercial mouse anti-human $\alpha_v\beta_3$ integrin or $\alpha_v\beta_5$ integrin mAb immobilized on immunoaffinity gel matrix beads were washed thrice in ice-cold Triton buffer [20 mmol/L Tris-HCl (pH 7.4), 150 mmol/L NaCl, 0.2% Triton X-100, 2 mmol/L $MgCl_2$, and 0.1 mmol/L $CaCl_2$] and incubated in 1 mL Triton buffer containing 1% BSA at 4°C for 30 minutes with gentle shaking. After washing thrice with 1 mL of ice-cold Triton buffer, the beads were gently shaken with or without 10 μg of $\alpha_v\beta_3$ integrin or $\alpha_v\beta_5$ integrin complex in 50 μL Triton buffer at 4°C for 10 minutes. The beads were then gently pelleted, the liquid was carefully removed, and the beads were washed in 1 mL Triton buffer. The beads were then resuspended in 1 mL buffer and separated into equal volume aliquots. An aliquot was gently shaken with buffer alone or buffer containing 500 nmol/L DMP1 or 500 nmol/L DMP1-KAE (in a final volume of 50 μL) at 4°C for 10 minutes. The beads were then pelleted, washed in 1 mL of Triton buffer, and incubated in 50 μL of Triton buffer containing 1 μg of proMMP-9 at 4°C for 10 minutes. The beads were pelleted and washed with 1 mL Triton buffer, and the MMP-9 was eluted from the beads with 80 μL of 1× zymogram sample buffer [2.5 mL of 0.5 mol/L Tris-HCl (pH 6.8) + 2 mL glycerol + 4 mL of 10% (w/v) SDS + 0.5 mL of 0.1% bromophenol blue adjusted to 20 mL with distilled water] and resolved by electrophoresis on a 10% (gelatin) zymogram gel.

SDS-PAGE and zymography. Samples in zymogram gel sample buffer were loaded on a 10% (gelatin) zymogram gel, subjected to electrophoresis, and processed as recommended by the manufacturer. Resulting Coomassie-stained gels were visualized by dynamic integrated exposure using an EagleEye II imaging system (Stratagene Corp., La Jolla, CA).

Labeling of purified human matrix metalloproteinase-9 with Alexa Fluor 488 dye. Latent protease (proMMP-9) was fluorescently labeled with the Alexa Fluor 488 protein-labeling kit according to the protocol of the manufacturer but adjusted to the smaller amount of protein being labeled. All steps were done at 4°C. Briefly, shipping buffer from 50 μg of proMMP-9 was changed into the reaction buffer (PBS) on ProbeQuant G-50 microcolumns, and the resulting eluant concentrated to ~50 μL with a prewashed Microcon YM-30 centrifugal filter device. Five microliters of 0.1 mol/L sodium bicarbonate were added to raise the pH to 7.5 to 8.5 for efficient labeling. The reactive dye was dissolved in 0.5 mL of PBS containing 0.1 mol/L sodium bicarbonate, 50 μL of Alexa Fluor 488 dye was added to the proMMP-9 solution, and the reaction mixture was stirred for 2 hours. The labeled proMMP-9 protein was then separated from the unreacted dye on a ProbeQuant G-50 microcolumn (in PBS) and stored as aliquots at −80°C until use.

Flow cytometry. Cells were detached from culture dishes with PBS containing 0.53 mmol/L EDTA, washed twice in HBSS, and then incubated at 2×10^6/mL at room temperature for 10 minutes with buffer alone or buffer containing either 500 nmol/L DMP1 or 500 nmol/L DMP1-KAE. For the studies involving the blocking antibodies, cells were incubated with buffer alone or buffer containing $\alpha_v\beta_3$ integrin antibody (LM609, 4 μg/mL), $\alpha_v\beta_5$ integrin antibody (P1F6, 4 μg/mL), CD44 antibody (BU75, 4 μg/mL), or control IgG (4 μg/mL) at room temperature for 10 minutes, and then the mixture was incubated with 500 nmol/L DMP1 or 500 nmol/L DMP1-KAE for another 10 minutes. In the final step for all samples, cells were pelleted, washed once in HBSS, and then incubated at room temperature with Alexa Fluor 488–labeled human proMMP-9 at 5 μg/mL for 10 minutes. The cells were pelleted, washed once, resuspended in HBSS, and analyzed immediately with a FACSCalibur cell sorter equipped with a 488 nm argon laser and Cellquest software (BD PharMingen, Bedford, MA).

Rabbit anti-human matrix metalloproteinase-9 polyclonal antibody (LF-184) production. The carboxy-terminal 23 amino acids of human MMP-9 (RSELNQVDQVGYVTYDILQCPED), a region with relatively low homology to human MMP-2, was synthesized and conjugated to maleimide-activated keyhole limpet hemocyanin (Pierce Biotechnology, Inc., Rockford, IL) through the cysteinyl residue. A New Zealand white rabbit was injected four times with ~1.0 mg of conjugate under an approved animal protocol at a contract facility (Covance, Inc., Denver, PA). ELISA showed good activity to authentic human MMP-9 but no cross-reactivity with authentic human MMP-2 or MMP-3. Synthetic peptide (1.6 mg) was conjugated to 2 mL column of SulfoLink agarose beads (Pierce Biotechnology) according to the instructions of the manufacturer. Antibodies were bound to the affinity column, washed sequentially with PBS, 0.05% Tween 20 in PBS (PBS-T), PBS, and then eluted in 0.1 mol/L glycine (pH 2.4). The fractions were immediately neutralized, dialyzed against PBS, and stored frozen at −80°C until use.

Immunohistochemistry. Immunohistochemistry was done on human colon adenocarcinoma serial sections cut from blocks obtained from the Cooperative Human Tissue Network, Mid-Atlantic Division (Charlottesville, VA) under Institutional Review Board approval. The Zymed ST5050 automated system (Zymed Lab, Inc., San Francisco, CA) was used with following primary antibodies: mouse anti-human DMP1 mAb (LFMb-31, 1:100; ref. 2), mouse anti-human CD44 (H-CAM, 1:100) mAb (MAB2140, Chemicon International), mouse anti-human α_v integrin (CD51, 1:50) mAb (407286), mouse anti-human β_3 integrin (CD61, 1:50) mAb (407314), mouse anti-human β_5 integrin mAb (407316, 1:50; all from EMD Biosciences, Inc., San Diego, CA), and the affinity purified rabbit anti-human MMP-9 polyclonal antibody (LF-184, 1:200). Briefly, the paraffin block containing a moderately differentiated colon adenocarcinoma was serially sectioned (5 μm thickness) and dried on silane-coated slides (Statlab Medical Products, Inc., Lewisville, TX). The sections were manually deparaffinized in xylene and rehydrated through a graded ethanol series (100%, 95%, and 70%). After the endogenous peroxidase activity was blocked with 3% hydrogen peroxide in methanol for 20 minutes, the sections were washed thrice in PBS for 5 minutes each and covered with PBS-T before loading the slides onto the preprogrammed ST5050 automated immunohistochemistry machine. The ST5050 was programmed to incubate each slide for 1 hour with appropriate primary antibody diluted in 10% normal goat serum in PBS. The slides thereafter went through a 4 × 1 minute wash cycle with PBS-T before incubation with SuperPicTure Polymer horseradish peroxidase (HRP)–conjugated broad-spectrum secondary antibody (Zymed Lab) for 10 minutes. The slides were processed through another wash cycle and then were developed with AEC Single Solution chromogen (Zymed Lab) for 2 minutes. Sections were lightly counterstained manually with Mayer's hematoxylin for 10 to 20 seconds before applying an overlay of Clearmount glaze (both from Zymed Lab) over the sections. After air drying, slides were coverslipped with Histomount (Zymed Lab). All steps were done at room temperature. Negative controls included the substitution of primary antibody with nonimmune rabbit serum or mouse IgG control (Zymed Lab). Sections were photographed with an AxioCam MR-MRGrab camera imaging system (Carl Zeiss Vision, Munich, Germany), which included an Axioplan2 microscope, an AxioCam MRm camera, and AxioVision 3.1 software.

Statistical analysis. Data are the mean of quadruplicate determinations and 95% confidence interval. Each experiment has been repeated at least twice. In each case, data from a single representative experiment are shown. Multiple comparisons were done with a one-way ANOVA followed by Dunnett's test for treatment versus control comparisons. Pairwise comparisons were done by performing nonparametric Mann-Whitney *U* test. In each analysis, differences were considered statistically significant for $P < 0.05$. All statistical tests were two sided.

Results

Dentin matrix protein 1 enhances invasiveness of colon cancer cell line, SW480, *in vitro*. Previous work showed that many human cancer cell lines that produced MMP-2 showed enhanced invasion by BSP/MMP-2 interactions but that addition of recombinant DMP1 had no such effect. Therefore, the invasiveness of SW480 colon cancer cells, which are known to express the partner protease of DMP1, MMP-9, but not MMP-2 (29) was measured using a modified Boyden chamber invasion assay. SW480 cells showed a clear dose-response increase in their invasiveness through the Matrigel barrier upon the addition of recombinant DMP1, with a maximum 3.9-fold increase at 100 nmol/L DMP1 (86.1 ± 13.9 versus 22.3 ± 9.8 for untreated cells, $P < 0.001$; Fig. 1). The increase in the invasiveness of the SW480 cell line by DMP1 was not due to enhancement of integrin-mediated cell attachment/migration alone because the same amount of recombinant human BSP or osteopontin, two other members of the SIBLING family that can support cell attachment/migration but cannot bind and activate MMP-9, did not increase the invasiveness of the SW480 cells (data not shown).

Dentin matrix protein 1–enhanced invasion requires matrix metalloproteinase-9 and cell surface receptors $\alpha_v\beta_3$ integrin, $\alpha_v\beta_5$ integrin, or CD44. Invasion enhancement studies were also done with DMP1-KAE, a recombinant DMP1 protein whose integrin-binding RGD sequence was replaced with the chemically

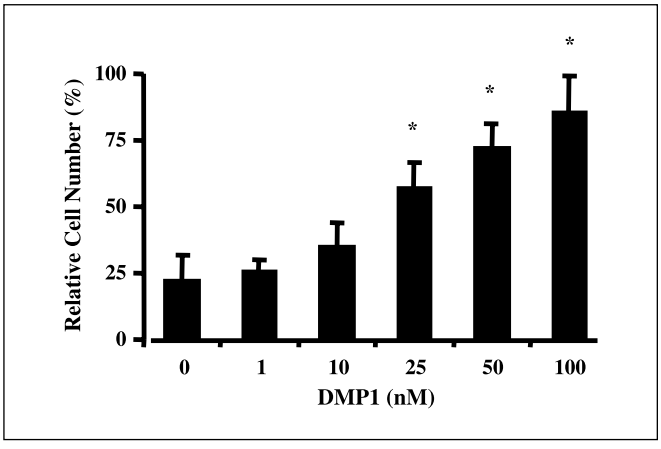

Figure 1. DMP1 and the invasion of the colon cancer cell line SW480 *in vitro*. Untreated or DMP1-treated SW480 colon cancer cells were placed in the top wells of separate Boyden chambers that each had Matrigel-coated UV-opaque transwell inserts. The lower chambers contained serum-free conditioned medium as a chemoattractant. The cells were incubated at 37°C for 24 hours. Invasive cells that penetrated the Matrigel artificial basement membrane barrier and moved into the lower chamber were then detected by calcein acetoxymethyl ester fluorescent dye activated by the live cells. The relative fluorescence in the lower chamber corresponded directly to the number of cells that digested their way through the barrier and migrated into to the lower chamber. *Columns,* means of triplicate samples; *bars,* 95% confidence intervals. $P < 0.001$ was obtained for multiple comparisons within the panel by use of one-way ANOVA. Each treatment group was also individually compared with the control (0 nmol/L DMP1) group by use of the Dunnett's test. *$P < 0.001$, compared with untreated cells by the Dunnett's test. All statistical tests were two-sided.

similar but inactive tripeptide, KAE. SW480 cells treated with DMP1-KAE showed a 2.4-fold increase at 100 nmol/L DMP1-KAE (83.6 ± 16.3 versus 34.4 ± 20.2 for untreated cells, $P < 0.01$; Fig. 2*A*). Although significantly less robust than the enhancement from normal DMP1, the mutant DMP1-KAE clearly aided the invasion by these cells without the ability to bind to RGD-dependent integrins. Addition of a blocking CD44 antibody completely inhibited the DMP1-KAE–enhanced invasion (12.7 ± 4.7 versus 11.1 ± 2.9; Fig. 2*B*), showing that DMP1 can act through both RGD-dependent integrins and CD44. To complete the study of cell surface proteins, blocking antibodies to the $\alpha_v\beta_3$ and $\alpha_v\beta_5$ integrins (both RGD-dependent) as well as to CD44 were separately added to SW480 cells before the addition of normal DMP1 in the invasion assay. Each lowered the efficiency of the DMP1-enhanced invasion but not to DMP1-free control levels, suggesting that each was contributing to a portion of the DMP1 enhancement (Fig. 2*C*). Simultaneous addition of all three antisera reduced the DMP1-enhanced invasion to control levels (Fig. 2*C*), suggesting that both $\alpha_v\beta_3$ and $\alpha_v\beta_5$ integrins contributed to the integrin-related DMP1 enhancement of invasion by SW480 cells.

Because integrins, CD44, and MMP-9 have previously been shown to be associated with cancer cell invasiveness (9, 16), and because DMP1 specifically binds to MMP-9 with nanomolar affinity (10), we hypothesized that DMP1 may bridge MMP-9 to the cell surface via CD44, $\alpha_v\beta_3$, and/or $\alpha_v\beta_5$ integrins where it could become more effective in digesting the Matrigel during the invasion process. Both DMP1- and DMP1-KAE–enhanced SW480 cell invasions were almost completely inhibited by the addition of a blocking antibody to MMP-9 (Fig. 2*D*).

Dentin matrix protein 1 bridges matrix metalloproteinase-9 to CD44, $\alpha_v\beta_3$, and $\alpha_v\beta_5$ integrins. Because DMP1 can separately form complexes with specific cell surface proteins and with MMP-9, DMP1 may be able to bridge MMP-9 to $\alpha_v\beta_3$ or $\alpha_v\beta_5$ integrins *in vitro*. The hypothesis was tested with pull-down experiments

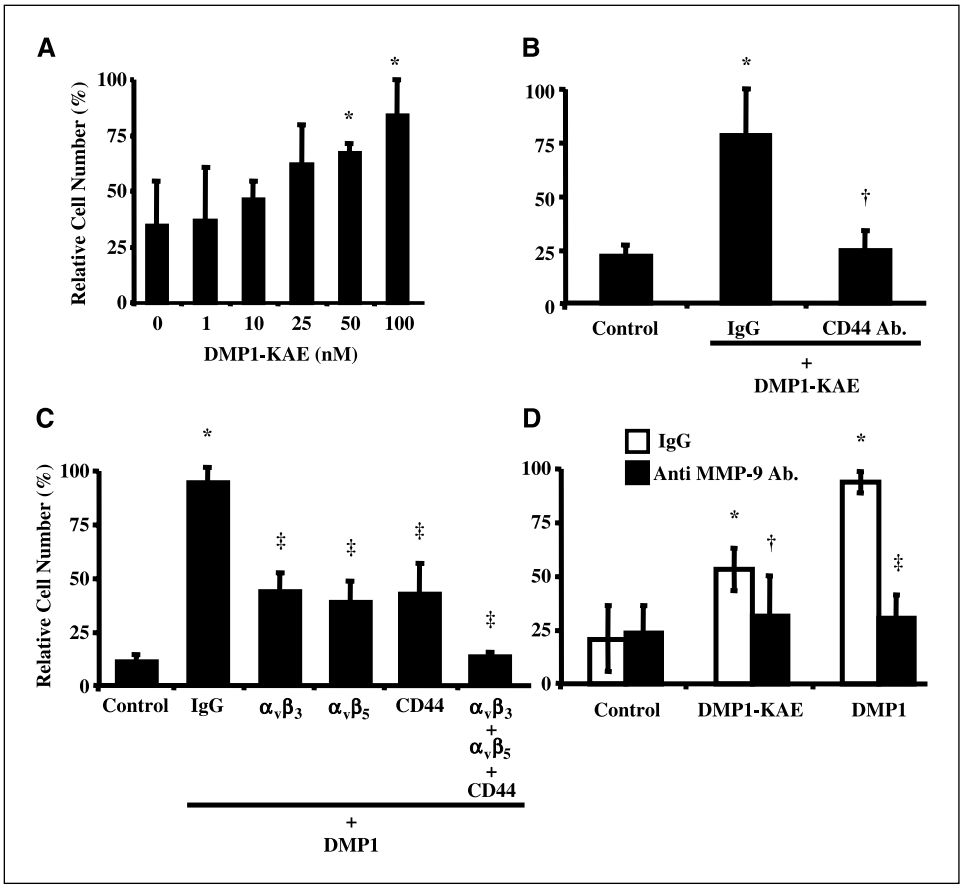

Figure 2. RGD-dependent integrins and CD44 are involved in the DMP1-enhanced invasion of colon cancer cells *in vitro*. *A,* SW480 cells treated with 0 to 100 nmol/L DMP1-KAE (in which the RGD domain of DMP1 was replaced with the integrin-inactive tripeptide, KAE) were placed in the upper portion of a modified Boyden chamber coated with Matrigel. The addition of DMP1-KAE resulted in a positive but less robust dose-response pattern compared with the integrin-binding native DMP1 (Fig. 1), showing that DMP1 does not have an absolute requirement to bind to RGD-dependent integrins to enhance invasion. *B,* addition of CD44 antibodies (*Ab.,* 20 μg/mL) to the DMP1-KAE treatment completely negates the enhanced invasion, showing that CD44 is the alternate cell surface–binding partner for DMP1. *C,* blocking mAbs to $\alpha_v\beta_3$ or $\alpha_v\beta_5$ integrins, or CD44 (20 μg/mL of each antibody), were each able to partially block DMP1-enhanced invasion but not to control levels, suggesting that DMP1 can act through each of these cell surface receptors. Combined, the antibodies completely block the DMP1-enhanced invasion. Nonspecific IgGs had no affect on the invasion enhancement. *D,* inhibition of MMP-9 activity by addition of blocking antibodies (20 μg/mL) returned both the DMP1- and DMP1-KAE–enhanced invasion to control levels. Relative fluorescence, which corresponds to the number of cells that migrated through the Matrigel, is as described in Fig. 1. *A, columns,* mean of quadruplicate samples; *bars,* 95% confidence intervals. A P value of <0.01 was obtained for multiple comparisons within each panel by use of one-way ANOVA. Each treatment group was also individually compared with the control, untreated group by use of the Dunnett's test. *, $P < 0.01$, compared with untreated cells by the Dunnett's test. All statistical tests were two-sided. *B* to *D, columns,* mean of quadruplicate samples from a representative experiment; *bars,* 95% confidence intervals. A Mann-Whitney *U* test was used for the pairwise comparisons. *, $P < 0.01$, obtained for SW480 cells treated DMP1-KAE or DMP1 versus untreated respective control cells. $P < 0.01$, obtained for SW480 cells treated with antibody + DMP-KAE (†) or DMP1 (‡) versus isotype control IgG + DMP-KAE or DMP1, respectively. All statistical tests were two sided.

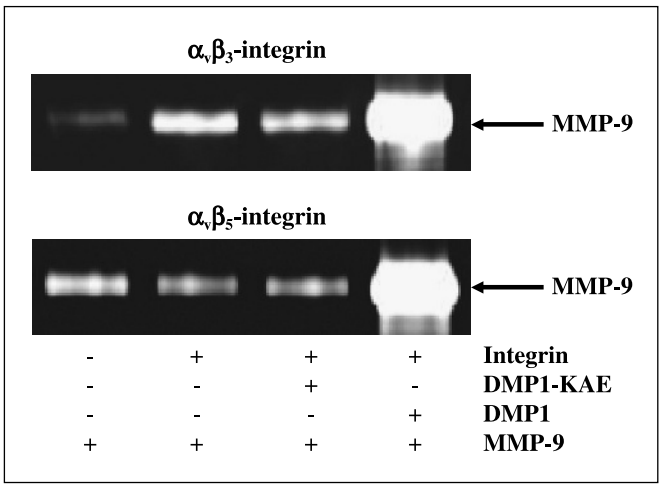

Figure 3. Pull-down experiments showing bridging of MMP-9 to $\alpha_v\beta_3$ integrin and $\alpha_v\beta_5$ integrin by DMP1. The $\alpha_v\beta_3$ or $\alpha_v\beta_5$ integrins were first bound to their respective mAbs previously attached to beads by the manufacturer. After washing, the beads were incubated with buffer alone or buffer containing 500 nmol/L DMP1-KAE or 500 nmol/L DMP1, washed, and subsequently treated with recombinant proMMP-9. The washed samples were then electrophoresed on 10% zymogram gelatin gels and examined by Coomassie blue staining after digestion conditions were done. Beads alone have low background level of MMP-9 binding (*lane 1*). Note that the addition of DMP1 (*lane 4*) but not DMP1-KAE (*lane 3*) enabled proMMP-9 to be pulled down with both sets of integrin-bound beads. Control levels of proMMP-9 were observed without addition of DMP1 (*lane 2*).

using purified components. Only a small amount of proMMP-9 was detected using just the beads, showing that the pull-down assay had a low background (Fig. 3, *lane 1*). Beads with bound $\alpha_v\beta_3$ or $\alpha_v\beta_5$ integrin but no DMP1 resulted in a similar, small amount of proMMP-9 pulled down with the beads (Fig. 3, *lane 2*). Addition of DMP1-KAE also gave background levels of bound proMMP-9 (Fig. 3, *lane 3*). However, addition of DMP1 to either $\alpha_v\beta_3$ or $\alpha_v\beta_5$ integrin–coated beads greatly increased the amount of bead-associated proMMP-9, indicating the bridging of proMMP-9 to each integrin (Fig. 3, *lane 4*). BSP and osteopontin are also known to be able to bind to $\alpha_v\beta_3$ and possibly $\alpha_v\beta_5$ integrins but substitution of recombinant BSP or osteopontin for DMP1 in the pull-down experiments resulted in only background levels of MMP-9, again illustrating the specificity of the DMP1 for proMMP-9 (data not shown). Because we were unable to obtain recombinant CD44, we could not test the formation of a proMMP-9/DMP1/CD44 complex *in vitro* using highly purified proteins in the pull-down experiments.

We were, however, able to detect proMMP-9/DMP1/CD44 complexes as well as proMMP-9/DMP1/integrin complexes on living cells through FACS analysis. Purified proMMP-9 was covalently labeled with the fluorescent dye, Alexa Fluor 488. Flow cytometry was used to determine the amount of labeled proMMP-9 bound to SW480 cells with and without DMP1 (or DMP1-KAE) treatment. Addition of DMP1 produced an 81% increase in the mean value of the signal of labeled proMMP-9 bound compared with that of cells not pretreated with DMP1 (Fig. 4*A*). The addition of DMP1-KAE produced a lower but significant increase of proMMP-9 binding (57%; Fig. 4*B*), verifying the earlier results showing that RGD-binding integrins were not the only cell surface protein that could be used by DMP1. Separate addition of blocking antibodies to $\alpha_v\beta_3$ integrin (Fig. 4*D*), $\alpha_v\beta_5$ integrin (Fig. 4*E*), or CD44 (Fig. 4*F*) before the treatment with DMP1 each partially blocked the DMP1-enhanced binding of the labeled proMMP-9 to SW480 cells. However, when cells were treated with the blocking antibodies against both integrins and CD44 together, labeled proMMP-9 binding decreased to the DMP1-free control levels (Fig. 4*G*). Furthermore, when cells were first treated with anti-CD44 mAb and then with DMP1-KAE, MMP-9 binding was reduced to the untreated control levels (Fig. 4*H*), supporting the hypothesis of the formation of a MMP-9/DMP1/CD44 complex on cell surfaces.

Indirect fluorescent immunocytochemistry experiments were done to show that added DMP1 and MMP-9 both localize to the

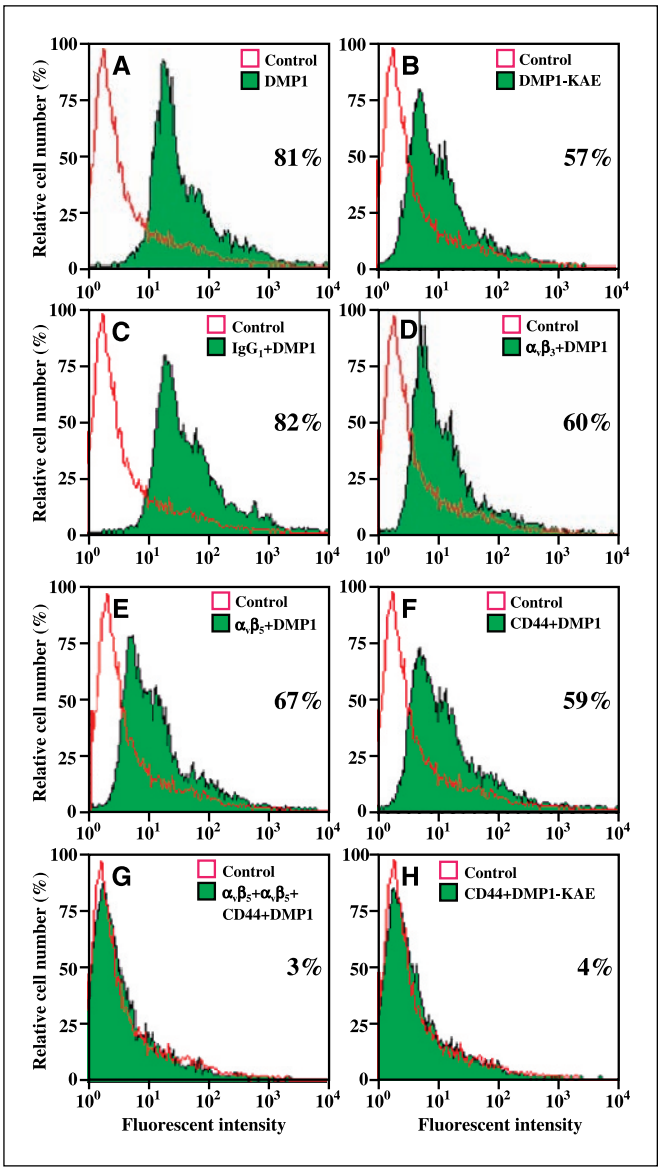

Figure 4. DMP1-enhanced binding of fluorescently labeled latent MMP-9 (proMMP-9) to SW480 cells. ProMMP-9 was labeled with Alexa Fluor 488 and incubated with cells treated as indicated or untreated cells (control). Pretreating the cells with DMP1 (*shaded area*) increased the amount of labeled proMMP-9 bound to the living cells, compared with untreated cells as analyzed by FACS (*A*). Pretreating cells with DMP1-KAE (*shaded area*) showed increased binding of labeled proMMP-9 compared with that of untreated cells (*open area*; *B*). Blocking cell surface molecules $\alpha_v\beta_3$ integrin (*D*), $\alpha_v\beta_5$ integrin (*E*), or CD44 (*F*) with their respective mAbs decreased the DMP1-enhanced binding of the labeled proMMP-9 but not to control levels. However, when all three antisera were added together ($\alpha_v\beta_3$ + $\alpha_v\beta_5$ + CD44), the DMP1-enhanced binding of labeled proMMP-9 was completely blocked (*G*). Treating cells with a nonimmune IgG had no affect on the ability of DMP1 to enhance the binding of proMMP-9 (*C*). DMP1-KAE–enhanced binding of labeled proMMP-9 was essentially blocked by CD44 mAb alone (*H*). *Numbers,* percentage of cells bound to labeled proMMP-9.

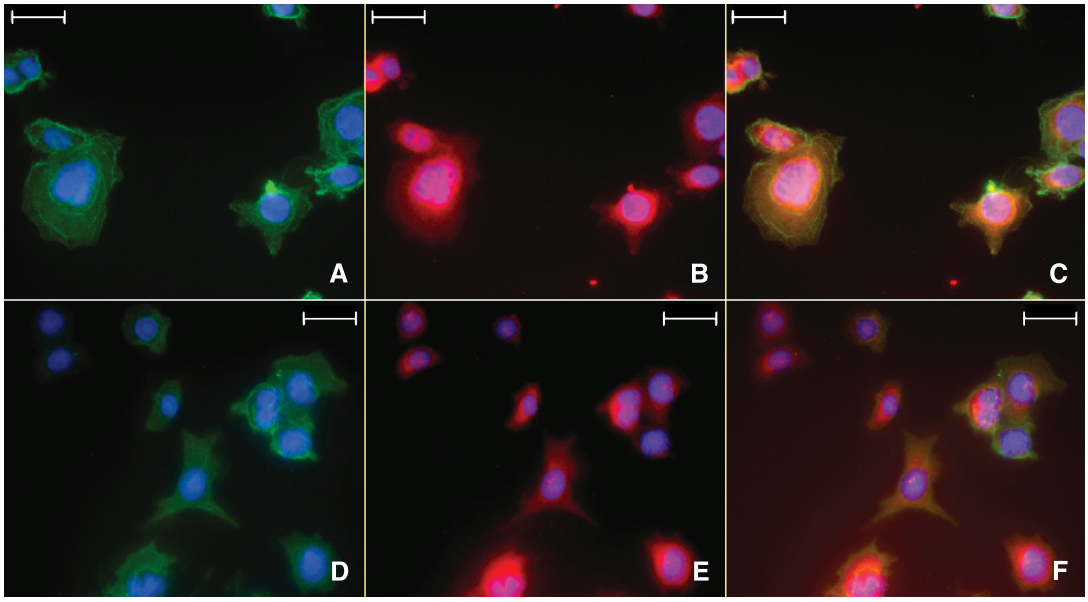

Figure 5. Colocalization of DMP1 and RGD-mutant DMP1 (DMP1-KAE) with MMP-9 on SW480 colon cancer cells. Cells were treated first with DMP1 and then with proMMP-9. The cells were incubated with a mouse mAb that can detect DMP1 as well as DMP1-KAE and an affinity purified rabbit polyclonal antibody against MMP-9. Bound antibodies were then detected by indirect immunofluorescence with Cy2-conjugated AffiniPure goat anti-mouse IgG for DMP1 or DMP1-KAE and Cy5-conjugated AffiniPure goat anti-rabbit IgG for MMP-9. *A, green,* location of DMP1. *B, red,* location of MMP-9. *C, yellow,* colocalization of DMP1 and MMP-9. *D, green,* location of DMP1-KAE. *E, red,* location of MMP-9. *F, yellow,* colocalization of DMP1-KAE and MMP-9. 4,6-Diamidino-2-phenylindole was used as a nuclear stain (*blue*). Bar, 20 μm.

same cells. DMP1 and MMP-9 were colocalized on the SW480 cells (Fig. 5*A-C*), suggesting that DMP1 rapidly localizes MMP-9 to the cell surface *in vitro* by binding to possibly both integrins and CD44 cell surface molecules. Added recombinant DMP1-KAE and MMP-9 were also detected at the same locations in these cells (Fig. 5*D-F*), suggesting that DMP1 also localizes MMP-9 to the cell surface *in vitro* through CD44. Like the SIBLINGs in most other established cancer cell lines, DMP1 was not detected in untreated SW480 cells but endogenous MMP-9 was weakly positive (data not shown).

Expression of dentin matrix protein 1, matrix metalloproteinase-9, CD44, and integrin subunits α_v, β_3, and β_5 in colon adenocarcinoma *in vivo*. The expression of MMP-9, CD44, as well as the α_v, β_3, and β_5 integrin subunits, in tumors have been shown separately and in some combinations many times previously. However, to illustrate that the MMP-9/DMP1/cell surface receptors are made by the same cells and, therefore, logically may form the complexes describe above *in vivo*, immunohistochemistry reactions were done on serial paraffin sections of a human colon adenocarcinoma. The results show that all six proteins are coexpressed in the same cells/areas, suggesting that the complexes could easily be locally formed by simple interactions (Fig. 6). The red/brown staining indicates the expression of DMP1 (Fig. 6A), CD44 (Fig. 6*B*), α_v integrin subunit (Fig. 6*C*), β_3 integrin subunit (Fig. 6*D*), β_5 integrin subunit (Fig. 6*E*), and MMP-9 (Fig. 6*F*). The negative controls, mouse IgG (Fig. 6*G*), and rabbit nonimmune serum (Fig. 6*H*) illustrate the low background for these assays.

Discussion

Cancer progression reaches a critical period when a tumor starts to invade and metastasize. One of the initial steps in metastasis requires invasion of tumor cells through basement membrane and nearby stroma. The presence of MMPs, various cell adhesion molecules, and SIBLING proteins during tumor development, growth, invasion, metastasis, and angiogenesis have been well documented. However, the mechanisms by which these molecules work in the coordination of tumor progression are less well elucidated. Several colocalization studies have reported that $\alpha_v\beta_3$ integrin may function not only as an adhesion and/or migration receptor but also to activate and properly distribute proteases that degrade the extracellular matrix during invasion (23, 24, 30). Three members of the SIBLING family (BSP, osteopontin, and DMP1) bind and activate proMMP-2, proMMP-3, and proMMP-9, respectively (10). Furthermore, the same pairings of SIBLINGs and active MMPs cause their respective TIMPs to be much less effective at inhibiting the proteases. Recombinant BSP has been shown to promote invasion of many MMP-2-expressing osteotropic cancer cell lines through formation of a MMP-2/BSP/$\alpha_v\beta_3$ integrin complex (18). DMP1, which has recently been shown to be expressed by various tumors (8, 9), had no effect on these same MMP-2-producing cell lines.

In this article, the role of DMP1 in an invasion assay was studied using a colon cancer cell line, SW480, that has been reported to express significant levels of MMP-9 but no MMP-2 (29). Recombinant DMP1 added to the Boyden chamber wells caused a dose-response increase in the invasiveness of the cells through a Matrigel barrier. Addition of two other SIBLING family members with similar cell attachment properties, BSP or osteopontin, did not increase the invasiveness of the SW480 cells suggesting that the action of DMP1 was not due to simple attachment and/or migration effects. This result is similar to the specific enhancement of invasion of several MMP-2-expressing cancer cell lines in

response to the addition of the SIBLING partner of MMP-2, BSP, but not to either osteopontin (partner of MMP-3) or DMP1. Negating the ability of DMP1 to bind to RGD-dependent integrins by mutation of the RGD to the inactive KAE or by the addition of antibodies that block $\alpha_v\beta_3$ integrin and $\alpha_v\beta_5$ integrin only partially affected the ability of DMP1 to enhance invasion. This suggests that DMP1 may also be using another of its known cell surface receptors, CD44. Antibodies to CD44 resulted in a partial block in the DMP1-enhanced invasion and a complete return to control levels when used with the DMP1-KAE protein. Used together, antibodies against $\alpha_v\beta_3$ integrin, $\alpha_v\beta_5$ integrin, and CD44 reduced the DMP1-enhanced invasion to nearly control levels.

The DMP1-enhanced invasion by the SW480 cells was also inhibited by a specific antibody for it protease partner, MMP-9. Pull-down studies using purified proteins showed the formation of MMP-9/DMP1/$\alpha_v\beta_3$ integrin and MMP-9/DMP1/$\alpha_v\beta_5$ integrin complexes *in vitro*. Because purified recombinant CD44 was not available, we did not look at the formation of the hypothesized MMP-9/DMP1/CD44 complex by this approach. However, the formation of the DMP1/MMP-9/CD44 as well as the other two integrin-related complexes at the cellular level by FACS analysis was shown. Together, these results suggest that cells use DMP1 as a bridge to link MMP-9 to its cell surface receptors, $\alpha_v\beta_3$ integrin, $\alpha_v\beta_5$ integrin, and/or CD44, thereby increasing their ability to invade through basement membranes and other connective tissues particularly in the absence of MMP-2. The modified Boyden chamber assay can measure only certain rate-limiting steps in this model system but one can hypothesize that *in vivo*, a cell may use a BSP/MMP-2/integrin complex to digest some matrix components and a DMP1/MMP-9/integrin or DMP1/MMP-9/CD44 complex to digest other proteins during the metastasis process. This may help to explain why some invasive tumors are found to express a combination of SIBLINGs and their MMP partners.

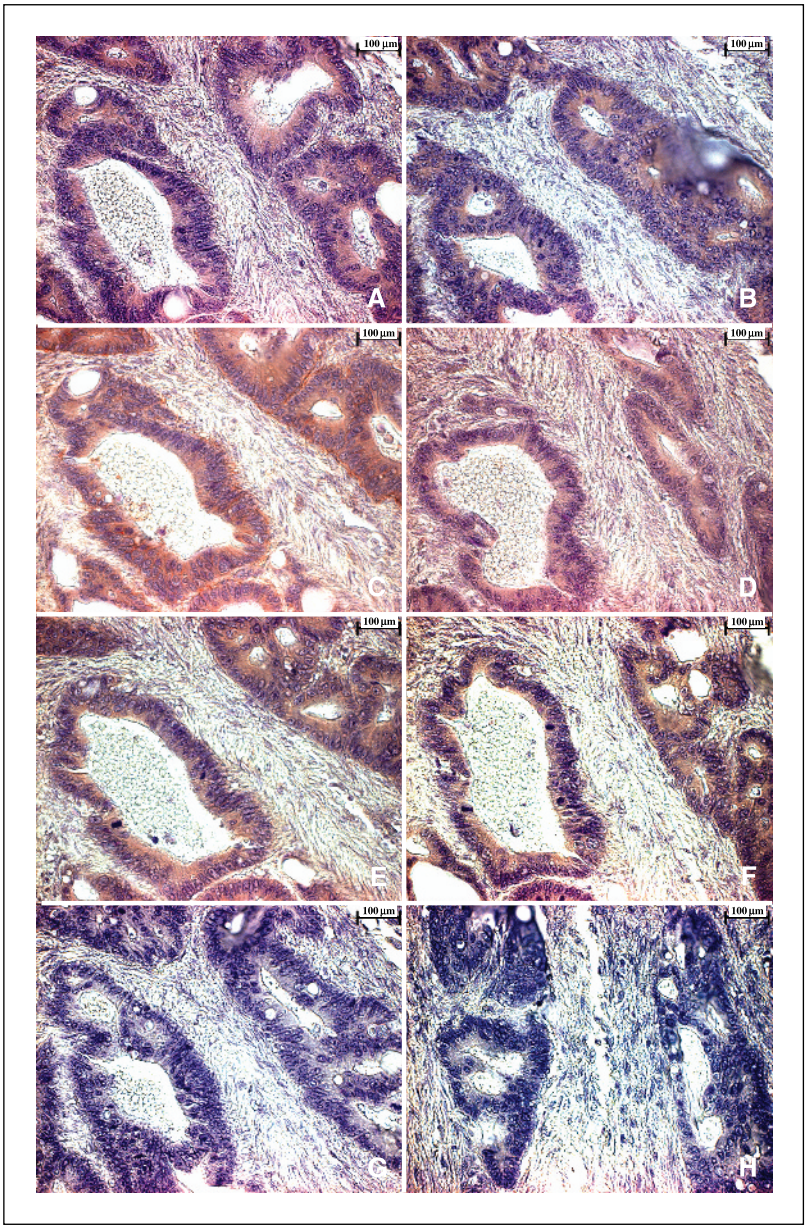

Figure 6. The expression of DMP1, MMP-9, CD44, and all three subunits of integrin $\alpha_v\beta_3$ and $\alpha_v\beta_5$ in near-serial sections of moderately differentiated colon adenocarcinoma. Deparaffinized sections of a colon adenocarcinoma were incubated separately with antibodies specific for DMP1, MMP-9, CD44, and the α_v, β_3, and β_5 integrin chains. Localization of the antibodies was determined with SuperPicture Polymer HRP-conjugated broad-spectrum secondary antibody and AEC Single Solution chromogen. *Red/brown color,* DMP1 (*A*), CD44 (*B*), α_v integrin (*C*), β_3 integrin (*D*), β_5 integrin (*E*), and MMP-9 (*F*) are all associated with the same cells, suggesting that all proteins required for formation of complexes of CD44, or integrins $\alpha_v\beta_3$ or $\alpha_v\beta_5$, DMP1, and MMP-9, are expressed in the same cells. The negative controls, mouse IgG (*G*), and rabbit immune serum (*H*), revealed no signal. Mayer's hematoxylin was used as a nuclear counterstain (*purple blue*). Bar, 100 μm.

In conclusion, it was shown that DMP1 can enhance the invasiveness of a model colon cancer cell *in vitro* by bridging MMP-9 to the cell surface in an RGD-dependent (with $\alpha_v\beta_3$ or $\alpha_v\beta_5$ integrin) and RGD-independent (with CD44) manner. Furthermore, it was shown that intact tumors can express all of these proteins within the same cellular structures, suggesting that these complexes studied *in vitro* will likely be formed *in vivo*.

Acknowledgments

Received 8/11/2005; accepted 10/5/2005.

Grant support: Intramural Research Program of the NIH, National Institute of Dental and Craniofacial Research.

The costs of publication of this article were defrayed in part by the payment of page charges. This article must therefore be hereby marked *advertisement* in accordance with 18 U.S.C. Section 1734 solely to indicate this fact.

We thank Li Li (National Institute of Dental and Craniofacial Research) for assistance during the sectioning and immunostaining of the paraffin tissue blocks.

References

1. Fisher LW, Torchia DA, Fohr B, Young MF, Fedarko NS. Flexible structures of SIBLING proteins, bone sialoprotein, and osteopontin. Biochem Biophys Res Commun 2001;280:460–5.

2. Ogbureke KU, Fisher LW. Expression of SIBLINGs and their partner MMPs in salivary glands. J Dent Res 2004;83:664–70.

3. Ogbureke KU, Fisher LW. Renal expression of SIBLING proteins and their partner matrix metalloproteinases (MMPs). Kidney Int 2005;68:155–66.

4. George A, Sabsay B, Simonian PA, Veis A. Characterization of a novel dentin matrix acidic phosphoprotein. Implications for induction of biomineralization. J Biol Chem 1993;268:12624–30.

5. MacDougall M, Gu TT, Luan X, Simmons D, Chen J. Identification of a novel isoform of mouse dentin matrix protein 1: spatial expression in mineralized tissues. J Bone Miner Res 1998;13:422–31.

6. Ye L, Mishina Y, Chen D, et al. Dentin matrix protein 1 (Dmp1) deficient mice display severe defects in cartilage formation responsible for a chondrodysplasia-like phenotype. J Biol Chem 2005;280:6197–203.

7. Jain A, Karadag A, Fohr B, Fisher LW, Fedarko NS. Three SIBLINGs (small integrin-binding ligand, N-linked glycoproteins) enhance factor H's cofactor activity enabling MCP-like cellular evasion of complement-mediated attack. J Biol Chem 2002;277:13700–8.

8. Chaplet M, De Leval L, Waltregny D, et al. Dentin matrix protein 1 is expressed in human lung cancer. J Bone Miner Res 2003;18:1506–12.

9. Fisher LW, Jain A, Tayback M, Fedarko NS. Small integrin binding ligand N-linked glycoprotein gene family expression in different cancers. Clin Cancer Res 2004;10:8501–11.

10. Fedarko NS, Jain A, Karadag A, Fisher LW. Three small integrin binding ligand N-linked glycoproteins (SIBLINGs) bind and activate specific matrix metalloproteinases. FASEB J 2004;18:734–6.

11. Mook OR, Frederiks WM, Van Noorden CJ. The role of gelatinases in colorectal cancer progression and metastasis. Biochim Biophys Acta 2004;1705:69–89.

12. Ishida H, Murata N, Tada M, et al. Determining the levels of matrix metalloproteinase-9 in portal and peripheral blood is useful for predicting liver metastasis of colorectal cancer. Jpn J Clin Oncol 2003;33:186–91.

13. Matsuyama Y, Takao S, Aikou T. Comparison of matrix metalloproteinase expression between primary tumors with or without liver metastasis in pancreatic and colorectal carcinomas. J Surg Oncol 2002;80:105–10.

14. Roeb E, Dietrich CG, Winograd R, et al. Activity and cellular origin of gelatinases in patients with colon and rectal carcinoma differential activity of matrix metalloproteinase-9. Cancer 2001;92:2680–91.

15. Reinmuth N, Liu W, Ahmad SA, et al. $\alpha_v\beta_3$ Integrin antagonist S247 decreases colon cancer metastasis and angiogenesis and improves survival in mice. Cancer Res 2003;63:2079–87.

16. Fujisaki T, Tanaka Y, Fujii K, et al. CD44 stimulation induces integrin-mediated adhesion of colon cancer cell lines to endothelial cells by up-regulation of integrins and c-Met and activation of integrins. Cancer Res 1999; 59:4427–34.

17. Murray D, Morrin M, McDonnell S. Increased invasion and expression of MMP-9 in human colorectal cell lines by a CD44-dependent mechanism. Anticancer Res 2004;24:489–94.

18. Karadag A, Ogbureke KU, Fedarko NS, Fisher LW. Bone sialoprotein, matrix metalloproteinase 2, and $\alpha(v)\beta3$ integrin in osteotropic cancer cell invasion. J Natl Cancer Inst 2004;96:956–65.

19. Matrisian LM. Cancer biology: extracellular proteinases in malignancy. Curr Biol 1999;9:R776–8.

20. Forget MA, Desrosiers RR, Beliveau R. Physiological roles of matrix metalloproteinases: implications for tumor growth and metastasis. Can J Physiol Pharmacol 1999;77:465–80.

21. Kleiner DE, Stetler-Stevenson WG. Matrix metalloproteinases and metastasis. Cancer Chemother Pharmacol 1999;43Suppl:S42–51.

22. Yu Q, Stamenkovic I. Localization of matrix metalloproteinase 9 to the cell surface provides a mechanism for CD44-mediated tumor invasion. Genes Dev 1999;13: 35–48.

23. Deryugina EI, Bourdon MA, Luo GX, Reisfeld RA, Strongin A. Matrix metalloproteinase-2 activation modulates glioma cell migration. J Cell Sci 1997;110: 2473–82.

24. Deryugina EI, Bourdon MA, Jungwirth K, Smith JW, Strongin AY. Functional activation of integrin $\alpha_V\beta_3$ in tumor cells expressing membrane-type 1 matrix metalloproteinase. Int J Cancer 2000;86:15–23.

25. Albini A, Iwamoto Y, Kleinman HK, et al. A rapid *in vitro* assay for quantitating the invasive potential of tumor cells. Cancer Res 1987;47:3239–45.

26. Hirst KL, Ibaraki-O'Connor K, Young MF, Dixon MJ. Cloning and expression analysis of the bovine dentin matrix acidic phosphoprotein gene. J Dent Res 1997;76: 754–60.

27. Becker TC, Noel RJ, Coats WS, et al. Use of recombinant adenovirus for metabolic engineering of mammalian cells. Methods Cell Biol 1994;43 Pt A:161–89.

28. Fedarko NS, Fohr B, Robey PG, Young MF, Fisher LW. Factor H binding to bone sialoprotein and osteopontin enables tumor cell evasion of complement-mediated attack. J Biol Chem 2000;275:16666–72.

29. Giambernardi TA, Grant GM, Taylor GP, et al. Overview of matrix metalloproteinase expression in cultured human cells. Matrix Biol 1998;16:483–96.

30. Brooks PC, Stromblad S, Sanders LC, et al. Localization of matrix metalloproteinase MMP-2 to the surface of invasive cells by interaction with integrin $\alpha_v\beta_3$. Cell 1996;85:683–93.

The SIBLING Family of Proteins: Activators of MMPs

Larry W. Fisher[1], Abdullah Karadag[1], Kalu Ogbureke[1], and Neal S. Fedarko[1,2]

[1]Craniofacial and Skeletal Diseases Branch, National Institute of Dental and Craniofacial Research, NIH, DHHS, Bethesda, MD, U.S.A.

[2]Division of Geriatrics, Department of Medicine, Johns Hopkins University, School of Medicine, Baltimore, MD, U.S.A.

The SIBLING family of proteins (BSP, DMP1, DSPP, MEPE and OPN) can modify hydroxyapatite initiation and growth *in vitro*. However, a variety of biochemical experiments proved that BSP, DMP1 and OPN can form stable complexes with MMP-2, MMP-9 and MMP-3, respectively. Furthermore, the complexes with proMMPs were active without removal of the propeptides and the propeptide-free MMP remained active in the presence of their inhibitors, TIMPs. Complement Factor H, with its higher affinity for the SIBLINGs, reversed both SIBLING-induced activations, suggesting that these activities may be limited to regions secreting the proteins. All five SIBLINGs as well as their three known MMP partners are co-expressed in cells of primate and rodent salivary glands, a mature, non-mineralizing tissue. These results suggest that the integrin-binding SIBLING family members may be playing important and perhaps related roles in the local activation of specific MMPs in both mineralizing and non-mineralizing tissues.

Keywords: SIBLING, MMP, BSP, OPN, DMP1, DSPP, MEPE

During the 1970s and 1980s, the acidic proteins entrapped within the mineralized matrices of bones and teeth were studied as possible hydroxyapatite nucleators and crystal growth modulators. Their biochemical properties permitted investigators to categorize the proteins into proteoglycans, phosphoglycoproteins, Gla-containing proteins, and other subgroups. The phosphoglycoproteins were so different in their primary protein sequences that it was difficult at that time to conclude that they were derived from a common primordial gene. Later, when the properties of the exon structures of bone sialoprotein (BSP), dentin matrix protein-1 (DMP1), dentin sialophosphoprotein (DSPP), osteopontin (OPN), and matrix extracellular phosphoglycoprotein (MEPE) genes were compared, we proposed that all five proteins were derived from a single ancient gene [1]. Some of the properties that were usually shared by the SIBLING (Small Integrin-Binding LIgand, N-linked Glycoprotein) family members were: a noncoding exon 1; a leader sequence plus the first two amino acids in exon 2; casein kinase II (CKII) phosphorylation consensus sequences in exons 3 and 5; a more proline-rich and often basic exon 4; and an integrin-binding tripeptide, RGD, within one of the last two much larger exons. Interestingly, exon 5, a short CKII domain, is often missing in natural splice variants of DMP1, OPN and MEPE. At the last meeting of the ICCBMT, the best data suggested that all five SIBLING genes were clustered within a 750,000 basepair region of human chromosome 4 [2]. A more refined analysis now shows them aligned with the same transcriptional orientation within a 372,000 bp region. Results for the mouse (chromosome 5) are similar.

Genetic analysis is interesting, but true families of proteins should also have related structures, binding partners, and functions. To date only two SIBLINGs (BSP and OPN) have had their structures solved and they were both found to be flexible (in solution) along their entire length within normal NMR timescales [1]. Flexibility is a common feature of proteins/domains that have many binding partners. All SIBLINGs are thought to bind to integrins via their RGD domain although rat DSPP (which lacks the RGD tripeptide) may use a unique, REDV fibronectin-like attachment domain. DMP1 and OPN have been shown to bind CD44 while BSP does not [3,4]. Complement Factor H binds with very high affinity to BSP, DMP1 and OPN in solution and can even mask the detection of SIBLINGs in serum [5]. BSP, DMP1 and OPN can bridge Factor H to cell surface integrins (all three) or CD44 (DMP1 and OPN) and protect the cell from the lytic pathway of complement [4,6]. Protection from complement may be important for the survival of a metastasizing cancer cell. DSPP and MEPE have not been purified in sufficient quantity to perform similar studies.

The newly-discovered ability of at least three members of the SIBLING family to bind and activate specific members of the MMP family of proteases was due to a fortuitous series of events. First, in 1996 Cheresh's group localized MMP-2 on the surface of invasive cells by direct interaction with $\alpha v\beta 3$ integrin [7]. Later we were making recombinant BSP, DMP1 and OPN in eukaryotic cells and gently purifying the proteins for structural analysis. We hypothesized that, since both the SIBLINGs family and MMP-2 bound to $\alpha v\beta 3$ integrin, it would be interesting to see if the SIBLINGs could displace the MMP-2 from the cell surface complex. Of course, in order to do this experiment, we had to be sure that none of the three purified SIBLINGs themselves were contaminated with MMP-2. To our surprise, small amounts of MMP-2 had co-purified with BSP while MMP-3 co-purified with OPN and MMP-9 co-purified with DMP1 under the non-denatur-

ing conditions. From there it was standard biochemistry using commercial sources of purified MMPs to show that purified SIBLINGs bound in a 1:1 stoichiometry with nM affinity to their partner MMPs but not to the other two MMPs. Upon binding of their partner MMPs, both the latent (proMMP) and active (MMP) forms underwent conformational changes that were easily detected using natural fluorescence of the MMP's tryptophan residues [8]. Furthermore, it was shown that when the SIBLING bound to its partner proMMP, the protease became active, apparently without removing the inhibitory propeptide (Figure 1A). This was a surprise because it is generally thought that the propeptide must be removed before the MMPs can be enzymatically active. It is reasonable to hypothesize that the conformational change induced in the MMPs by the bound SIBLING caused the propeptides to have lower affinities for their own binding domains, move out of the active sites, and allow substrates to be digested. Active MMPs that had been previously inhibited by addition of their corresponding purified tissue inhibitors of metalloproteinases (TIMPs) became re-activated upon binding of the appropriate SIBLING (Figure 1C). The TIMPs appear to have had their inhibitory binding sites within the MMPs altered by the SIBLING-induced conformational changes losing their ability to bind strongly and inhibit the MMPs [8]. To date, DSPP and MEPE have not been shown to have MMP partners with similar action.

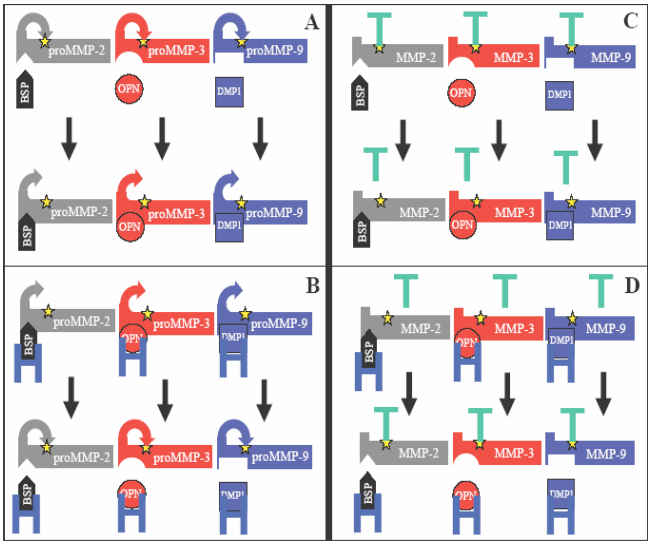

Figure 1. Latent MMPs with propeptide in active (star) site (A, top) upon binding partner SIBLING undergoes a conformational change exposing the active site to substrates (A, bottom). Factor H binds to the SIBLINGs (B, top), removing them and permitting the propeptide to reinsert into the active site (B, bottom). Propeptide-free MMPs inhibited by TIMPs (green T) (C, top) bind SIBLINGs, thereby inducing a conformational change. The TIMPs are released (C, bottom) activating the MMPs. Factor H removes the SIBLING from the complex allowing the TIMPs to bind and inhibit the MMPs (D).

Mechanisms for activating latent MMPs and/or interfering with the action of the TIMPs would not likely evolve unless there was also a mechanism for reversing these activation pathways. Fortunately, we knew from previous results mentioned above that complement Factor H has an approximately 100-fold higher affinity for BSP, DMP1 and OPN than the SIBLINGs have for their respective MMP partners. Factor H, which is present in the blood at about 1 mg/ml, apparently binds to the SIBLINGs on the latent (Figure 1B) and active (Figure 1D) MMPs and removes them from the protease complex [8]. The propeptides and TIMPs can then re-inhibit the protease activity. Therefore SIBLING-activation of MMPs will likely be local events, occurring within a short distance of their secretion.

At this point, all of the results discussed have been found using highly purified proteins in biochemical experiments. We next set out to determine if the SIBLING-MMP complexes could be shown to be important in experiments with living cells. Because many different types of cancers have been shown in paraffin sections to express high levels of various SIBLINGs, we used a number of cancer cell lines in a modified Boyden chamber assay to determine if any of the proteins could enhance invasion potential. BSP, but not DMP1 or OPN, could enhance the invasion potential of many cell lines derived from breast, prostate, lung, and thyroid cancers through a model basement membrane system, Matrigel [9,10]. The specificity of BSP suggested that MMP-2 may have been involved and, indeed, inhibitors of MMP-2 stopped the BSP-enhanced invasion. Because mutating the integrin-binding tripeptide, RGD, to the chemically similar but inactive KAE also stopped the enhanced invasion, we hypothesized that integrins were involved. Blocking the activity of αvβ3 integrin with an antibody stopped the BSP-enhanced invasion. Together these observations suggested that BSP bridges MMP-2 to αvβ3 integrin. In fact, beads with bound αvβ3 integrin were able to pull down much more MMP-2 if pre-treated with BSP compared to untreated beads or ones treated with BSP-KAE [9].

To be a biologically useful model of MMP activation, however, each SIBLING must also be shown to be co-expressed with its partner MMP by a cell *in vivo*. All SIBLINGs and the three MMPs are expressed in normal growing bones and/or teeth, but we were also interested in their co-expression in normal epithelial tissues, the cells that upon transformation become the tumors studied above. OPN had been known for many years to be expressed in normal salivary gland [11] and we first chose to look carefully at this tissue. Similar to the photomicrographs presented in a recent publication [12], Figure 2 shows that all five SIBLINGs as well as MMP-2, -3 and -9 are expressed in normal human salivary gland ducts. In primates, all eight proteins are limited to the intercalated duct, striated duct, and to some degree the collecting ducts. Mature mouse salivary gland differed in two ways. First, all three of the MMPs and four of the five SIBLINGs are also expressed in the acini of mice. DSPP

expression remains limited to the rodent ducts. Second, mature male mouse ducts under the strict control of androgens become almost exclusively granulated convoluted tubules (GCT) and express none of the eight proteins. Salivary glands therefore show that a SIBLING and its MMP partner are always co-expressed and can be reasonably expected to form active complexes in the pericellular and extracellular spaces near these epithelial cells. These epithelial cells persist for many months or years and do not appear to be assisted by any other cell type in the maintenance of local matrix proteins.

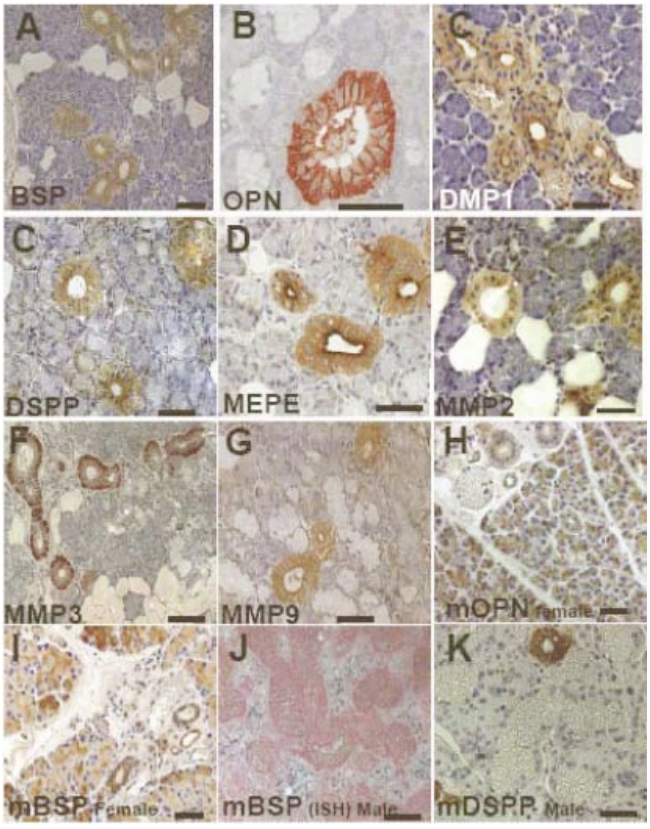

Figure 2. Immunolocalization (red/brown) of SIBLINGs and MMPs in the ducts of human salivary glands (A-G). Mouse salivary glands have staining also in the acini (OPN, H and BSP, I are shown). *In situ* hybridization of BSP (blue/purple) in mouse gland shows mRNA in acini but not granulated convoluted tubules (GCT) (J). DSPP immunostaining (red/brown) is only in non-GCT ducts (K), not in acini. Bar = 50 micrometers.

It is our hypothesis that the SIBLING/MMP partners are involved in the turnover of the pericellular and/or extracellular proteins of these metabolically active cells.

In summary, three SIBLINGs have been shown to bind and activate three different MMPs *in vitro* and the proteins are co-expressed *in vivo*, suggesting that these activities are likely to be biologically important.

REFERENCES

1. Fisher, L.W., Torchia, D.A., Fohr, B., Young, M.F., and Fedarko, N.S. (2001). Flexible structures of SIBLING proteins, bone sialoprotein, and osteopontin. *Biochem. Biophys. Res. Commun.* 280, 460-465.

2. Fisher, L.W., and Fedarko, N.S. (2003). Six genes expressed in bones and teeth encode the current members of the SIBLING family of proteins. *Proc. 7th ICCBMT. Connect. Tissue Res.* 44, 33-40.

3. Weber, G.F., Ashkar, S., Glimcher, M.J., and Cantor, H. (1996). Receptor-ligand interaction between CD44 and osteopontin (Eta-1). *Science* 271, 509-512.

4. Jain, A., Karadag, A., Fohr, B., Fisher, L.W., and Fedarko, N.S. (2002). Three SIBLINGs (small integrin-binding ligand, N-linked glycoproteins) enhance factor H's cofactor activity enabling MCP-like cellular evasion of complement-mediated attack. *J. Biol. Chem.* 277, 13700-13708.

5. Fedarko, N.S., Jain, A., Karadag, A., Van Eman, M.R., and Fisher, L.W. (2001). Elevated serum bone sialoprotein and osteopontin in colon, breast, prostate, and lung cancer. *Clin. Cancer Res.* 7, 4060-4066.

6. Fedarko, N.S., Fohr, B., Robey, P.G., Young, M.F., and Fisher, L.W. (2000). Factor H binding to bone sialoprotein and osteopontin enables tumor cell evasion of complement-mediated attack. *J. Biol. Chem.* 275, 16666-16672.

7. Brooks, P.C., Stromblad, S., Sanders, L.C., von Schalscha, T.L., Aimes, R.T., Stetler-Stevenson, W.G., Quigley, J.P., and Cheresh, D.A. (1996). Localization of matrix metalloproteinase MMP-2 to the surface of invasive cells by interaction with integrin alpha v beta 3. *Cell* 85, 683-693.

8. Fedarko, N.S., Jain, A., Karadag, A., and Fisher, L.W. (2004). Three small integrin binding ligand N-linked glycoproteins (SIBLINGs) bind and activate specific matrix metalloproteinases. *FASEB J.* 18, 734-736.

9. Karadag, A., Ogbureke, K.U., Fedarko, N.S., and Fisher, L.W. (2004). Bone sialoprotein, matrix metalloproteinase 2, and alpha(v)beta3 integrin in osteotropic cancer cell invasion. *J. Natl. Cancer Inst.* 96, 956-965.

10. Karadag, A., Fedarko, N.S., and Fisher, L.W. (2004). "The Formation of alpha-v beta-3 Integrin/Bone Sialoprotein/Matrix Metalloproteinase-2 Complex on the Cell Surface in Invasion by Breast Cancer Cells in vitro". In: *Proc. 8th ICCBMT*. W.J. Landis and J. Sodek (eds.), pp 170-173 (University of Toronto Press, Toronto).

11. Brown, L.F., Berse, B., Van de Water, L., Papadopoulos-Sergiou, A., Perruzzi, C.A., Manseau, E.J., Dvorak, H.F., and Senger, D.R. (1992). Expression and distribution of osteopontin in human tissues: widespread association with luminal epithelial surfaces. *Mol. Biol. Cell* 3, 1169-1180.

12. Ogbureke, K.U., and Fisher, L.W. (2004). Expression of SIBLINGs and their partner MMPs in salivary glands. *J. Dent. Res.* 83, 664-670.

BONE SIALOPROTEIN BINDING TO MATRIX METALLOPROTEINASE-2 ALTERS ENZYME INHIBITION KINETICS.

Alka Jain[*], Larry W. Fisher[#], and Neal S. Fedarko[*]

From the [*]Department of Medicine, Johns Hopkins University, Baltimore, MD 21224 and [#]Craniofacial and Skeletal Diseases Branch, NIDCR, NIH, DHHS, Bethesda, MD. 20892.

Bone sialoprotein (BSP) is induced by multiple neoplasms *in vivo*, its expression levels correlate with tumor stage and it can modulate the activity of matrix metalloproteinase-2 (MMP-2). In this study, the hypothesis that BSP acts biologically to lessen the effectiveness of MMP inhibitors was investigated. Solution and solid phase binding assays were carried out demonstrating that binding between recombinant BSP and latent as well as active MMP-2 does not require the hemopexin domain. BSP binding restored activity to hemopexin-deleted MMP-2 inhibited by tissue inhibitor of matrix metalloproteinase-2 (TIMP2) when activity was measured using both natural, large macromolecular substrates and synthetic, small molecular weight, freely diffusable substrates. BSP effects on TIMP2 inhibition of wild type active MMP-2 were quantified by varying small molecular weight substrate concentrations at different fixed inhibitor concentrations, and solving a general linear mixed inhibition rate equation with a global curve fitting program. The results indicate a 15 to 30-fold increase in the competitive inhibition constant and an ~ 6-fold increase in uncompetitive inhibition constant for the MMP-2+BSP complex. To address whether the failure of clinical trials of MMP inhibitors may be explained at least in part by the activity of BSP, the effect of BSP binding to MMP-2 on inhibition by a small molecular weight drug (illomastat) was similarly determined. An over 30-fold increase in K_I was observed. The ability of BSP to modulate MMP inhibitor action in an *in vitro* angiogenesis model system was tested. When human umbilical vein endothelial cells co-cultured with dermal fibroblasts in defined medium were treated with either nM TIMP2 or illomastat, the degree of tubule formation was reduced while the addition of equimolar BSP restored vessel formation.

The Small Integrin Binding LIgand N-linked Glycoprotein (SIBLING) gene family is clustered on human chromosome 4 and its members include bone sialoprotein (BSP), osteopontin, dentin matrix protein 1, matrix extracellular phosphoglycoprotein, and dentin sialophosphoprotein (1). BSP was once thought to be restricted in expression to mineralizing tissue such as bones and teeth (2) but has recently been shown to be expressed in ductal elements of salivary gland (3) and kidney (4). SIBLINGs, including BSP, are also induced in certain neoplasms (5-15). SIBLINGs can be co-localized to the cell surface through binding of $\alpha_V\beta_3$ and/or CD44 (16-18); exhibit correlation between expression levels and tumor stage (19); and bind and modulate the activity of different but specific matrix metalloproteinases (MMP)s (20). Indeed, BSP has been shown to enhance the invasion potential of many human cancer cell lines in vitro by bridging MMP-2 to the cell surface of the cells through the $\alpha_V\beta_3$ integrin (18).

MMPs are a family of structurally and functionally related endoproteinases that are involved in development and tissue repair as well as cancer angiogenesis and metastasis. We have recently shown that active MMPs inhibited by either tissue inhibitors of MMPs (TIMPs) or low molecular weight synthetic inhibitors can be reactivated by equimolar amounts of the appropriate SIBLING partner (20). The current study was undertaken to determine whether BSP action on MMP-2 inhibition involves the hemopexin domain, and to see if the SIBLING alters MMP affinity for substrates, TIMP2 or small molecular weight inhibitors. The biological consequences of these interactions were tested in an *in vitro* model system of angiogenesis.

Materials and Methods

Reagents. Pro- and active human MMP-2 was obtained from Oncogene Research Products (Boston, MA) and Research Diagnostic Systems, Inc. (Minneapolis, MN). Recombinant human

MMP-2 lacking the hemopexin domain was purchased from Biomol Research Laboratories, Inc. (Plymouth Meeting, PA). The inhibitor illomastat (GM6001, or N-[(2R)-2-(hydroxamido-carbonylmethyl)-4-methylpentanoyl]-L-tryptophan methylamide), substrate Ac-PLG-[2-mercapto-4-methyl-pentanoyl]-LG-OC_2H_5 , and 5,5'-dithio-bis-2-nitrobenzoic acid *(*DTNB) were obtained from Calbiochem (La Jolla, CA). TIMP2 was a generous gift of Dr. H. Birkedal-Hansen, NIDCR, NIH. Human serum adsorbed goat anti-rabbit IgG conjugated to horseradish peroxidase (HRP) was obtained from Kirkegaard & Perry (Gaithersburg, MD). Recombinant human BSP that included post translational modifications was made using an adenovirus construct and eukaryotic cells and purified (> 95% purity as defined by acrylamide gel electrophoresis) as previously described (16).

Fluorescent binding studies. Intrinsic tryptophan fluorescence binding studies of BSP and mutant hemopexin-deleted MMP-2 were carried out as previously described (20). BSP contains no tryptophan groups while the hemopexin-deleted MMP-2, contains 8, so the intrinsic fluorescence changes are a result of the change in conformation of the MMP alone. Briefly, the relative change in fluorescence in the area under the emission curve (300 to 500 nm at 295 nm excitation) was used to determine binding curves. Fractional acceptor saturation (f_a) as a function of nM BSP added was determined by calculating $f_a = (y - y_f)/(y_b - y_f)$, where y_f and y_b are the area under the curve of the fluorescent emission profile of free and fully bound MMP-2. Scatchard plots were made by fitting the transformed data to the function $r/[BSP] = n/K_d - r/K_d$., where r represents the binding function, *[BSP]*, BSP concentration, n the number of binding sites and K_d the dissociation constant.

Solid phase binding assays. The binding of BSP to purified and immobilized MMP-2 was measured by an indirect sandwich assay. Plates were coated with the different forms of MMP-2 by adding 0.1 ml of 3.5 nM recombinant purified MMP-2 in 50 mM $NaHCO_3$, pH 9.0 to each well of a Greiner high-binding 96-well microtiter plates (stock # 655061, Greiner Bio-One, Longwood, FL) incubated overnight at 4°C. The plates were blocked with 5 % (w/v) nonfat dry milk in TBS for 60 min and then rinsed three times with TBS containing 0.05 % Tween 20. BSP was added in nM equivalents in TBS-Tween and incubated for 120 min at room temperature. After a second round of three washes, bound ligand was quantified by the addition of a 1:50,000 dilution of specific rabbit anti-BSP antibody, LF100 (21), followed by a 60 min incubation. After three washes, secondary antibody (1:2000 goat anti-rabbit horseradish peroxidase conjugated antibody) was added and incubated for a further 60 min. Color was developed using diaminobenzamidine substrate and the absorbance at 405 nm was measured. Non-specific binding was measured by determining the ligand binding to wells coated with BSA alone, and these values were subtracted from the corresponding values for MMP-coated wells.

High molecular weight substrate studies. Fluorescein-conjugated gelatin (Molecular Probes, Inc., Eugene, OR) substrate was used to follow proteolytic activity as previously described (20). This substrate is highly substituted with fluorescein moieties so that the fluorescent signal is self-quenched until proteolytic cleavage liberates fragments and a robust fluorescent emission is measured. The reaction mixture consisted of the fluorescein-substrate conjugate with 1.4 nM mutant hemopexin-free MMP-2 reacted with either 10 nM TIMP2, 10 nM TIMP2 + 10 nM BSP, 10 nM BSP, or buffer alone (50 mM Tris, pH 7.6, 150 mM NaCl, 5 mM $CaCl_2$). Relative velocity plots were determined by varying the substrate concentration between 0.025 and 15 µg/ml and determining the change in fluorescence over the first hour of reaction. Inhibitor titrations were carried out by varying TIMP2 concentration from 1.6 to 1600 nM. Fluorescent data was acquired with excitation at 485 nm and emission at 535 nm. Reactions were run in duplicate.

Low molecular weight substrates. The activities of mutant and wild type MMP-2 in the presence and absence of inhibitors (TIMP2 or illomastat) and BSP were measured using a small molecular weight thiopeptide substrate (Ac-PLG-[2-mercapto-4-methyl-pentanoyl]-LG-OC_2H_5). Substrate was incubated in assay buffer (50 mM HEPES, 10 mM $CaCl_2$, 0.05% Brij-35, 1 mM

DTNB, pH 7.5) with 10 nM MMP-2 + different concentrations of inhibtor, a 10 nM [MMP-2+BSP] preformed complex or MMP2 + inhibitor + BSP added simultaneously. Data from the first six minutes were used to calculate velocity (pmols/sec) values. Substrate cleavage was monitored using a Perkin Elmer Victor 2 multilabel plate reader and absorbance was measured at 412 nM. Preformed complexes of [MMP-2+BSP] were formed by incubation at 37 C for 30 minutes prior to addition to the reaction mixture. Global curve-fitting of the family of substrate-velocity curves was performed using Prism 4 software (GraphPad Software, Inc.,) with V_{max}, K_m, K_{ic} and K_{iu} set as shared parameters.

SDS PAGE, zymography. 10% zymogram gelatin gels were obtained from Invitrogen, Inc., (Carlsbad, CA). Samples in zymogram gel sample buffer were electrophoresed at a constant 125 V for 90 min. Gels were processed for zymography according to the manufacture's instructions, stained with 0.5% Coomassie Brilliant Blue R250, and bands were visualized by dynamic integrated exposure using an AlphaInotech imaging system (Alpha Inotech Corp., San Leandro, CA).

In vitro angiogenesis. Human umbilical vein endothelial cell (HUVEC) and human dermal fibroblast co-cultures and EGM-2 defined medium were obtained from TCS Cell Works (Botolph Claydon, UK). The functional readout from this *in vitro* assay was tubule formation. Tubule formation was defined by the total number of tubules, total tubule length, mean tubule length, and number of branches. Test conditions were run in triplicate wells with 8 conditions per 24 well plate. The cells were treated starting on day six of culture with 5 nM BSP, 5 nM TIMP2, 5 nM BSP + TIMP2, 5 nM GM6001, 5 nM GM6001 + BSP, or buffer alone. Medium was changed every other day with fresh medium containing experimental conditions. Cells were fixed in 70 % ethanol on day 12 and tubule formation was quantified following immunostaining with a mouse anti-human PECAM-1 monoclonal antibody (TCS Cell Works), and the secondary antibody being goat anti-mouse IgG alkaline phosphatase coupled antibody, with 5-bromo-4-chloro-3-indolyl phosphate/ nitro blue tetrazolium (BCIP/NBT; Sigma) as substrate. Images were visualized on a Nikon Diaphot inverted microscope and digitized with a Polaroid CCD digital camera and software. Two images per well were captured, digitized and the number of tubules, the number of branch points (junctions) between tubules, as well as the total tubule length (in pixels) determined using AngioSys Version 1.0 software. (TCS Cell Works, Botolph Claydon, UK).

For zymographic analyses of MMP-2, a membrane-associated fraction was prepared from the HUVEC cocultures essentially as described by Ward et al. (22). Briefly, HUVEC cells were scraped from culture wells in cold 5 mM Tris HCl (pH 7.8), homogenized, and crude membranes were prepared by centrifugation of the cell lysate at 10,000 x g for 15 minutes at 4°C. The supernatant was centrifuged at 105,000 x g for 1 hour at 4°C; then, the supernatant was removed and saved, and the membrane fraction was resuspended in 20 mM Tris HCl (pH 7.8), 10 mM $CaCl_2$, and 0.05% Brij 35.

RESULTS

Bone sialoprotein binding does not require the hemopexin domain. MMPs consist of a catalytic domain and a hemopexin-like domain thought to be essential for the binding of many natural substrates. TIMPs have binding sites in both the hemopexin and catalytic domains (23). We have shown previously that BSP can bind to both pro- and active MMP-2 (20). Whether BSP interacts with the hemopexin domain or, at least in part, with the catalytic region was investigated by studying the binding characteristic of BSP to recombinant human MMP-2 that lacks the hemopexin domain. When the intrinsic tryptophan fluorescence of the mutant MMP-2 was followed during titration with BSP, quenching of the signal similar to that previously seen for the intact MMP-2 was observed (Fig. 1). The area under the emission peaks was quantified and used to determine the change in fluorescence and calculate both the fractional acceptor saturation as a function of nM BSP added and a corresponding Scatchard plot. BSP binding was saturable and its affinity for the mutant protein was actually higher than that for intact MMP-2 (K_d = 0.07 ± 0.03 nM for mutant MMP-2 versus 0.32 ± 0.02 nM for active MMP-2, and 2.9 ± 0.9 nM for pro-MMP-2).

An alternative method to confirm BSP and MMP-2 binding was employed. Solid phase binding assays were developed to measure BSP binding to immobilized forms of MMP-2. Microtiter plates coated with either proMMP-2, active MMP-2 or hemopexin-deleted MMP-2 were reacted with increasing concentrations of BSP and the amount bound quantified by specific antibodies (Fig. 1D). The binding of BSP to MMP variants was saturable. Scatchard plot analysis revealed BSP binding with a K_d = 0.39 ± 0.04 nM for mutant MMP-2 versus 0.36 ± 0.04 nM for active MMP-2 and 2.1 ± 0.1 nM for pro- MMP-2 (Fig. 1E). While the pro- and active forms of MMP-2 exhibited essentially similar binding constants by the two different binding methods, the mutant form of MMP-2 exhibited a distinct K_d value which may be reflecting differences in solid phase binding orientation in the absence of the hemopexin domain. Attempts to measure BSP binding to TIMP2 by either intrinsic tryptophan fluorescence spectroscopy (TIMP2 contains 4 internal tryptophans, BSP none) or by solid phase binding assay were negative (data not shown).

Bone sialoprotein modulation of MMP-2 activity does not require the hemopexin domain. We recently reported that BSP can restore enzymatic activity to MMP-2 incubated with TIMP2 when activity was followed using a natural, large molecular weight substrate (gelatin) (20). The effect of BSP on the activity of the mutant MMP-2 was therefore investigated using the gelatin-fluorescein large molecular weight substrate assay (Fig. 2 A-D). The change in substrate fluorescence caused by mutant MMP-2 alone compared to a complex of equimolar mutant MMP-2 + BSP was not significantly different. As expected, the addition of equimolar TIMP2 to mutant MMP-2 caused a significant decrease in the rate of fluorescence change. However, inclusion of equimolar BSP to mutant MMP-2 + TIMP2 complexes restored the rate of fluorescence change to that of mutant MMP-2 alone showing that the TIMP2 became ineffective in the presence of bound BSP. Substrate velocity plots as a function of substrate concentration yielded no significant difference for mutant MMP-2 in the presence or absence of BSP. Titration with TIMP2 of mutant MMP-2 and the large molecular weight substrate revealed that over a 100-fold excess of TIMP2 was required to inhibit activity to 20 % (Fig. 2 C). For complexes of equimolar mutant MMP-2 + TIMP2, the rate of the reaction was decreased to 67 %, while the presence of equimolar BSP restored activity to 97 %. Increasing the concentration of BSP in mixes of equimolar TIMP2 and mutant MMP-2 further increased the reaction rate (Fig. 2 D).

A low molecular weight freely diffusible peptide substrate assay was next used and enabled kinetic parameters to be evaluated (Fig. 2 E-H). Similar to results with the large molecular weight substrate, the addition of BSP alone did not significantly alter mutant MMP-2 enzyme product evolution. Furthermore, the TIMP2 inhibited product evolution as expected and the addition of BSP to the preformed mutant MMP-2/TIMP2 complex returned the digestion to uninhibited levels. Substrate velocity plots of mutant MMP-2 ± BSP yielded no statistically significant difference in fitted K_m or v_{max} values (Table I) verifying the observations with the larger substrate that the conformational changes induced by BSP did not significantly affect the actions of the active site itself. Titration of the small molecular weight substrate and mutant MMP-2 with varying concentrations of TIMP2 indicated that at 10-fold excess, TIMP2 inhibited mutant MMP-2 activity to 20 %, while equimolar TIMP2 inhibited mutant MMP-2 and to 34 % (Fig. 2 G). The addition of equimolar BSP was able to restore the activity of mutant MMP-2 treated with TIMP2 to 85 %. Increasing the concentration of BSP in reaction mixtures of small molecular weight substrate + equimolar TIMP2 and mutant MMP-2 restored activity further (Fig. 2 H). These data suggest that BSP reactivation of TIMP2-inhibited MMP-2 does not require the hemopexin domain of MMP-2.

TIMP Inhibition kinetics. To determine the effect of BSP on active wild type MMP-2 and TIMP2 reaction kinetics, the small molecular weight substrate was employed to follow product evolution over time. MMP-2 incubated with increasing concentrations of TIMP2 exhibited the expected dose-dependent inhibition (Fig. 3A). The inhibition by TIMP2 was significantly decreased by the presence of either a performed complex of [MMP-2+BSP] or by the simultaneous addition of BSP and TIMP2 to MMP-2 (Fig. 3B, C). To

investigate whether decreased inhibition of MMP-2 by TIMP2 in the presence of BSP was associated with an altered affinity, substrate-velocity plots were obtained by varying substrate concentrations of each at different but fixed inhibitor concentrations. Reaction conditions included either TIMP2 + 10 nM MMP-2, TIMP2 + preformed equimolar complexes of 10 nM [MMP-2+BSP], or simultaneous mixes of TIMP2 + 10 nM MMP-2 + 10 nM BSP (Fig. 3D - E).

Because there are two distinct binding sites for TIMP2 on MMP-2, TIMP2 does not act purely as a competitive inhibitor (24). The common types of inhibition (competitive, uncompetitive, noncompetitive) are all special cases of linear mixed inhibition (25). The generalized linear mixed inhibition equation $v = V_{max}[S]/\{K_m(1+ [I]/K_{ic}) + [S](1+[I]/K_{iu})\}$, was employed to determine the reaction rate. V_{max} is the limiting rate, K_m is the Michaelis constant, K_{ic} is the competitive inhibition constant and K_{iu} is the uncompetitive inhibition constant. For competitive inhibition, $[I]/K_{iu}$ is negligible while for uncompetitive inhibition $[I]/K_{ic}$ is negligible. In pure noncompetitive inhibition the inhibition constants are equal.

Global curve-fitting of the family of substrate-velocity curves (Fig. 3D-F) revealed a significant increase in K_{ic} and K_{iu} values for the [MMP-2+BSP] complex as well as the simultaneously added MMP-2 + BSP (Table I). This indicates a relatively poor affinity of the inhibitor for MMP-2 in the presence of BSP. The order of magnitude change in apparent inhibitor affinity for MMP-2 in the presence of BSP indicates that SIBLING modulation of MMPs is physiologically significant.

Illomastat inhibitor kinetics. The MMP inhibitor illomastat was utilized to test whether small molecular weight drug inhibition of MMP-2 activity could be modulated by BSP. Illomastat at a 1 nM concentration inhibited the initial velocity of MMP-2 activity to 39 % of control activity, while the same concentration of inhibitor reduced the activity of the MMP-2 + BSP to only 70 % of control suggesting that the inhibitor is much less effective against MMP-2 in the conformation resulting from the binding of BSP (Figure 4A). Titration of a mix of 10 nM MMP-2 + 1 nM illomastat with increasing concentrations of BSP revealed a dose-dependent decrease to the inhibitor's action (Fig. 4B).. To quantify the effects of BSP on MMP-2 inhibitor kinetics, substrate-velocity plots were obtained by varying substrate concentrations of each at different but fixed illomastat concentrations. Reaction conditions were either 10 nM MMP-2 alone, or with 10 nM equimolar MMP-2 + BSP (Fig. 4C, D).

Because Illomastat is a competitive inhibitor, kinetic parameters in the presence and absence of BSP can be determined by fitting the substrate-velocity curves to the equation for competitive inhibition: $v = v_{max}[S]/K_m(1+[I]/K_{Ic})+[S]$; where V_{max} is the limiting rate, K_m is the Michaelis constant, K_{Ic} is the competitive inhibition constant, $[S]$ is substrate concentration and $[I]$ is illomastat concentration. The results indicated a significant increase (> 30-fold) in K_{Ic} value for the MMP-2 + BSP (Table I). Thus illomastat exhibited a reduced affinity for MMP-2 in the presence of BSP.

BSP restores activity to inhibited MMPs in vitro. The ability of BSP to restore enzymatic activity to TIMP2- and illomastat-inhibited MMP-2 in a purified component assay led to a screen of the effects of BSP on MMP inhibitors in an *in vitro* angiogenesis system. 5 nM BSP alone stimulated tubule formation by HUVEC cells while separately illomastat (GM6001) and TIMP2 inhibited tubule formation below control levels (Figure 5). The inclusion of BSP with MMP-specific inhibitors restored tubule formation. Quantification of tubule formation using AngioSys Ver. 1.0 software revealed that the addition of BSP to TIMP2 or illomastat-treated cells restored not only the number of tubules but also the number of branch points and total tubule length (in pixels) to values not significantly different from BSP enhancement alone (Figure 6). The effect of BSP on MMP-2 levels and activity in the *in vitro* angiogenesis system was also studied by two other, complementary systems. MMP activity measured by the fluorescein-gelatin substrate assay and a rate of digestion of gelatin by zymography. Both assays exhibited a consistent

pattern of increased enzymatic activity in BSP-treated conditions.

DISCUSSION

BSP is a member of the SIBLING gene family (2). It is extended and flexible in solution and such lack of ordered structure is shared by a number proteins that have multiple binding partners (1). BSP can bind the $\alpha_V\beta_3$ integrin via its RGD sequence (26,27) and to complement Factor H (16). BSP can also bind to and modulate the activity of MMP-2 (20). Binding of BSP to MMP-2 was associated with conformational changes as indicated by fluorescent quenching during BSP binding titration (indicating a change in the microenvironment of the MMP's tryptophans); and by increased susceptibility of a BSP–proMMP-2 complex to plasmin cleavage. BSP binding to latent MMP-2 was associated with increased proteolytic activity and BSP binding to TIMP2-inhibited MMP-2 restored activity (20). Taken together the data suggest that conformational changes in MMP-2 induced by BSP binding may include changes in the shape of the active site and inhibitor binding domains. A trimolecular complex of BSP, $\alpha_V\beta_3$ and MMP-2 can be demonstrated by immunoprecipitation, flow cytometry, and *in situ* hybridization in cancer cells grown *in vitro* (18). BSP message was induced in multiple cancers and its expression correlated with paired MMP-2 expression as well as tumor stage (19).

MMP-2, a gelatinase that can degrade components of the extracellular matrix at physiological pH, is regulated *in vivo* by the naturally occurring TIMPs and RECK (28,29). TIMP2 binding to MMP-2 involves distinct domains on both the inhibitor and the enzyme (30-32). The binding and kinetics of MMP-2 and TIMP2 are more complex than simple competitive inhibition. In our analyses we have used a mixed linear model of mixed inhibition (25) and observed inhibition constants in the $\leq$ nM range. K_I values in sub-nanamolar range for TIMP2 and MMP-2 using the same substrate have been reported in the literature (33-35), though a more recent analysis has yielded 3- to 4-fold higher estimation (23). The different reported values are most likely due to differences in sources and concentrations of substrate, enzyme and inhibitor.

SIBLING binding to active MMPs inhibited by TIMP or small molecular weight MMP-specific inhibitors could restore activity through multiple mechanisms. Possible mechanisms include blocking inhibitor access (steric blocking), binding to the inhibitor (stripping), or by altering inhibitor affinity. The analysis of inhibitor kinetic parameters as well as binding order effects can be used to distinguish between steric blocking or affinity changes. Based on the current studies with BSP, MMP-2 and TIMP2, SIBLING binding to MMP did not significantly alter K_m values but did alter the MMP's affinity for its inhibitor. SIBLING binding to inhibitor (stripping) was not observed.

BSP was found to significantly reduce the affinity of a small molecular weight synthetic inhibitor (illomastat) for MMP-2. Illomastat as a hydroxamate class inhibitor blocks the activity of multiple MMPs and has been used to disrupt angiogenesis and metastasis (36-38). Illomastat blocked TNFα processing (39), experimental autoimmune encephalitis (40), angiogenesis and metastasis (36-38). The magnitude of change in apparent inhibitor affinity for MMP-2 in the presence of BSP indicates that SIBLING modulation of MMP inhibition by small molecular weight drugs can be physiologically significant.

Finally, a cell culture model system was used to test whether BSP modulation of MMP-2 inhibition occurs *in vitro*. The *in vitro* model of angiogenesis utilized human umbilical vein endothelial cells (HUVECs) co-cultured with normal adult human diploid dermal fibroblasts. The endothelial cells form small islands amongst the fibroblasts, proliferate, and migrate through the co-culture matrix to form thread-like tubule structures. These cord-like structures join up to form a network of anastomosing tubules. These linked tubules produce endothelial cell-specific components such as von Willebrand Factor and PECAM-1 (CD31) that can be stained immunohistochemically and quantified. The observed effects of BSP (stimulating basal tubule formation and restoring formation to TIMP2- or illomastat-inhibited cultures) was consistent with BSP modulating MMP-2 activity. Profiling MMP-2 levels and activity in the *in vitro* system (by

zymography and fluorescent substrate assays) demonstrated changes with BSP treatment. BSP has been shown to promote angiogenesis in the chick chorioallantoic membrane system (41). Thus, BSP has biochemical and biological plausibility to be playing active roles in tumor progression *in vivo.* BSP is induced by multiple neoplasms *in vivo* and its modulation of MMP activity might contribute to the relative lack of efficacy seen in the recent clinical trials of MMP inhibitors in numerous cancers (42).

Literature Cited

1. Fisher, L. W., Torchia, D. A., Fohr, B., Young, M. F., and Fedarko, N. S. (2001) *Biochem. Bophys. Res. Comm.* **280**, 460-465
2. Fisher, L. W., and Fedarko, N. S. (2003) *Connect Tissue Res* **44 Suppl 1**, 33-40
3. Ogbureke, K. U., and Fisher, L. W. (2004) *J Dent Res* **83**(9), 664-670
4. Ogbureke, K. U., and Fisher, L. W. (2005) *Kidney Int* **68**(1), 155-166
5. Craig, A. M., Bowden, G. T., Chambers, A. F., Spearman, M. A., Greenberg, A. H., Wright, J. A., McLeod, M., and Denhardt, D. T. (1990) *Int J Cancer* **46**(1), 133-137
6. Gillespie, M. T., Thomas, R. J., Pu, Z. Y., Zhou, H., Martin, T. J., and Findlay, D. M. (1997) *Int J Cancer* **73**(6), 812-815
7. Hirota, S., Nakajima, Y., Yoshimine, T., Kohri, K., Nomura, S., Taneda, M., Hayakawa, T., and Kitamura, Y. (1995) *J Neuropathol Exp Neurol* **54**(5), 698-703
8. Senger, D. R., Perruzzi, C. A., and Papadopoulos, A. (1989) *Anticancer Res* **9**(5), 1291-1299
9. Sung, V., Stubbs, J. T., 3rd, Fisher, L., Aaron, A. D., and Thompson, E. W. (1998) *J Cell Physiol* **176**(3), 482-494
10. Bellahcene, A., Kroll, M., Liebens, F., and Castronovo, V. (1996) *J Bone Miner Res* **11**(5), 665-670
11. Bellahcene, A., Albert, V., Pollina, L., Basolo, F., Fisher, L. W., and Castronovo, V. (1998) *Thyroid* **8**(8), 637-641
12. Bellahcene, A., Merville, M. P., and Castronovo, V. (1994) *Cancer Res* **54**(11), 2823-2826
13. Bellahcene, A., Maloujahmoum, N., Fisher, L. W., Pastorino, H., Tagliabue, E., Menard, S., and Castronovo, V. (1997) *Calcif Tissue Int* **61**(3), 183-188
14. Chaplet, M., De Leval, L., Waltregny, D., Detry, C., Fornaciari, G., Bevilacqua, G., Fisher, L. W., Castronovo, V., and Bellahcene, A. (2003) *J Bone Miner Res* **18**(8), 1506-1512
15. Rowe, P. S., de Zoysa, P. A., Dong, R., Wang, H. R., White, K. E., Econs, M. J., and Oudet, C. L. (2000) *Genomics* **67**(1), 54-68
16. Fedarko, N. S., Fohr, B., Gehron Robey, P., Young, M. F., and Fisher, L. W. (2000) *J. Biol. Chem.* **275**, 16666-16672
17. Jain, A., Karadag, A., Fohr, B., Fisher, L. W., and Fedarko, N. S. (2002) *J Biol Chem* **277**(16), 13700-13708
18. Karadag, A., Ogburke, K. U. E., Fedarko, N. S., and Fisher, L. W. (2004) *J. Natl. Cancer Inst.* **96**(12), In press.
19. Fisher, L. W., Jain, A., Tayback, M., and Fedarko, N. S. (2004) *Clin. Can. Res* **10**(24), 8501-8511
20. Fedarko, N. S., Jain, A., Karadag, A., and Fisher, L. W. (2004) *Faseb J* **18**(6), 734-736
21. Mintz, K. P., Grzesik, W. J., Midura, R. J., Robey, P. G., Termine, J. D., and Fisher, L. W. (1993) *J Bone Miner Res* **8**(8), 985-995
22. Ward, R. V., Atkinson, S. J., Slocombe, P. M., Docherty, A. J. P., Reynolds, J. J., and Murphy, G. (1991) *Biochim Biophys Acta.* **1079**, 242 –246.
23. Olson, M. W., Gervasi, D. C., Mobashery, S., and Fridman, R. (1997) *Journal of Biological Chemistry* **272**, 29975-29983.

24. Kleiner, D. E., Jr., Unsworth, E. J., Krutzsch, H. C., and Stetler-Stevenson, W. G. (1992) *Biochemistry* **31**(6), 1665-1672
25. Cortes, A., Cascante, M., Cardenas, M. L., and Cornish-Bowden, A. (2001) *Biochem J* **357**(Pt 1), 263-268
26. Oldberg, A., Franzen, A., and Heinegard, D. (1986) *Proc Natl Acad Sci U S A* **83**(23), 8819-8823
27. Fisher, L. W., McBride, O. W., Termine, J. D., and Young, M. F. (1990) *J Biol Chem* **265**(4), 2347-2351
28. Giannelli, G., and Antonaci, S. (2002) *Histol Histopathol* **17**(1), 339-345
29. Oh, J., Takahashi, R., Kondo, S., Mizoguchi, A., Adachi, E., Sasahara, R. M., Nishimura, S., Imamura, Y., Kitayama, H., Alexander, D. B., Ide, C., Horan, T. P., Arakawa, T., Yoshida, H., Nishikawa, S., Itoh, Y., Seiki, M., Itohara, S., Takahashi, C., and Noda, M. (2001) *Cell* **107**(6), 789-800
30. Willenbrock, F., Crabbe, T., Slocombe, P. M., Sutton, C. W., Docherty, A. J., Cockett, M. I., O'Shea, M., Brocklehurst, K., Phillips, I. R., and Murphy, G. (1993) *Biochemistry* **32**(16), 4330-4337
31. Nguyen, Q., Willenbrock, F., Cockett, M. I., O'Shea, M., Docherty, A. J., and Murphy, G. (1994) *Biochemistry* **33**(8), 2089-2095
32. Hutton, M., Willenbrock, F., Brocklehurst, K., and Murphy, G. (1998) *Biochemistry* **37**(28), 10094-10098
33. O'Shea, M., Willenbrock, F., Williamson, R. A., Cockett, M. I., Freedman, R. B., Reynolds, J. J., Docherty, A. J., and Murphy, G. (1992) *Biochemistry* **31**(42), 10146-10152
34. Murphy, G., and Docherty, A. J. (1992) *Am J Respir Cell Mol Biol* **7**(2), 120-125
35. O'Connell, J. P., Willenbrock, F., Docherty, A. J., Eaton, D., and Murphy, G. (1994) *J Biol Chem* **269**(21), 14967-14973
36. Boghaert, E. R., Chan, S. K., Zimmer, C., Grobelny, D., Galardy, R. E., Vanaman, T. C., and Zimmer, S. G. (1994) *J Neurooncol* **21**(2), 141-150
37. Galardy, R. E., Grobelny, D., Foellmer, H. G., and Fernandez, L. A. (1994) *Cancer Res* **54**(17), 4715-4718
38. Winding, B., NicAmhlaoibh, R., Misander, H., Hoegh-Andersen, P., Andersen, T. L., Holst-Hansen, C., Heegaard, A. M., Foged, N. T., Brunner, N., and Delaisse, J. M. (2002) *Clin Cancer Res* **8**(6), 1932-1939
39. Solorzano, C. C., Ksontini, R., Pruitt, J. H., Auffenberg, T., Tannahill, C., Galardy, R. E., Schultz, G. P., MacKay, S. L., Copeland, E. M., 3rd, and Moldawer, L. L. (1997) *Shock* **7**(6), 427-431
40. Gijbels, K., Galardy, R. E., and Steinman, L. (1994) *J Clin Invest* **94**(6), 2177-2182
41. Bellahcene, A., Bonjean, K., Fohr, B., Fedarko, N. S., Robey, F. A., Young, M. F., Fisher, L. W., and Castronovo, V. (2000) *Circ Res* **86**(8), 885-891
42. Mandal, M., Mandal, A., Das, S., Chakraborti, T., and Sajal, C. (2003) *Mol Cell Biochem* **252**(1-2), 305-329

FIGURE LEGENDS

Figure 1. BSP binding to MMP-2 does not require the hemopexin domain. Binding interactions between mutant MMP-2 lacking the hemopexin domain and BSP were followed by intrinsic tryptophan fluorescence of the MMP-2 protein (BSP has no tryptophans). 1 nM mutant MMP-2 was reacted with increasing concentration of BSP. Intrinsic tryptophan fluorescence was monitored by excitation at 295 nm and recording emission from 300 to 500 nm using a Photon Technology International Series M fluorimeter (A). Binding saturation was followed by monitoring the change in the area under the emission peak curve (inset). The area under the emission peak curve was used to determine a binding curve by calculating fractional acceptor saturation versus nM BSP added (B) and the corresponding Scatchard plot (C). The binding interaction between BSP and latent MMP-2 (◇), active MMP-2 (○) and mutant hemopexin-free MMP-2 (□) were investigated by solid phase binding assays (D). Scatchard plots derived from solid phase binding assays of BSP and latent MMP-2, active MMP-2 and hemopexin-deleted MMP-2 were determined (E.).

Figure 2. BSP binding to hemopexin-deleted MMP-2 keeps TIMP2 from inhibiting the protease activity. The effect of BSP on the activity of the mutant MMP-2 was profiled using the fluorescein-labeled large molecular weight (gelatin) substrate assay (A). Reaction conditions included mutant MMP2 (□), mutant MMP2 + BSP (○), mutant MMP2 + TIMP2 (△), and mutant MMP2 + TIMP2 +BSP (▲). The effect of a varying substrate concentration on the relative velocity of the mutant enzyme in the presence (○) or absence (□) of BSP was analyzed by linear regression analysis over the first hour and the slope determined at each substrate concentration (B). Similarly, the relative rates of 12.5 µg/ml substrate cleavage by 1.4 nM mutant MMP-2 in the presence of increasing concentrations of TIMP2 were compared by plotting the fluorescent change/min at each dose (C). Conditions included mutant MMP2 alone (□), mutant MMP2 + TIMP2 (△), and mutant MMP2 + TIMP2 + BSP (▲). The effect of BSP on mutant MMP-2 inhibition was studied by titrating a reaction mixture of 10 nM mutant MMP-2 + 10 nM TIMP2 with increasing concentrations of BSP (D). Conditions included mutant MMP2 + TIMP2 (△) and mutant MMP2 + TIMP2 + BSP (▲). The action of BSP on mutant MMP2 activity using a small molecular weight substrate was determined by following pmol product evolution over time (E), velocity plots (F), TIMP2 inhibition curves (G)., and BSP dose response of inhibition by 10 nM TIMP2 + 10 nM mutant MMP-2 (H). Reaction conditions included mutant MMP2 (□), mutant MMP2 + BSP (○), mutant MMP2 + TIMP2 (△), and mutant MMP2 + TIMP2 +BSP (▲). For substrate titrations and TIMP2 dose response, three separate experiments were combined and values plotted present the mean with error bars representing the standard deviation.

Figure 3. BSP effects on TIMP2 inhibition of MMP-2. Small molecular weight substrate was incubated in assay buffer at a final concentration of 100 µM with (A) 10 nM MMP-2 and different concentrations of TIMP2 or (B) 10 nM preformed complex of [MMP-2+BSP] incubated with increasing concentrations of TIMP2, or (C) simultaneously added 10 nM MMP-2 + BSP and different concentrations of TIMP2. TIMP2 concentrations ranged from 0 (□), 1 (○), 5 (△), 10 (◇), and 20 (▽) nM TIMP2. MMP-2 and BSP concentration was 10 nM. Reaction rates were profiled by increasing substrate concentration from 10 to 200 µM. Data from the first six minutes of each reaction condition were used to calculate V_0 (pmols/sec) values. Substrate-velocity plots of MMP-2 incubated with different concentrations of TIMP2 (D), of [MMP-2+BSP] complexes incubated with varying concentrations of TIMP2 (E), or of MMP-2 incubated simultaneously with TIMP2 and BSP (F) were determined. Preformed complexes of [MMP-2+BSP] were formed by incubation at 37°C for 30 minutes prior to addition to the reaction mixture. Six separate experiments were combined for each condition and values shown represent the mean ± the standard deviation.

Figure 4. BSP effects on illomastat (GM6001) inhibition of MMP-2. 100 µM peptide substrate was incubated with 10 nM MMP-2 (□), 10 nM MMP2 + 1 nM illomastat (△), or [10 nM MMP2+10 nM BSP] + 1 nM illomastat (▲) and the evolution of product followed by absorbance at 405 nm (A). In parallel

experiments, peptide substrate was incubated with 10 nM MMP-2 (□), 10 nM MMP2 + 1 nM illomastat (△), or 10 nM MMP2 + 1 nM illomastat + varying concentrations of BSP (▲) to profile a dose response (B). Substrate-velocity plots were generated by increasing substrate concentration at different fixed inhibitor concentrations with the slope over the first six minutes being used to calculate V_0 values (C, D). Active MMP-2 was incubated with illomastat whose concentration varied from 0 (□), 0.1 (○), 0.5 (△), 1 (◇), 5 (▽), and 10 (✣) nM. The inhibitor was added to either directly to MMP-2 (C) or to MMP-2+BSP (D).

Figure 5. BSP stimulates angiogenesis and overcomes MMP-2 inhibitors *in vitro*. HUVEC cells were treated starting on day 6 of culture with vehicle alone (A), 5 nM GM6001 (B), 5 nM TIMP2 (C), 5 nM BSP (D), as well as combinations of 5 nM BSP + 5 nM GM6001 (E) or 5 nM BSP + 5 nM TIMP2 (F). The cells were fixed on day 12 and probed with a PECAM1 antibody (blue) to visualize tubule formation. Note that BSP stimulated tubule formation and in equimolar amounts overcame the inhibitory effects of both natural (TIMP) and synthetic (GM6001) MMP-2 inhibitors.

Figure 6. Quantification of the effects of recombinant BSP on tubule formation and in overcoming the effects of MMP-2 inhibitors. Two distinct fields from each triplicate well of the experimental conditions described were digitized as TIFF files and analyzed using AngioSys Ver. 1.0 software (TCS Cell Works, Buckingham UK). The image analysis package determined the number of tubules (A), the number of branch points or junctions (B) between tubules, as well as the total tubule length in pixels (C). In each case BSP stimulated the angiogenesis parameters even in the presence of the normally inhibitory effect of both natural (TIMP) and synthetic (GM6001) MMP-2 protease inhibitors. In addition a cell surface-associated pool from day 10 cohort cultures was assayed for MMP activity by the large fluorescein-gelatin substrate assay (D) and by zymography (E). Note that BSP caused increased cell surface accumulation of MMP-2 activity in the presence and absence of inhibitors. C, control, B, BSP; T, TIMP2; T+B, TIMP2 + BSP: G, GM6001; G+B, GM6001 + BSP. The region of the zymogram corresponding to active MMP-2 is shown. Asterisks represent ANOVA p values with *, $p \leq 0.05$ and **, $p \leq 0.01$.

TABLES

Table I. BSP & MMP-2 kinetic values.

	K_m	V_{max}	K_{ic}	K_{iu}
mMMP2	96 ± 13	0.20 ± 0.01		
mMMP2+BSP	59 ± 14	0.18 ± 0.02		
MMP2	103 ± 14	1.9 ± 0.1		
MMP2+BSP	90 ± 10	2.1 ± 2		
MMP2+TIMP2	103 ± 9	1.9 ± 0.8	0.67 ± 0.06	1.4 ± 0.2
[MMP2+BSP]+TIMP2	127 ± 18	2.1 ± 0.2	24 ± 12	9 ± 4
MMP2+TIMP2+BSP	98 ± 14	1.8 ± 0.1	10 ± 3	9 ± 2
MMP2+GM6001	106 ± 23	1.8 ± 0.5	0.3 ± 0.1	-
MMP2+BSP+GM6001	88 ± 10	1.6 ± 0.2	9.8 ± 0.3	-

For the small molecular weight substrate peptide substrate, K_m values are µM and for TIMP2 and illomastat the K_I values are nM. Abreviations: mMMP2, mutant hemopexin-deleted MMP-2; BSP, bone sialoprotein; TIMP2, tissue inhibitor of matrix metalloproteinase-2; GM6001, illomastat. K_{ic} and K_{iu} values were determined by fitting the generalized linear mixed inhibition equation and K_I values determined using the equation for competitive inhibition.

FOOTNOTES

[1] The abbreviations used are: SIBLING, Small, Integrin-Binding LIgand, N-linked Glycoprotein; BSP, bone sialoprotein; MMP, matrix metalloproteinase; proMMP, pro-matrix metalloproteinase; TIMP, tissue inhibitor of matrix metalloproteinase; TBS, Tris buffered saline; HRP, horse radish peroxidase; r, binding function; C_S, total ligand concentration; C_A total acceptor concentration; f_a, fractional acceptor saturation.

ACKNOWLEDGEMENTS

This research was supported in part by DAMD 17-02-0684 (N.S.F.) and by the Intramural Research Program of the NIH, NIDCR (L.W.F.).

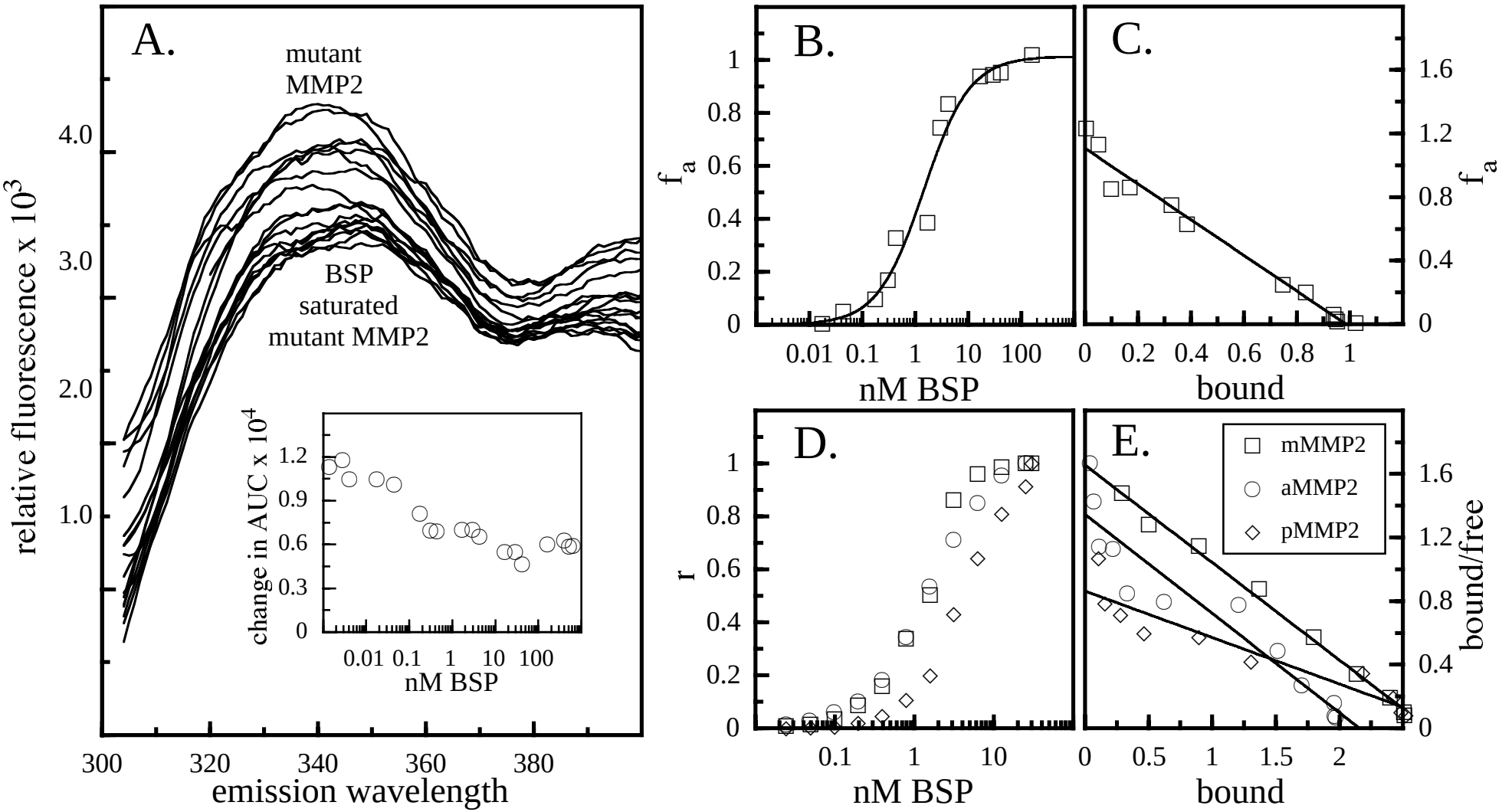
A.
mutant
MMP2
BSP
saturated
mutant MMP2
relative fluorescence x 10^3
emission wavelength
change in AUC x 10^4
nM BSP
B.
f_a
nM BSP
C.
f_a
bound
D.
r
nM BSP
E.
mMMP2
aMMP2
pMMP2
bound/free
bound

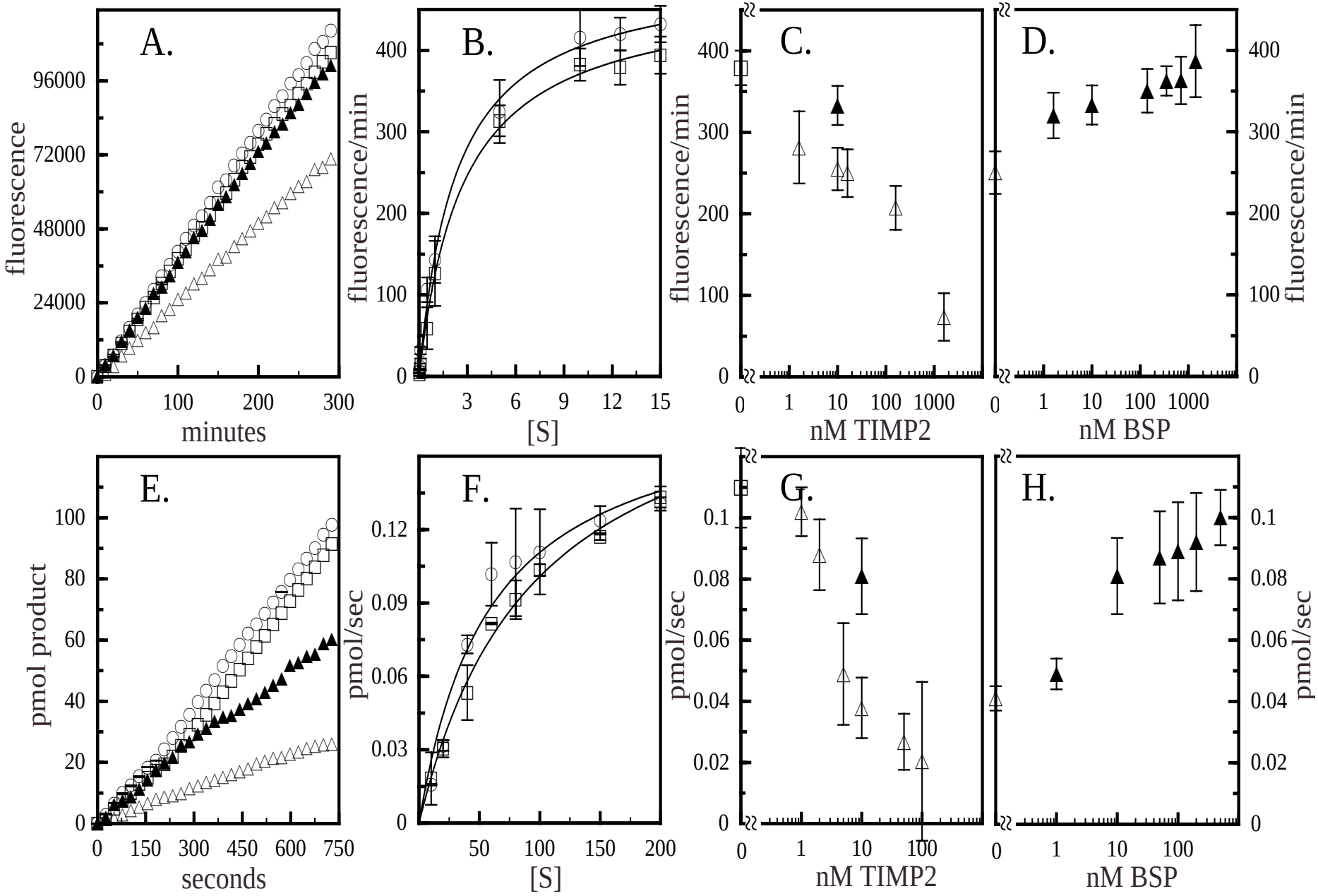
A.
fluorescence
96000
72000
48000
24000
0
0
100
200
300
minutes
B.
fluorescence/min
400
300
200
100
0
3
6
9
12
15
[S]
C.
fluorescence/min
400
300
200
100
0
0
1
10
100
1000
nM TIMP2
D.
fluorescence/min
400
300
200
100
0
0
1
10
100
1000
nM BSP
E.
pmol product
100
80
60
40
20
0
0
150
300
450
600
750
seconds
F.
pmol/sec
0.12
0.09
0.06
0.03
0
50
100
150
200
[S]
G.
pmol/sec
0.1
0.08
0.06
0.04
0.02
0
0
1
10
100
nM TIMP2
H.
pmol/sec
0.1
0.08
0.06
0.04
0.02
0
0
1
10
100
nM BSP

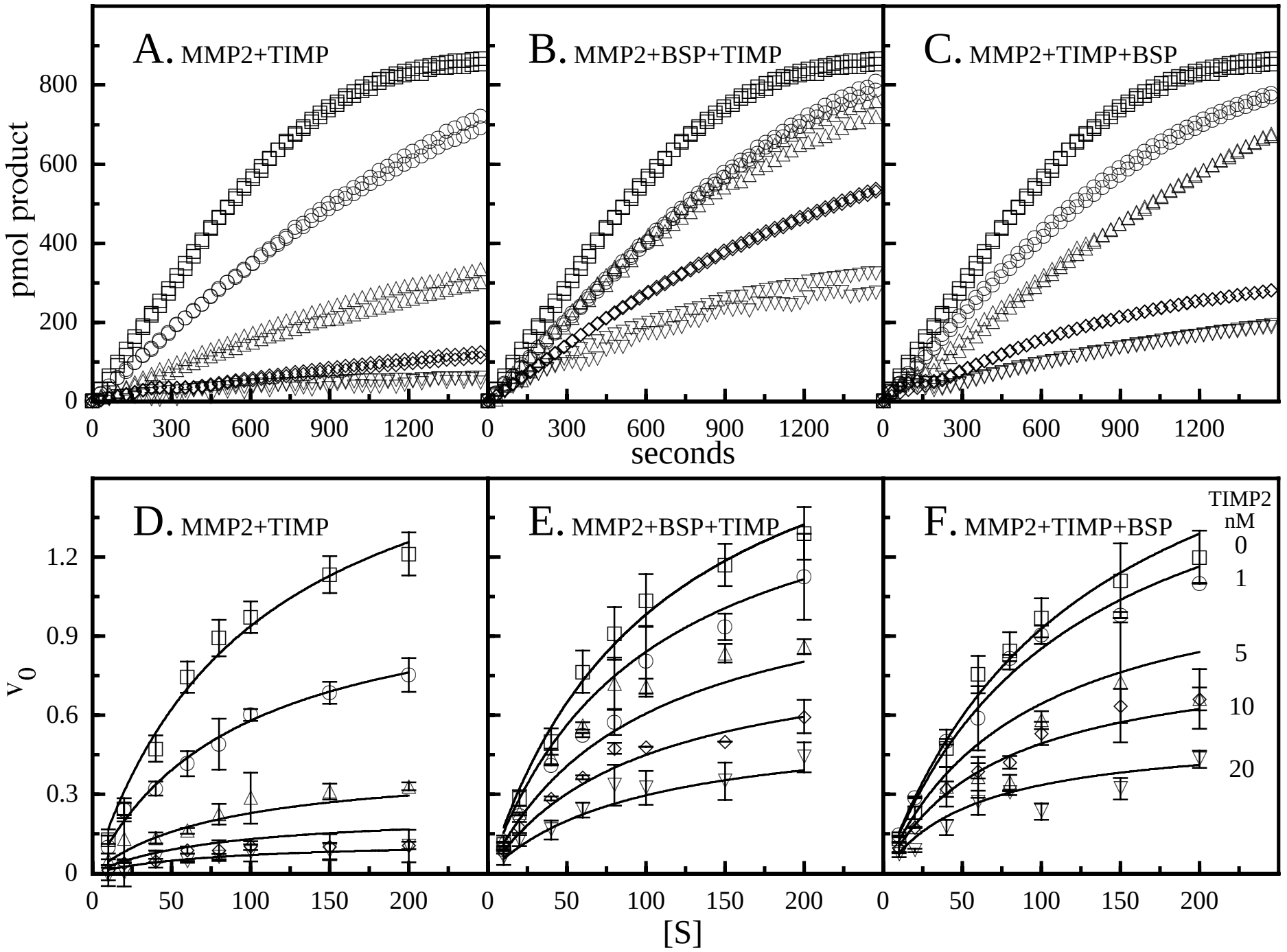
A. MMP2+TIMP
B. MMP2+BSP+TIMP
C. MMP2+TIMP+BSP
pmol product
seconds
D. MMP2+TIMP
E. MMP2+BSP+TIMP
F. MMP2+TIMP+BSP
TIMP2 nM
0
1
5
10
20
v0
[S]

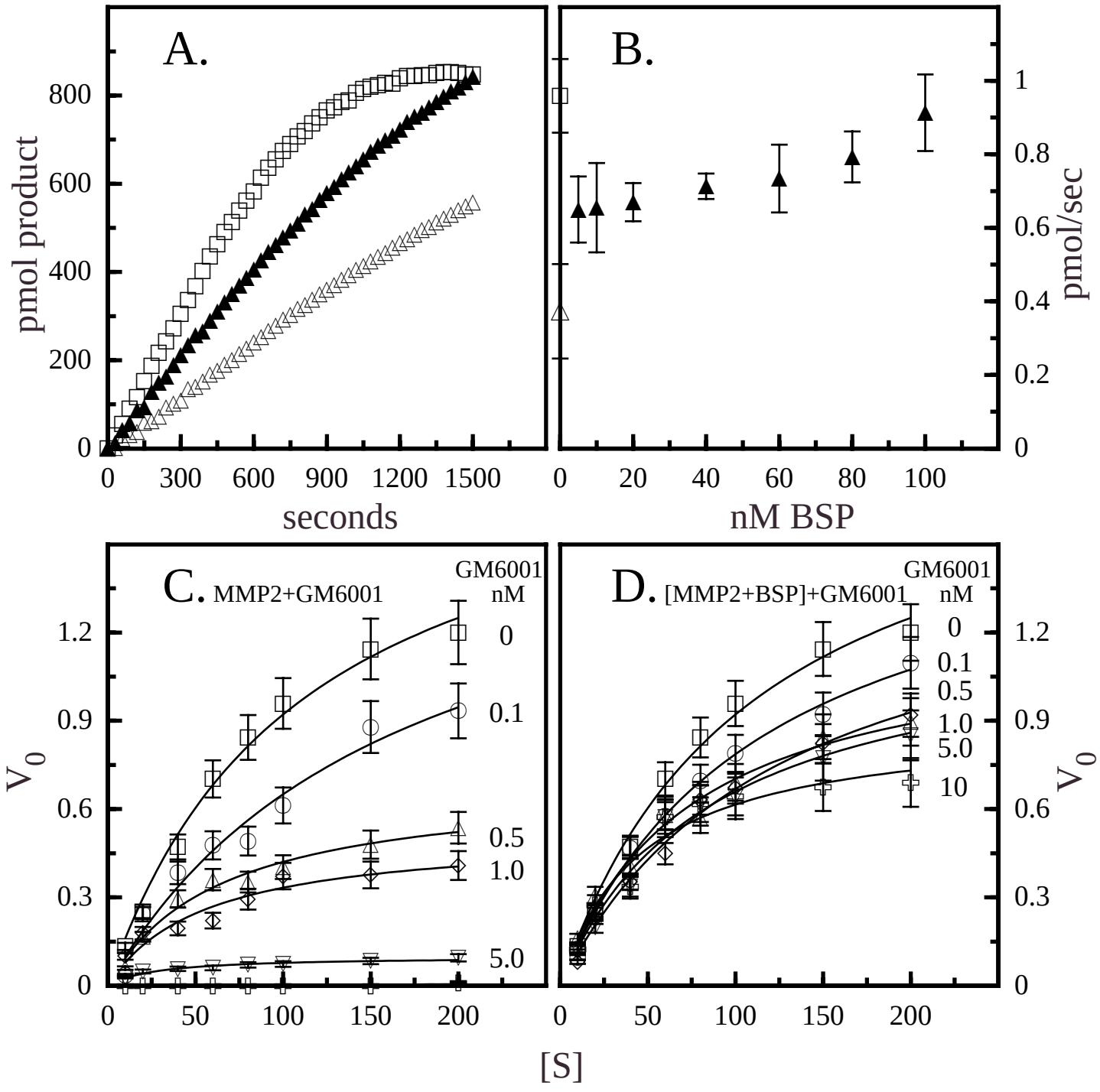
A.
B.
C. MMP2+GM6001
D. [MMP2+BSP]+GM6001
GM6001
nM
0
0.1
0.5
1.0
5.0
10
pmol product
seconds
nM BSP
pmol/sec
V0
[S]

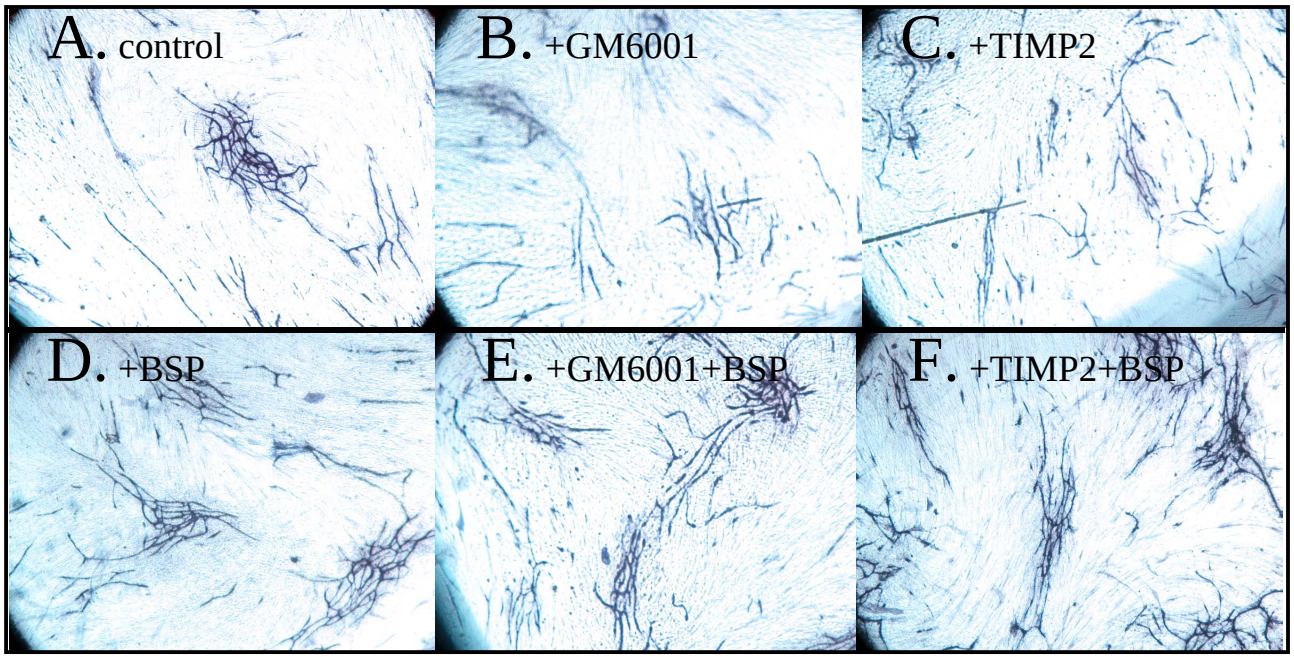
A. control
B. +GM6001
C. +TIMP2
D. +BSP
E. +GM6001+BSP
F. +TIMP2+BSP

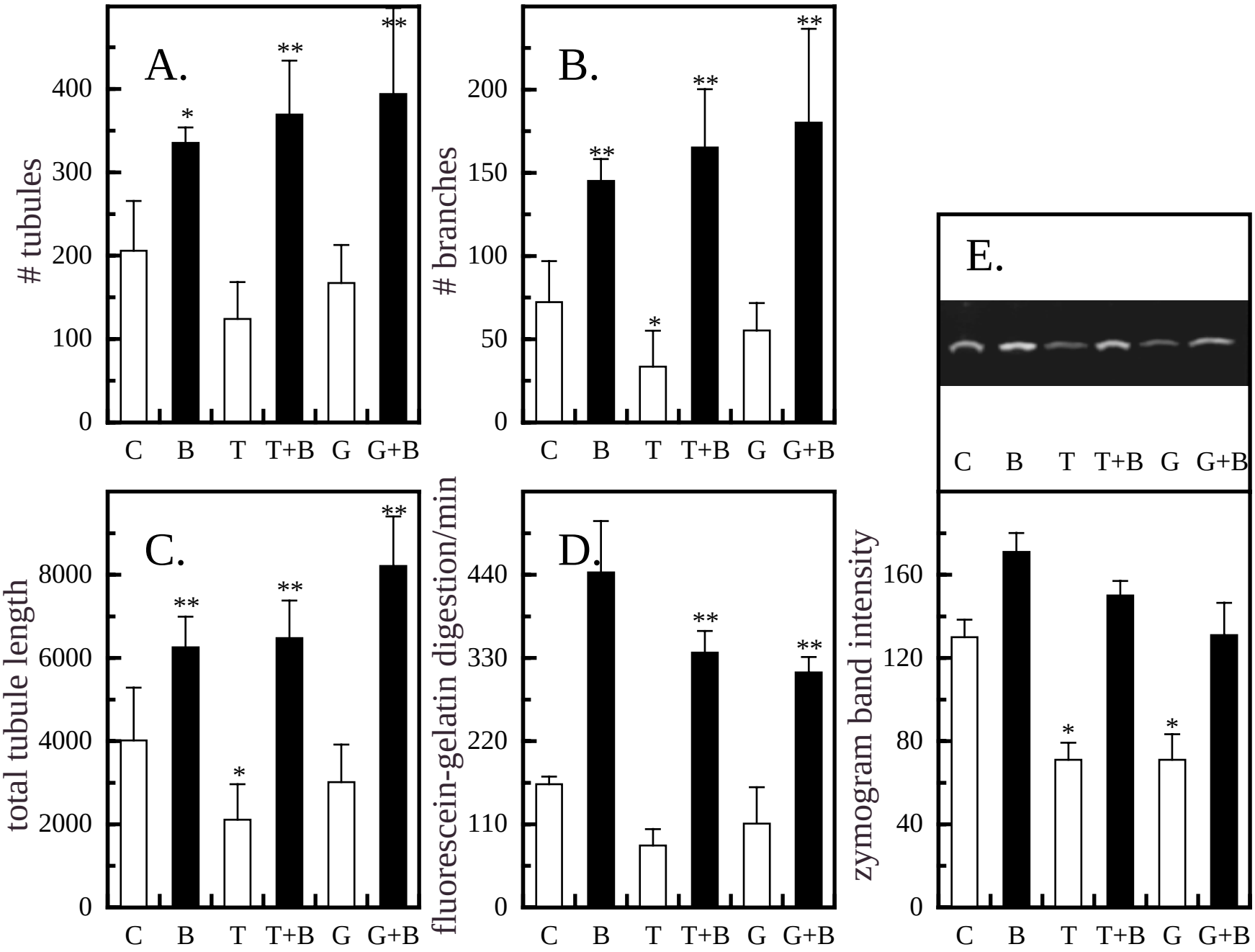
A.
tubules
0
100
200
300
400
C B T T+B G G+B
B.
branches
0
50
100
150
200
C B T T+B G G+B
C.
total tubule length
0
2000
4000
6000
8000
C B T T+B G G+B
D.
fluorescein-gelatin digestion/min
0
110
220
330
440
C B T T+B G G+B
E.
C B T T+B G G+B
zymogram band intensity
0
40
80
120
160
C B T T+B G G+B